

## STRING THEORY, GRAVITY AND EXPERIMENT

Thibault Damour<sup>1</sup> and Marc Lilley<sup>2</sup>

<sup>1</sup> *Institut des Hautes Etudes Scientifiques, 35 route de Chartres, F-91440 Bures-sur-Yvette, France*

<sup>2</sup> *Institut d'Astrophysique de Paris, 98, bis Blvd. Arago, F-75014 Paris, France*

## Contents

1. Introduction	3
2. Classical black holes as dissipative branes	4
2.1. Global properties of black holes	5
2.2. Black hole electrodynamics	13
2.3. Black hole viscosity	19
2.4. Irreversible thermodynamics of black holes	23
2.5. Hawking Radiation	25
3. Experimental tests of gravity	32
3.1. Universal coupling of matter to gravity	33
3.2. Experimental tests of the coupling of matter to gravity	36
3.2.1. How constant are the constants?	36
3.2.2. Tests of local Lorentz invariance	37
3.2.3. Universality of free fall	38
3.2.4. Universality of the gravitational redshift	39
3.3. Tests of the dynamics of the gravitational field	39
3.3.1. Brief review of the theoretical background	39
3.3.2. Experimental tests in the solar system	45
3.3.3. Objects with strong self-gravity: binary pulsars	47
3.3.4. Tests of gravity on very large scales	51
4. String-inspired phenomenology of the gravitational sector	52
4.1. Overview	52
4.2. Long range modifications of gravity	54
4.2.1. The cosmological attractor mechanism	55
4.2.2. Observable consequences of the Cosmological Attractor Mechanism	57
5. String-related signals in cosmology	62
5.1. Alternatives to slow-roll inflation	62
5.2. Cosmic superstrings	63
5.2.1. Phenomenological origin	63
5.2.2. Observational signatures	65
5.2.3. String dynamics	67
5.2.4. Gravitational waves from a cosmological string network	71
6. Conclusion	72
Bibliography	72

## Abstract

The aim of these lectures is to give an introduction to several topics which lie at the intersection of string theory, gravity theory and gravity phenomenology. One successively reviews: (i) the “membrane” approach to the dissipative dynamics of classical black holes, (ii) the current experimental tests of gravity, and their theoretical interpretation, (iii) some aspects of the string-inspired phenomenology of the gravitational sector, and (iv) some possibilities for observing string-related signals in cosmology (including a discussion of gravitational wave signals from cosmic superstrings).

## 1. Introduction

The common theme of these lectures is *gravity*, and their aim is to discuss a few cases where string theory might have an interesting interplay either with gravity theory, or with gravity phenomenology. We shall discuss the following topics:

- *Classical black holes as dissipative branes.* The idea here is to review the “classic” work on black holes of the seventies which led to the picture of black holes as being analog to dissipative branes endowed with finite electrical resistivity, and finite surface viscosity. In particular, we shall review the derivation of the (classical) surface viscosity of black holes, which has recently acquired a new (quantum) interest in view of AdS/CFT duality.

- *Hawking radiation from black holes.* To complete our classical account of irreversible properties of black holes, we shall also give a direct derivation of the phenomenon of Hawking radiation, because of its crucial importance in fixing the coefficient between the area of the horizon and black hole “entropy”.

- *Experimental tests of gravity.* Before discussing possible phenomenological consequences of string theory in the gravitational sector, we find useful to summarize the present status of experimental tests of gravity, as well as the theoretical frameworks used to interpret them. In particular, we emphasize that binary pulsar experiments have already given us accurate tests of some aspects of strong-field (and radiative) relativistic gravity.

- *String-inspired phenomenology of the gravitational sector.* In this section we shall discuss (without any attempt at completeness) some of the ideas that have been suggested about observable signals possibly connected to string theory. In

particular, we shall discuss the *cosmological attractor mechanism* which leads to a rather rich gravitational phenomenology that will be probed soon by various gravitational experiments.

- *String-related signals in cosmology.* After discussing a few alternatives to slow-roll inflation (and the possible relaxation of the Lyth bound when using non-linear kinetic terms for the inflaton), one discusses in some detail *cosmic superstrings*. We explain, in particular, how one computes the *gravitational wave burst signal* emitted by the cusps that periodically form during the dynamical evolution of generic string loops.

A final warning: by lack of time (and energy), no attempt has been made to give exhaustive and fair references to original and/or relevant work. The given references are indicative, and should be viewed as entry points into the relevant literature. With the modern, web-based, easy access to the scientific literature it is hoped that the reader will have no difficulty in using the few given references as starting points for an instructive navigation on the vast sea of the physics literature.

## 2. Classical black holes as dissipative branes

Early work on (Schwarzschild, Reissner-Nordström, or Kerr-Newman) black holes (BHs) in the 1950's and 1960's treated them as *passive objects*, *i.e.*, as given geometrical backgrounds (and potential wells). This viewpoint changed in the early 1970's when the study of the *dynamics* of BHs was initiated by Penrose [1], Christodoulou and Ruffini [2, 3], Hawking [4], and Bardeen, Carter and Hawking [5]. In the works [1–5], only the *global dynamics* of BHs was considered, *i.e.*, their total mass, their total angular momentum, their total irreducible mass, and the variation of these quantities. This viewpoint further evolved in the works of Hartle and Hawking [6], Hanni and Ruffini [7], Damour [8–10], and Znajek [11], which studied the *local dynamics of BH horizons*. In this new approach (which was later called the “membrane paradigm” [12]) a BH horizon is interpreted as a brane with dissipative properties, such as, for instance, an electrical resistivity  $\rho$ , equal to 377 Ohms [8, 11] independently of the type of BH, and a surface (shear) viscosity, equal to  $\eta = \frac{1}{16\pi}$  [9, 10]. When divided by the entropy density found by Hawking ( $S/A = \frac{1}{4}$ ), the latter shear viscosity yields the ratio  $\frac{1}{4\pi}$ , a result which has recently raised a renewed interest in connection with AdS/CFT, through the work of Kovtun, Son, and Starinets [13, 14].

### 2.1. Global properties of black holes

Let us start by reviewing the study of the *global dynamics* of BHs. Initially, BHs were thought of as given geometrical backgrounds. In the case of a spherically symmetric object of mass  $M$  without any additional attribute, Schwarzschild derived the first exact solution of Einstein's equations only a few weeks after Einstein had obtained the final form of the field equations. Schwarzschild's solution is as follows. In  $3+1$  dimensions, setting  $G = c = 1$ , the metric for a spherically symmetric background can be written in the form

$$ds^2 = -A(r)dT^2 + B(r)dr^2 + r^2 (d\theta^2 + \sin^2\theta d\varphi^2) \quad (2.1)$$

where  $T$  denotes the usual Schwarzschild-type time coordinate, and where the coefficients  $A(r)$  and  $B(r)$  read

$$\begin{aligned} A(r) &= 1 - \frac{2GM}{r}, \\ B(r) &= \frac{1}{A(r)}. \end{aligned} \quad (2.2)$$

This result was generalized in independent works by Reissner, and by Nordström (1918) for electrically charged spherically symmetric objects, in which case  $A(r)$  and  $B(r)$  are given by

$$\begin{aligned} A(r) &= 1 - \frac{2M}{r} + \frac{Q^2}{r^2}, \\ B(r) &= \frac{1}{A(r)}. \end{aligned} \quad (2.3)$$

We shall not review here the long historical path which led to interpreting the above solutions, as well as their later generalizations due to Kerr (who added to the mass  $M$  the spin  $J^1$ ), and Newman *et al.* (mass, spin and charge), as BHs. Up to the 1960's BHs were viewed only as *passive* gravitational wells. For instance, one could think of adiabatically lowering a small mass  $m$  at the end of a string until it disappears within the BH, thereby converting its mass-energy  $mc^2$  into work. More realistically, one was thinking of matter orbiting a BH and radiating away its potential energy (up to a maximum, given by the binding energy of the last stable circular orbit around a BH). This viewpoint changed in the 1970's, when BHs started being considered as *dynamical* objects, able to exchange mass, angular momentum and charge with the external world. Whereas in the simplest case above, one uses the attractive potential well created by the mass  $M$  without extracting energy from the BH, Penrose [1], showed that energy could in principle be *extracted* from a BH itself by means of what is now called a (gedanken) "Penrose process" (see FIG. 1). Namely, if one considers a time-independent

<sup>1</sup>Note that in the case of a spinning BH, one often introduces the useful quantity  $a = J/M$ , *i.e.*, the ratio of the total angular momentum to the mass of the BH, which has the dimension of length.

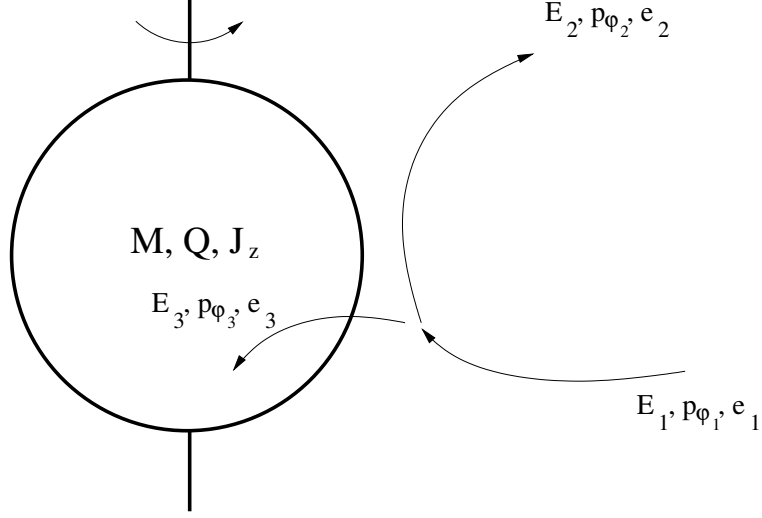


Figure 1. In this figure, we schematically illustrate the “Penrose process”, *i.e.*, the splitting of an ingoing particle into one that falls into the BH and another that exits at infinity.

background and a BH that is more complicated than Schwarzschild’s, say a Kerr BH, one may extract energy using a test particle 1 coming in from infinity with energy  $E_1$ , angular momentum  $p_{\phi_1}$ , and electric charge  $e_1$ . By Noether’s theorem, the time-translation, axial and  $U(1)$  gauge symmetries of the background guarantee the conservation of  $E$ ,  $p_{\phi}$  and  $e$  during the “fall” of the test particle. Moreover, if, in a quantum process, the test particle 1 splits, near the BH, into two particles 2 and 3, with  $E_2, p_{\phi_2}, e_2$ , and  $E_3, p_{\phi_3}, e_3$  respectively, then, under certain conditions, one finds that particle 3 can be absorbed by the BH, and that particle 2 may come out at infinity with more energy than the incoming particle 1. A detailed analysis of the efficiency of such gedanken Penrose processes by Christodoulou and Ruffini [2, 3] then led to the understanding of the existence of a fundamental *irreversibility* in BH dynamics, and to the discovery of the BH *mass formula*. Let us explain these results.

The basic idea is to explore the physics of BHs through a sequence of infinitesimal changes of their state obtained by injecting in them some test particles. One starts by writing that the total mass-energy, spin and charge of the BH change, by absorption of particle 3, as

$$\begin{aligned} \delta M &= E_3 = E_1 - E_2, \\ \delta J &= J_3 = J_1 - J_2, \\ \delta Q &= e_3 = e_1 - e_2. \end{aligned} \tag{2.4}$$

This preliminary result can be further exploited by making use of the Hamilton-Jacobi equation. Considering an on-shell particle of mass  $\mu$ , and adopting the  $(-+++)$  signature, the Hamilton-Jacobi equation reads

$$g^{\mu\nu} (p_\mu - eA_\mu) (p_\nu - eA_\nu) = -\mu^2, \quad (2.5)$$

in which  $p_\mu = \partial S / \partial x^\mu$ ,  $S$  is the action and the partial derivatives are taken w.r.t. the coordinates  $x^\mu$ . The details of the splitting process will be irrelevant, as only particle 3 matters in the calculation. In an axially symmetric and time-independent background,  $S$  can be taken as a linear function of  $T$  and  $\varphi$ ,

$$S = -ET + p_\varphi \varphi + S(r, \theta). \quad (2.6)$$

where  $E = -p_T = -p_0$  is the conserved energy,  $p_\varphi$  is the conserved  $\varphi$ -component of angular momentum and the last term is the contribution from terms that depend on the angle  $\theta$  and on the radial distance  $r$ . Let us consider the case of a Reissner-Nordström BH, where calculations are easier: the inverse metric is easily computed and (2.5) can then be written explicitly as

$$-\frac{1}{A(r)} (p_0 - eA_0)^2 + A(r)p_r^2 + \frac{1}{r^2} \left( p_\theta^2 + \frac{1}{\sin^2 \theta} p_\varphi^2 \right) = -\mu^2 \quad (2.7)$$

which we re-write as

$$(p_0 - eA_0)^2 = A(r)^2 p_r^2 + A(r) \left( \mu^2 + \frac{L^2}{r^2} \right) \quad (2.8)$$

The electric potential is  $-A_0 = +V = +Q/r$ . The above expression is quadratic in  $E$  (it is the generalization of the famous flat-spacetime  $E^2 = \mu^2 + \mathbf{p}^2$ ) and one finds two possible solutions for the energy as a function of momenta and charge (see FIG. 2):

$$E = \frac{eQ}{r} \pm \sqrt{A(r)^2 p_r^2 + A(r) \left( \mu^2 + \frac{L^2}{r^2} \right)}. \quad (2.9)$$

In flat space,  $A(r) = 1$ , so that, if we ignore charge, we recover the usual Dirac dichotomy on the choice of the  $+$  or  $-$  sign between particle and antiparticle:  $E = \pm \sqrt{\mu^2 + \mathbf{p}^2}$ . This shows that one should take the *plus sign* in the equation above. We remind the reader that for a charged BH, there exists a regular horizon only if  $Q < M$  (which can be interpreted as a BPS bound). [We have set  $G = 1$ ]. Remembering that  $A(r) = 1 - 2M/r + Q^2/r^2$ , there exists both an outer and an inner horizon defined by  $r_\pm = M \pm \sqrt{M^2 - Q^2}$  (which are the two roots

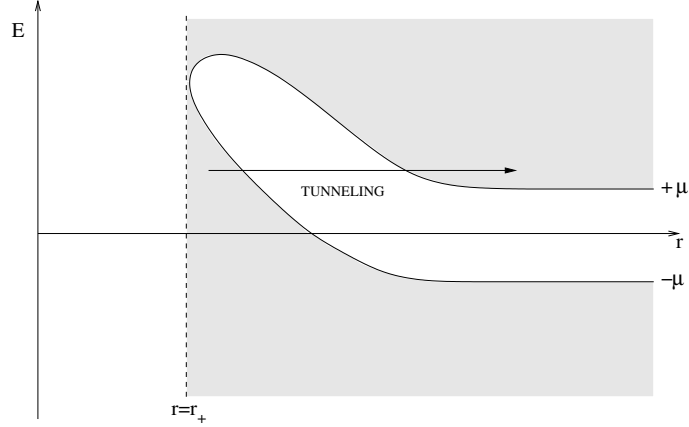


Figure 2. This figure depicts the classically allowed energy levels (shaded region) as a function of radius, for test particles in the neighborhood of a BH. There exist positive- and negative-energy solutions, corresponding (after second quantization) to particles and anti-particles. Classically (as in the Penrose process) one should consider only the “positive-square-root” energy levels, located in the upper shaded region. The white region is classically forbidden. Note the possibility of tunneling (this corresponds to particle creation via the “super-radiant”, non-thermal mechanism briefly mentioned below).

of  $A(r) = 0$ . The horizon of relevance for BH physics is the outer one  $r_+ = M + \sqrt{M^2 - Q^2}$  (it gives the usual result  $2M$  when  $Q = 0$ ). As particle 3 is absorbed by the BH, we can compute its (conserved) energy when it crosses the horizon, *i.e.*, in the limit where the radial coordinate  $r$  is equal to  $r_+$ . This simplifies the expression of  $E_3$  to

$$E_3 = \frac{e_3 Q}{r_+} + |p^r|, \quad (2.10)$$

where we have introduced the contravariant component  $p^r = g^{rr} p_r = A(r) p_r$ , which has a finite limit on the horizon. Note the presence of the *absolute value* of  $p^r$  (coming from the limit of a positive square-root). The change in the mass of the BH is equal to the energy  $E_3$  of the particle absorbed, *i.e.*, particle 3. Using  $e_3 = \delta Q$ , this yields

$$\delta M = \frac{Q \delta Q}{r_+(M, Q)} + |p^r|. \quad (2.11)$$

From the positivity of  $|p^r|$  we deduce that

$$\delta M \geq \frac{Q \delta Q}{r_+(M, Q)}. \quad (2.12)$$



We have derived an *inequality* and have thereby demonstrated (by following Christodoulou and Ruffini) the irreversibility property of BH energetics. There exist two types of processes, the *reversible* ones with an ‘=’ sign in (2.12), and the *irreversible* ones with an ‘>’ sign. The former ones are reversible because if a BH first absorbs a particle of charge  $+e$  with vanishing  $|p^r|$  (thereby changing its mass by  $\delta'M = eQ/r_+(M, Q)$  and its charge by  $\delta'Q = e$ ), and then a particle of charge  $-e$  with vanishing  $|p^r|$  (thereby changing its mass by  $\delta''M = -eQ/r_+(M, Q)$  and its charge by  $\delta''Q = -e$ ), it will be left, at the end, in the same state as the original one (with mass  $M + \delta'M + \delta''M = M$  and charge  $Q + \delta'Q + \delta''Q = Q$ ). Evidently, such reversible transformations are delicate to perform, and one expects that irreversibility will occur in most BH processes. The situation here is clearly similar to the relation between reversible and irreversible processes in thermodynamics.

The same computation as for the Reissner-Nordström BH can be performed for the Kerr-Newman BH. One obtains in that case, by a slightly more complicated calculation,

$$\delta M - \frac{a\delta J + r_+Q\delta Q}{r_+^2 + a^2} = \frac{r_+^2 + a^2 \cos^2\theta}{r_+^2 + a^2} |p^r|. \quad (2.13)$$

in which  $r_+(M, J, Q) = M + \sqrt{M^2 - Q^2 - a^2}$ . We recall that  $a = J/M$ , and that one has the bound  $Q^2 + (J/M)^2 \leq M^2$ .

The idea now is to consider an infinite sequence of infinitesimal reversible changes (*i.e.*,  $p^r \rightarrow 0$ ), and to study the BH states which are reversibly connected to some initial BH state with given mass  $M$ , angular momentum  $J$  and charge  $Q$ . This leads to a partial differential equation for  $\delta M$ ,

$$\delta M = \frac{a\delta J + r_+Q\delta Q}{r_+^2 + a^2}, \quad (2.14)$$

which is found to be integrable. Integrating it, one finds the Christodoulou-Ruffini mass formula [3]

$$M^2 = \left( M_{\text{irr}} + \frac{Q^2}{4M_{\text{irr}}} \right)^2 + \frac{J^2}{4M_{\text{irr}}^2}. \quad (2.15)$$

Here the *irreducible mass*  $M_{\text{irr}} = \frac{1}{2}\sqrt{r_+^2 + a^2}$  appears as an integration constant. The mass squared thus appears as a function of three contributions, with one term containing the square of the sum of the irreducible mass and of the Coulomb energy, and the other one containing the rotational energy. Inserting this expression into Eq. (2.13), one finds

$$\delta M_{\text{irr}} \geq 0 \quad (2.16)$$

with  $\delta M_{\text{irr}} = 0$  under reversible transformations and  $\delta M_{\text{irr}} > 0$  under irreversible transformations. The irreducible mass  $M_{\text{irr}}$  can only increase or stay constant. This behaviour is certainly reminiscent of the second law of thermodynamics. The free energy of a BH is therefore  $M - M_{\text{irr}}$ , *i.e.*, this is the maximum extractable energy. In this view, BHs are no longer passive geometrical backgrounds but contain stored energy that can be extracted. Actually, the stored energy can be enormous because a BH can store up to 29 % of its mass as rotational energy, and up to 50 % as Coulomb energy!

The irreducible mass is related to the area of the horizon of the BH, by  $A = 16\pi M_{\text{irr}}^2$  so that in a reversible process  $\delta A = 0$ , while in an irreversible one  $\delta A > 0$ . Hawking showed [4] that this irreversible evolution of the area of the horizon was a general consequence of Einstein's equations, when assuming the weak energy condition. He also showed that in the merging of two BHs of area  $A_1$  and  $A_2$ , the total final area satisfied  $A_{\text{tot}} \geq A_1 + A_2$ .

Such results evidently evoke the second law of thermodynamics. The analog of the first law [ $dE(S, \text{extensive parameters}) = dW + dQ$ , where the work  $dW$  is linked to the variation of extensive parameters (volume, etc.) and where  $dQ = TdS$  is the heat exchange] reads, for BH processes,

$$dM(Q, J, A) = VdQ + \Omega dJ + \frac{g}{8\pi} dA. \quad (2.17)$$

Comparing this result with expression (2.13), one has

$$\begin{aligned} V &= \frac{Qr_+}{r_+^2 + a^2}, \\ \Omega &= \frac{a}{r_+^2 + a^2}, \end{aligned} \quad (2.18)$$

and

$$g = \frac{1}{2} \frac{r_+ - r_-}{r_+^2 + a^2}, \quad (2.19)$$

which, in the Kerr-Newman case, is given by

$$g = \frac{\sqrt{M^2 - a^2 - Q^2}}{r_+^2 + a^2}. \quad (2.20)$$

$V$  is interpreted as the electric potential of the BH, and  $\Omega$  as its angular velocity. Expression (2.17) resembles the usual form of the first law of thermodynamics in which the area term has to be interpreted as some kind of entropy. The parameter  $g$  is called the "surface gravity". [In the Schwarzschild case, it reduces to  $M/r_+^2$  (in  $G = 1$  units), *i.e.*, the usual formula for the surface gravitational acceleration  $g = GM/R^2$ ]. In the Les Houches Summer School of 1972, a more general

version of the first law was derived, that included the presence of matter around the BH, and energy exchange [5]. An analog of the zeroth law was also derived [15], in the sense that the surface gravity  $g$  (which is analog to the temperature) was found to be uniform on the surface of a BH in equilibrium.

In 1974, Bekenstein went further in taking seriously (and no longer as a simple analogy) the thermodynamics of BHs. First, note that one can write the formal BH “heat exchange” term in various ways

$$dQ = TdS = \frac{gdA}{8\pi} = 4gM_{\text{irr}}dM_{\text{irr}}. \quad (2.21)$$

In light of this, is the appropriate physical analog of the entropy the irreducible mass or the area of a BH? Is the analog of temperature proportional to the surface gravity  $g$  or to the product  $M_{\text{irr}}g$ ? Can one give a physical meaning to the temperature and entropy of a BH? To address such questions, Bekenstein used several different approaches.

In particular, he used Carnot-cycle-type arguments. For instance, one may extract work from a BH by slowly lowering into it a box of radiation of infinitesimal size. In fact, in this ideal case, one can theoretically convert all the energy of the box of radiation,  $mc^2$ , into work. The efficiency of Carnot cycles is defined in terms of both a hot and a cold source as

$$\eta = 1 - \frac{T_{\text{cold}}}{T_{\text{hot}}}. \quad (2.22)$$

From what we just said, it would seem that the efficiency of classical BHs as thermodynamic engines is 100%,  $\eta = 1$ . This would then correspond to a BH temperature (= the cold source)  $T_{\text{BH}} = T_{\text{cold}} = 0$ . The point made by Bekenstein was that this classical result will be modified by quantum effects. Indeed, one expects (because of the uncertainty principle) that a box of thermal radiation at temperature  $T$  (made of typical wavelengths  $\lambda \sim 1/T$ ) cannot be made infinitesimally small, but will have a minimum finite size  $\sim \lambda$ . From this limit on the size of the box, Bekenstein then deduced an upper bound on the efficiency  $\eta$ , and therefore a lower bound on the BH temperature  $T_{\text{BH}} \neq 0$ .

Let us indicate another reasoning (of Bekenstein) which suggests that the absorption of a single particle by a BH augments its surface by a finite amount proportional to  $\hbar$ . As we said above the change of BH energy as it absorbs a particle is (when  $a = 0$ , for simplicity)

$$E_3 = \frac{eQ}{r_+} + \lim_{r \rightarrow r_+} |p^r| \quad (2.23)$$

We also showed that the transformation will be reversible (*i.e.*, will *not* increase the surface area of the BH) only if  $\lim_{r \rightarrow r_+} |p^r| = 0$ . However, for this to be

true *both* the (radial) position and the (radial) momentum of the particle must be exactly fixed: namely,  $r = r_+$  and  $p^r = 0$ . This would clearly be in contradiction with the Heisenberg uncertainty principle. Technically, we must consider the conjugate momentum to the position  $r$  which is the *covariant* component  $p_r$  of the radial momentum (instead of the *contravariant* component  $p^r$  used in the equation above). The uncertainty relation therefore reads

$$\delta r \delta p_r \geq \frac{1}{2} \hbar. \quad (2.24)$$

Near the horizon (i.e. when  $\delta r \equiv r - r_+$  is small), the contravariant radial momentum reads (using  $g^{rr} = 1/g_{rr} = A(r)$ )

$$\begin{aligned} p^r &= \frac{A(r)p_r}{(r - r_+)(r - r_-)} \\ &= \frac{r^2}{\delta r} \frac{(r_+ - r_-)}{r_+^2} p_r \\ &\simeq \left( \frac{\partial A}{\partial r} \right)_{r_+} \delta r p_r, \end{aligned} \quad (2.25)$$

so that Heisenberg's uncertainty relation yields a *lower bound* for  $p^r$ . We can reexpress this lower bound in terms of the BH surface gravity  $g$  introduced above by noting that the partial derivative of  $A$  w.r.t.  $r$ ,  $\left( \frac{\partial A}{\partial r} \right)_{r_+}$ , entering the last equation, is proportional to  $g$ :

$$\left( \frac{\partial A}{\partial r} \right)_{r_+} = 2g. \quad (2.26)$$

This then gives

$$p^r \simeq 2g \delta r \delta p_r \geq g \hbar \quad (2.27)$$

>From the relation  $\delta M = \frac{Q \delta Q}{r_+(M, Q)} + |p^r|_{r_+}$ , we finally obtain

$$\delta M - \frac{Q \delta Q}{r_+} = |p^r| \geq g \hbar, \quad (2.28)$$

which can be rewritten as

$$\delta A \geq 8\pi \hbar. \quad (2.29)$$

In other words, quantum mechanics tells us that when one lets a particle fall into a BH, one cannot do so in a perfectly reversible way. The area must increase by a quantity of order  $\hbar$ . If (still following Bekenstein) one considers that the irreversible absorption of a particle by a BH corresponds to the loss of one bit of information (for the outside world), we are led to the idea of attributing to

a BH an entropy (in the sense of “negentropy”) equal (after re-introducing the constants  $c$  and  $G$ ) to [16]

$$S_{\text{BH}} = \hat{\alpha} \frac{c^3}{\hbar G} A, \quad (2.30)$$

with a dimensionless numerical coefficient equal to  $\hat{\alpha} = \ln 2/8\pi$  according to the reasoning just made. More generally, Bekenstein suggested that the above formula should hold with a dimensionless coefficient  $\hat{\alpha} \approx \mathcal{O}(1)$ , without being able to fix in a unique, and convincing, manner the value of  $\hat{\alpha}$ . This result in turn implies (by applying the law of thermodynamics) that one should attribute to a BH a temperature equal to

$$T_{\text{BH}} = \frac{1}{8\pi\hat{\alpha}} \frac{\hbar}{c} g. \quad (2.31)$$

This attribution of a finite temperature to a BH looked rather strange in view of the definition of a BH has being “black”, *i.e.*, as allowing no radiation to come out of it. In particular, Stephen Hawking resisted this idea, and tried to prove it wrong by studying quantum field theory in a BH background. However, much to his own surprise, he so discovered (in 1974) the phenomenon of quantum radiation from BH horizons (see below) which remarkably vindicated the physical correctness of Bekenstein’s suggestion. Hawking’s calculation also unambiguously fixed the numerical value of  $\hat{\alpha}$  to be  $\hat{\alpha} = \frac{1}{4}$  [17]. [We shall give below a simple derivation (from Ref. [18]) of Hawking’s radiation.]

Summarizing so far: The results on BH dynamics and thermodynamics of the early 1970’s modified the early view of BHs as passive potential wells by endowing them with *global* dynamical and thermodynamical quantities, such as mass, charge, irreducible mass, entropy, and temperature. In the following section, we shall review the further changes in viewpoint brought by work in the mid and late 1970’s ([6, 8–11]) which attributed *local* dynamical and thermodynamical quantities to BHs, and led to considering BH horizons as some kind of *dissipative branes*. Note that, in the following section, we shall no longer consider only Kerr-Newman BHs (*i.e.*, stationary BHs in equilibrium, which are not distorted by sources at infinity). We shall consider more general non-stationary BHs distorted by outside forces.

## 2.2. Black hole electrodynamics

The description of BHs we give from here on is essentially “holographic” in nature since it will consist of excising the interior of a BH, and replacing the description of the interior BH physics by quantities and phenomena taking place entirely on the “surface of the BH” (*i.e.*, the horizon). The surface of the BH is defined as being a null hypersurface, *i.e.*, a surface everywhere tangent to the lightcone, separating the region inside the BH from the region outside. As just

said, we ignore the region inside, including the spacetime singularity, and consider the physics in the outside region, completing it with suitable “boundary effects” on the horizon. These boundary effects are fictitious, and do not really exist on the BH surface but play the role of representing, in a holographic sense, the physics that goes on inside. In the end, we shall have a horizon, a set of surface quantities on the horizon and a set of bulk properties outside the horizon. We first consider Maxwell’s equations, namely  $F_{\mu\nu} = \partial_\mu A_\nu - \partial_\nu A_\mu$ , and

$$\begin{aligned}\nabla_\nu F^{\mu\nu} &= 4\pi J^\mu, \\ \nabla_\mu J^\mu &= 0.\end{aligned}\tag{2.32}$$

A priori, the electromagnetic field  $F_{\mu\nu}$  permeates the full space time, existing both inside and outside the horizon, and the current, *i.e.*, the source term of  $F_{\mu\nu}$  that carries charge, is also distributed both outside and inside the BH. In order to replace the internal electrodynamics of the BH by surface effects, we replace the real  $F_{\mu\nu}(x)$  by  $F_{\mu\nu}(x)\Theta_H$ , where  $\Theta_H$  is a Heaviside-like step function, equal to 1 outside the BH and 0 inside. Then we consider what equations are satisfied by this  $\Theta_H$ -modified electromagnetic field. The corresponding modified Maxwell equations contain two types of source terms,

$$\begin{aligned}\nabla_\nu (F^{\mu\nu}\Theta) &= (\nabla_\nu F^{\mu\nu})\Theta + F^{\mu\nu}\nabla_\nu\Theta \\ &= 4\pi (J^\mu\Theta + j_H^\mu),\end{aligned}\tag{2.33}$$

where we have introduced a *BH surface current*  $j_H^\mu$  as

$$j_H^\mu = \frac{1}{4\pi} F^{\mu\nu}\nabla_\nu\Theta.\tag{2.34}$$

This surface current contains a Dirac  $\delta$ -function which restricts it to the horizon. Indeed, let us consider a scalar function  $\varphi(x)$  such that  $\varphi(x) = 0$  on the horizon, with  $\varphi(x) < 0$  inside the BH, and  $\varphi(x) > 0$  outside it. The BH  $\Theta$ -function introduced above is simply equal to  $\Theta_H = \theta(\varphi(x))$ , where  $\theta$  denotes the standard step function of one real variable. Therefore, the gradient of  $\Theta_H$  reads

$$\partial_\mu\Theta_H = \partial_\mu\theta(\varphi(x)) = \delta(\varphi(x))\partial_\mu\varphi,\tag{2.35}$$

where  $\delta$  is the (one dimensional) usual Dirac delta, so that  $\delta(\varphi(x))$  is a delta function with support on the horizon. Morally, the gradient  $\partial_\mu\varphi$  yields a vector “normal to the horizon”. In the case of a BH (by contrast to the usual case of a hypersurface in Euclidean space), there exists an extra subtlety in the exact definition of the normal to the horizon. The horizon is a null hypersurface which by definition is normal to a null covariant vector  $\ell_\mu$  satisfying both  $\ell_\mu\ell^\mu = 0$  and  $\ell_\mu dx^\mu$  for any infinitesimal displacement  $dx^\mu$  within the hypersurface. Since  $\ell_\mu$

is null, it cannot be normalized in the same way as in Euclidean space. This leads to an ambiguity in the physical observables related to  $\ell_\mu$ . In stationary-axisymmetric spacetimes, one uniquely normalizes  $\ell_\mu$  by demanding that the corresponding directional gradient  $\ell^\mu \partial_\mu$  be of the form  $\partial/\partial t + \Omega \partial/\partial \phi$  (with a coefficient one in front of the time-derivative term). We shall assume (in the general non-stationary case) that  $\ell_\mu$  is normalized so that its normalization is compatible with the usual normalization when considering the limiting case of stationary-axisymmetric spacetimes. Anyway, given any normalization, there exists a scalar  $\omega$  such that

$$\ell_\mu = \omega \partial_\mu \varphi, \quad (2.36)$$

and we can then define an ‘‘horizon  $\delta$ -function’’

$$\delta_H = \frac{1}{\omega} \delta(\varphi), \quad (2.37)$$

such that

$$\partial_\mu \Theta_H = \ell_\mu \delta_H. \quad (2.38)$$

This leads to defining a ‘‘BH surface current density’’

$$K^\mu = \frac{1}{4\pi} F^{\mu\nu} \ell_\nu. \quad (2.39)$$

With this definition, the BH current  $j_H^\mu$  reads

$$j_H^\mu = K^\mu \delta_H, \quad (2.40)$$

and satisfies

$$\nabla_\mu (\Theta_H J^\mu + K^\mu \delta_H) = 0, \quad (2.41)$$

which is a conservation law for the sum of the outside bulk current  $\Theta_H J^\mu$  and of the boundary current  $K^\mu \delta_H$ . In picturesque terms, the surface current  $K^\mu \delta_H$  effectively ‘‘closes’’ the external current lines penetrating the BH (analogously to the case of external currents being injected in a perfect conductor and leading to currents flowing on its surface). In addition, Eq. (2.39) shows that this surface current is linked to the electromagnetic fields which are on the horizon. We have thus endowed the horizon with surface quantities, defined uniquely and locally on the horizon.

Before we proceed, we introduce a convenient coordinate system to describe the physics on the horizon of a general BH. We assume some regular ‘‘slicing’’ of the horizon and its neighbourhood by some (advanced) Eddington-Finkelstein-like time coordinate  $t = x^0$ . Then we assume that the first coordinate  $x^1$  is such that it is equal to zero on the horizon (like  $r - r_+$  in the Kerr-Newman

case). Finally  $x^A$  for  $A = 2, 3$  denote some angular-like coordinates on the two-dimensional spatial slice  $S_t$  ( $x^0 = t$ ) of the horizon. In this coordinate system, we normalize  $\ell^\mu$  such that

$$\ell^\mu \partial_\mu = \frac{\partial}{\partial t} + v^A \frac{\partial}{\partial x^A}. \quad (2.42)$$

Here, we have used the fact that the “normal” vector  $\ell^\mu$ , being null, is also *tangent* to the horizon, so that  $\ell^\mu \partial_\mu$  is a general combination of  $\partial/\partial t$  and  $\partial/\partial x^A$  but has no component along the “radial” (or “transverse”) coordinate  $x^1$ . Because  $\ell^\mu$  is a vector tangent to the hypersurface, we can consider its integral lines  $\ell^\mu = dx^\mu/dt$ , which lie within the horizon. These integral curves are called the *generators* of the horizon. They are null geodesics curves, lying entirely within the horizon.

Expression (2.42) for the directional gradient along  $\ell^\mu$  suggests that  $v^A$  be interpreted as the velocity of some “fluid particles” on the horizon, which are the “constituents” of a null membrane. Similarly to the usual description of the motion of a fluid, one has to keep track of the changes in the distance between two fluid particles as the fluid expands and shears. For a usual fluid, one considers the gradient of the velocity field, splitting it into its symmetric and anti-symmetric parts. The antisymmetric part is simply a local rotation which has no incidence on the physics and can be ignored. The symmetric part is further split into its trace and tracefree parts, namely

$$\frac{1}{2} (\partial_i v_j + \partial_j v_i) = \sigma_{ij} + \frac{1}{d} \partial \cdot v \delta_{ij} \quad (2.43)$$

where  $d$  is the spatial dimension of the considered fluid (which will be  $d = 2$  in our case). Here the first term describes the shear, and the second describes the rate of expansion. We will see later how the BH analogs of these quantities are defined. For the moment let us consider the distances on the horizon. They are measured by considering the restriction to the horizon of the spacetime metric (which is assumed to satisfy Einstein’s equations). As we are considering a null hypersurface, we have

$$ds^2|_{x^1=0} = \gamma_{AB}(t, x^C) (dx^A - v^A dt) (dx^B - v^B dt) \quad (2.44)$$

where  $v^A = \frac{dx^A}{dt}$ . Note that  $ds^2$  is a degenerate metric: indeed, on a (three-dimensional) null hypersurface, there is no real time direction ( $ds^2$  vanishes along the generators). One has only two positive-definite space dimensions along, e.g., the spatial slices  $S_t$ . This metric describes the geometry on the horizon from which one can compute the area element of the spatial sections  $S_t$

$$dA = \sqrt{\det \gamma_{AB}} dx^2 \wedge dx^3. \quad (2.45)$$



One can decompose the current density  $K^\mu$  into a time component  $\sigma_H = K^0$ , and two spatial components  $K^A$  tangent to the spatial slices  $S_t$  ( $t = \text{const.}$ ) of the horizon,

$$K^\mu \partial_\mu = \sigma_H \partial_t + K^A \partial_A \quad (2.46)$$

in which  $\partial_t = \ell^\mu \partial_\mu - v^A \partial_A$  so that

$$K^\mu \partial_\mu = \sigma_H \ell^\mu + (K^A - \sigma_H v^A) \partial_A \quad (2.47)$$

The total electric charge of the spacetime is defined by a surface integral at  $\infty$ , say

$$Q_{\text{tot}} = \frac{1}{4\pi} \oint_{S_\infty} \frac{1}{2} F^{\mu\nu} dS_{\mu\nu}. \quad (2.48)$$

This result can be re-written as the sum of a surface integral on the horizon and a volume integral in between the horizon and  $\infty$ . The volume integral is simply the usual charge contained in space, so that we can define the BH charge  $Q_H$  as

$$Q_H = \frac{1}{4\pi} \oint_H \frac{1}{2} F^{\mu\nu} dS_{\mu\nu}, \quad (2.49)$$

where the tensorial horizon surface element reads  $dS_{\mu\nu} = \frac{1}{2} \varepsilon_{\mu\nu\rho\sigma} dx^\rho \wedge dx^\sigma = (n_\mu \ell_\nu - n_\nu \ell_\mu) dA$ . Here,  $n^\mu$  is a second null vector, which is transverse to the horizon, and which is orthogonal to the spatial sections  $S_t$ . It is normalized such that  $n^\mu \ell_\mu = +1$ . Using the definitions above of the BH surface current, one easily finds that the total BH charge can be rewritten as

$$Q_H = \oint_H \sigma_H dA, \quad (2.50)$$

where  $\sigma_H$  is the time component of the BH surface current introduced above. Though it is a priori only the integrated BH charge which has a clear physical meaning, it is natural to consider the density  $\sigma_H$  appearing in the above surface integral as defining a charge distribution on the horizon. Then the link

$$\sigma_H = K^\mu n_\mu = \frac{1}{4\pi} F^{\mu\nu} n_\mu \ell_\nu \quad (2.51)$$

can be thought of as being analog to the result  $\sigma = \frac{1}{4\pi} E^i n_i$  giving the electric charge distribution on a metallic object. This can again be viewed as part of a holographic approach in which the interior of the BH is replaced by boundary effects. This analogy extends to the (spatial) currents flowing along the surface of the BH. Indeed, using the conservation law  $\nabla_\mu (\Theta_H J^\mu + K^\mu \delta_H) = 0$ , which is just a Bianchi identity, one has

$$\frac{1}{\sqrt{\gamma}} \frac{\partial}{\partial t} (\sqrt{\gamma} \sigma_H) + \frac{1}{\sqrt{\gamma}} \frac{\partial}{\partial x^A} (\sqrt{\gamma} K^A) = -J^\mu \ell_\mu. \quad (2.52)$$

This shows, in a mathematically precise way, how an external current injected “normally” to the horizon “closes” onto a combination of currents flowing along the horizon, and/or of an increase in the local horizon charge density. One can also introduce the electromagnetic 2-form and restrict it on the horizon. It then defines the electric and magnetic fields on the horizon according to

$$\frac{1}{2}F_{\mu\nu}dx^\mu \wedge dx^\nu|_H = E_A dx^A \wedge dt + B_\perp dA. \quad (2.53)$$

Taking the exterior derivative of the left-hand-side then gives

$$\nabla \times \vec{E} = -\frac{1}{\sqrt{\gamma}}\partial_t(\sqrt{\gamma}B_\perp). \quad (2.54)$$

which relates the electric and magnetic fields on the horizon.

>From the various formal definitions above, one also gets the following relation

$$E_A + \epsilon_{AB}B_\perp v^B = 4\pi\gamma_{AB}(K^B - \sigma_H v^B), \quad (2.55)$$

or

$$\vec{E} + \vec{v} \times \vec{B}_\perp = 4\pi(\vec{K} - \sigma_H \vec{v}). \quad (2.56)$$

We recognize here a BH analog of the usual Ohm’s law relating the electric field to the current (especially in the case where  $v \rightarrow 0$ , i.e., in the absence of the various “convection effects” linked to the horizon “velocity”  $\vec{v}$ ). From this form of Ohm’s law, we can read off that BHs have a *surface electric resistivity* equal to  $\rho = 4\pi = 377$  Ohm [8, 11].

Let us give an example in which this BH Ohm’s law can be “applied” to a specific system. We consider for simplicity the case of a Schwarzschild BH and set up an electric circuit “on the surface of the BH” by injecting on the North pole (through an electrode penetrating the horizon under a polar angle  $\theta_1$ , with, say,  $\theta_1 \ll 1$ ) an electric current  $I$ , and letting it escape<sup>2</sup> from the South pole (via an electrode penetrating the horizon under a polar angle  $\theta_2$ , with, say,  $\pi - \theta_2 \ll 1$ ). When viewing the BH as a membrane with surface resistivity  $\rho$ , this set up will give rise to a fictitious current flow on the horizon, closing the circuit between the North and the South poles. Associated to the current flow on the horizon, there will be a potential drop  $V$  between the poles. This potential drop is simply given by the usual Ohm’s law,  $V = RI$ , i.e., the product of the current  $I$  by a “resistance”  $R$ :

$$V = -A_0(\theta_1) + A_0(\theta_2) = RI. \quad (2.57)$$

<sup>2</sup>Actually, as (classical) charges cannot escape from a BH, we need to inject in the South electrode a flow of negative charges (while injecting a flow of positive charges down the North pole).

The BH resistance  $R$  can be computed in two different ways, either by solving Maxwell's equations in a Schwarzschild background, or by computing, in usual Euclidean space, the total resistance of a spherical metallic shell with a uniform surface resistivity  $\rho = 4\pi$  (by decomposing the problem in many elementary resistances, some being in parallel, and others in series). Both methods give the same answer, namely

$$R = 2 \ln \frac{\tan \frac{\theta_2}{2}}{\tan \frac{\theta_1}{2}}, \quad (2.58)$$

expressed in units of  $30 \Omega$ .<sup>3</sup> This result is saying that the typical total resistivity of a BH is of the order of  $30 \Omega$ . In addition, if one considers a rotating BH placed in a magnetic field out of alignment with its axis of rotation (a field uniform at  $\infty$ , but distorted on the horizon), one expects to find eddy currents on the horizon, currents which dissipate the energy. These currents exist, can be computed and do indeed brake the rotation of the BH. In such a situation, one also finds a torque which acts to restore the alignment of the BH with the field [8].

### 2.3. Black hole viscosity

In the previous section, we introduced the electromagnetic dissipative properties of a BH, using a holographic approach which kept the physics outside up to infinity, and replaced the physics inside the BH by defining suitable quantities on the horizon, and then showed that they satisfied equations similar to well-known ones (such as Ohm's law). We now turn to the viscous properties of BHs and show how suitably defined "surface hydrodynamical" quantities satisfy a sort of Navier-Stokes equation. Technically, we would like to do, for the gravitational surface properties, something similar to what we did for the electrodynamic properties. Namely, we would like to replace the spacetime connection, say  $\omega$ , by some sort of "screened connection"  $\Theta_H \omega$ , and see what kind of quantities and physics will be so induced on the surface of the BH. However, Einstein's equations being nonlinear, one cannot simply use a BH step function  $\Theta_H$  as was done for BH electrodynamics. We shall therefore motivate the definition of suitable "surface quantities" related to  $\omega$  in a slightly different way and then study the evolution of these surface quantities and their connection to the physics outside the horizon, up to  $\infty$ . Our presentation will be sketchy; for technical details, see [9, 10, 19, 20].

Let us start by considering an axisymmetric spacetime. Then there exists a Killing vector  $\vec{m} = m^\mu \partial / \partial x^\mu = \partial / \partial \varphi$ , to which, by Noether's theorem, one

---

<sup>3</sup>Indeed, in CGS-Gaussian units (as used, say, in the treatise of Landau and Lifshitz)  $30 \text{ ohms}$  is equal to the velocity of light (or its inverse, depending on whether one uses esu or emu). Then, when using (as we do here) units where  $c = 1$ ,  $30\Omega = 1$ .

can associate a conserved total angular momentum, which can be written as a surface integral at  $\infty$ . The total angular momentum  $J_z$  w.r.t.  $\varphi$  reads

$$J_\infty = -\frac{1}{8\pi} \int_{S_\infty} \frac{1}{2} \nabla^\nu m^\mu dS_{\mu\nu}, \quad (2.59)$$

where  $dS_{\mu\nu} = \frac{1}{2} \varepsilon_{\mu\nu\rho\sigma} dx^\rho \wedge dx^\sigma$ ,  $\nabla^\nu$  denotes a covariant derivative, and the surface integral is performed over the 2-sphere,  $S_\infty$ . This starting point is the analog of the surface-integral expression for the total electric charge used above to motivate the definition of a BH surface charge distribution.

In a way similar to what was done in the electromagnetic case, we can use Gauss' theorem to rewrite this integral as the sum of two contributions: (i) a volume integral (over the 3-volume contained between the horizon and infinity) measuring the angular momentum of the matter present outside the horizon, and (ii) a surface integral over a (topological) 2-sphere  $S_H$  at the horizon, representing what we can call the BH angular momentum  $J_H$ , *i.e.*,

$$J = J_{\text{matter}} + J_H, \quad (2.60)$$

where  $J_H$  is given by the same surface-integral formula as  $J_\infty$ , except for the replacement of  $S_\infty$  by  $S_H$  as integration domain.

The horizon being tangent to the lightcone, one defines on the horizon, as above, a null vector  $\ell_\mu$  both normal and tangent to it.  $\ell_\mu$  can in turn be complemented by another null vector  $n_\mu$  such that  $\ell^\mu n_\mu = 1$  and such that the surface element  $dS_{\mu\nu}$  can then be re-expressed as  $(n_\mu \ell_\nu - n_\nu \ell_\mu) dA$ . Remembering that the Killing symmetry preserves the generators of the horizon *i.e.*, the commutator  $[\vec{\ell}, \vec{m}] = 0$ , one has  $\ell^\nu \nabla_\nu m^\mu = m^\nu \nabla_\nu \ell^\mu$ , so that we can re-express the BH angular momentum  $J_H$  as the following surface integral

$$J_H = -\frac{1}{8\pi} \int_{S_H} n_\mu m^\nu \nabla_\nu \ell^\mu dA. \quad (2.61)$$

This result involves the directional (covariant) derivative of the horizon *normal vector*  $\vec{\ell}$  along a vector  $\vec{m}$  which is *tangent* to the horizon. The crucial point now is to realize that, very generally, given any hypersurface, the parallel transport along some *tangent* direction, say  $\vec{t}$ , of the (normalized) vector  $\vec{\ell}$  normal to the hypersurface yields *another tangent vector*. The technical proof of this fact consists of starting from the fact that  $\vec{\ell} \cdot \vec{\ell} = \epsilon$ , where  $\epsilon$  is a *constant* which is equal to  $\pm 1$  in the case of a time-like or spacelike hypersurface, and to 0 in the case (of interest here) of a null hypersurface. Then, taking the directional gradient of this starting equality along an arbitrary tangent vector  $\vec{t}$  yields  $(\nabla_{\vec{t}} \vec{\ell}) \cdot \vec{\ell} = 0$ . From this result, one deduces that the vector  $(\nabla_{\vec{t}} \vec{\ell})$  must be *tangent* to the hypersurface. Therefore, there exists a certain linear map  $K$ , acting in the tangent plane

to the hypersurface, such that  $\nabla_{\vec{t}}\vec{\ell} = K(\vec{t})$ . For a usual (time-like or space-like) hypersurface, the linear map  $K$  is called the “Weingarten map” and is simply the mixed-component  $K_j^i$  version of the extrinsic curvature of the hypersurface (usually thought of as being a symmetric covariant tensor  $K_{ij}$ ). On the other hand, in the case of a null hypersurface, there is no unique way to define the analog of the covariant tensor  $K_{ij}$  (where the indices  $i, j$  are “tangent” to the hypersurface), but it is natural, and useful, to consider the mixed-component tensor  $K_j^i$ , intrinsically defined as the Weingarten map  $K$  in  $\nabla_{\vec{t}}\vec{\ell} = K(\vec{t})$ .

To explicitly write out the various components of the linear map  $K$  (acting on the hypersurface tangent plane), we need to define a basis of vectors tangent to the horizon. This basis contains the null vector  $\vec{\ell}$  (which is both normal and tangent to the horizon), and two spacelike vectors. Using a coordinate system  $x^0, x^1, x^A$  ( $A = 2, 3$ ) of the type already introduced (with the horizon being located at  $x^1 = 0$ ), we can choose, as two spacelike horizon tangent vectors, the vectors  $\vec{e}_A = \partial_A$ . Then one finds that the Weingarten map  $K$  is fully described by the set of equations

$$\begin{aligned}\nabla_{\vec{\ell}}\vec{\ell} &= g\vec{\ell}, \\ \nabla_A\vec{\ell} &= \Omega_A\vec{\ell} + D_A^B\vec{e}_B.\end{aligned}\tag{2.62}$$

The first equation follows from the fact that  $\vec{\ell}$  is tangent to a null geodesic lying within the null hypersurface. [In turn, this follows from the fact that  $\vec{\ell}$  is proportional to the gradient of some scalar, say  $\varphi$  (satisfying the eikonal equation  $(\nabla\varphi)^2 = 0$ ).] The coefficient  $g$  entering the first equation defines (in the most general manner) the *surface gravity* of the BH. We see that it represents one component of the Weingarten map  $K$ . The other components are the two-vector  $\Omega_A$ , and the mixed two-tensor  $D_A^B$ . One can show that the components  $D_A^B$  are the mixed components of a symmetric two-tensor  $D_{AB}$ , which measures the “deformation”, in time, of the geometry of the horizon. We remind the reader of the expression of the horizon metric, introduced above,  $ds^2|_H = \gamma_{AB}(t, \vec{x})(dx^A - v^A dt)(dx^B - v^B dt)$ . Here,  $\gamma_{AB}(t, \vec{x})$  is a symmetric rank 2 tensor *i.e.*, a time-dependent 2-metric such that the horizon may be viewed as a 2-dimensional brane. In addition, we have the generators, which are the vectors tangent to  $\vec{\ell}$ . When decomposing  $\vec{\ell} = \partial_t + v^A\partial_A$  w.r.t. our coordinate system, they appear to have a “velocity”  $v^A$  which can also be viewed as the velocity of a fluid particle on the horizon.  $D_{AB}$  is then defined as the deformation tensor of the horizon geometry, namely  $D_{AB} = \gamma_{BC}D_A^C = \frac{1}{2}\frac{D\gamma_{AB}}{dt}$ , where  $D/dt$  denotes

the *Lie derivative* along  $\vec{\ell} = \partial_t + v^A \partial_A$ . It is explicitly given by

$$\begin{aligned} D_{AB} &= \frac{1}{2} (\partial_t \gamma_{AB} + v^C \partial_C \gamma_{AB} + \partial_A v^C \gamma_{CB} + \partial_B v^C \gamma_{AC}) \\ &= \frac{1}{2} (\partial_t \gamma_{AB} + v_{A|B} + v_{B|A}) \end{aligned} \quad (2.63)$$

where ‘ $|$ ’ denotes a covariant derivative w.r.t. the Christoffel symbols of the 2-geometry  $\gamma_{AB}$ . Note the contribution from the ordinary time derivative of  $\gamma_{AB}$ , and that from the variation of the generators of velocity  $v^A$  along the horizon. It is then convenient to split the deformation tensor  $D_{AB}$  into a tracefree part and a trace, *i.e.*,  $D_{AB} = \sigma_{AB} + \frac{1}{2} \theta \gamma_{AB}$ , where the tracefree part  $\sigma_{AB}$  is the “shear tensor” and the trace,  $\theta = \bar{D}_A^A = \frac{1}{2} \gamma^{AB} \partial_t \gamma_{AB} + v_{|A}^A$ , the “expansion”. The remaining component of the Weingarten map, namely the 2-vector  $\Omega_A$ , is defined as  $\Omega_A = \vec{n} \cdot \nabla_A \vec{\ell}$  with  $\vec{\ell} \cdot \vec{n} = 1$ . Its physical meaning can be seen from looking at the BH angular momentum  $J_H$ .

Indeed, from the definition above of  $J_H$ , one finds that the total BH angular momentum is the projection of  $\Omega_A$  on the direction of the rotational Killing vector  $\vec{m} = \partial_\varphi$  introduced at the beginning of this section, so that we have

$$J_H = -\frac{1}{8\pi} \oint_S m^A \Omega_A dA, \quad (2.64)$$

where  $m^A \Omega_A$  is the  $\varphi$ -component of  $\Omega_A$ . It is therefore natural to define, for a BH, a “surface density of linear momentum” as  $\pi_A = -\frac{1}{8\pi} \Omega_A = -\frac{1}{8\pi} \vec{n} \cdot \nabla_A \vec{\ell}$ . With this definition, one has

$$J_H = \int_S \pi_\varphi dA, \quad (2.65)$$

which is similar to the result above giving the BH electric charge as the surface integral of the “charge surface density”  $\sigma_H$ .

Having so defined some (fictitious) “hydrodynamical” quantities on the surface of a BH (fluid velocity, linear momentum density, shear tensor, expansion rate, etc.), let us now see what evolution equations they satisfy as a consequence of Einstein’s equations. By contracting Einstein’s equations with the normal to the horizon, we can relate the quantities just defined to the flux of the energy-momentum tensor  $T_{\mu\nu}$  into the horizon. For instance, by projecting Einstein’s equations along  $\ell^\mu e_A^\nu$ , one finds

$$\frac{D\pi_A}{dt} = -\frac{\partial}{\partial x^A} \left( \frac{g}{8\pi} \right) + \frac{1}{8\pi} \sigma_{A|B}^B - \frac{1}{16\pi} \partial_A \theta - \ell^\mu T_{\mu A} \quad (2.66)$$

where

$$\begin{aligned}\frac{D\pi_A}{dt} &= (\partial_t + \theta)\pi_A + v^B\pi_{A|B} + v_{|A}^B\pi_B, \\ \sigma_{AB} &= \frac{1}{2}(\partial_t\gamma_{AB} + v_{A|B} + v_{B|A}) - \frac{1}{2}\theta\gamma_{AB}, \\ \theta &= \frac{\partial_t\sqrt{\gamma}}{\sqrt{\gamma}} + v_{|A}^A\end{aligned}\quad (2.67)$$

correspond to a convective derivative, a shear and an expansion rate respectively. Let us recall that the Navier-Stokes equation for a viscous fluid reads

$$(\partial_t + \theta)\pi_i + v^k\pi_{i,k} = -\frac{\partial}{\partial x^i}p + 2\eta\sigma_{i,k}^k + \zeta\theta_{,i} + f_i, \quad (2.68)$$

where  $\pi_i$  is the momentum density,  $p$  the pressure,  $\eta$  the shear viscosity,  $\sigma_{ij} = \frac{1}{2}(v_{i,j} + v_{j,i}) - \text{Trace}$ , the shear tensor,  $\zeta$  the bulk viscosity,  $\theta = v^i_{,i}$  the expansion rate, and  $f_i$  the external force density. The two equations are remarkably similar. This suggests that a BH can be viewed as a (non-relativistic<sup>4</sup>) brane with (positive<sup>5</sup>) surface pressure  $p = +\frac{g}{8\pi}$ , external force-density  $f_A = -\ell^\mu T_{\mu A}$  which corresponds to the flow of external linear momentum, surface shear viscosity  $\eta = +\frac{1}{16\pi}$ , and surface bulk viscosity  $\zeta = -\frac{1}{16\pi}$  (in units where  $G = 1$ ). Note, finally, that both the surface shear viscosity and the surface bulk viscosity apply to any type of deformed non-stationary BH.

#### 2.4. Irreversible thermodynamics of black holes

In previous sections, we have introduced some electrodynamic and fluid dynamical quantities associated to a kind of dissipative dynamics of BH horizons. In addition, following Bekenstein, we would like to endow a BH with a surface density of entropy equal to a dimensionless constant  $\hat{\alpha}$  (in units where  $\hbar = G = c = 1$ ). Any dissipative system verifying Ohm's law and the Navier-Stokes equation is also expected to satisfy corresponding thermodynamic dissipative equations, namely Joule's law and the usual expression of the viscous heat rate proportional to the sum of the squares of the shear tensor and of the expansion rate. More precisely, we would expect to have a "heat production rate" in each surface element  $dA$  of the form

$$\dot{q} = dA \left[ 2\eta\sigma_{AB}\sigma^{AB} + \zeta\theta^2 + \rho \left( \vec{\mathcal{K}} - \sigma_H\vec{v} \right)^2 \right], \quad (2.69)$$

<sup>4</sup>The non-relativistic character of the BH hydrodynamical-like equations may seem surprising in view of the "ultra-relativistic" nature of a BH. This non-relativistic-looking character is due to our use of an adapted "light-cone frame" ( $\ell, n, e_A$ ). It is well-known that light-cone-gauge results have a distinct "non-relativistic" flavour.

<sup>5</sup>This is consistent with the idea that the BH surface pressure must counteract the self-gravity.

where  $\rho$  is the surface resistivity, and  $\eta$  and  $\zeta$  the shear and bulk viscosities. In addition, one expects that this heat production rate should be associated with a corresponding local increase of the entropy  $s = \hat{\alpha}dA$  contained in any local surface element of the form

$$\frac{ds}{dt} = \frac{\dot{q}}{T}. \quad (2.70)$$

with a local temperature  $T$  expected to be equal to  $T = \frac{g}{8\pi\hat{\alpha}}$ .

Remarkably, the ‘‘scalar’’ ( $\ell^\mu\ell^\nu$ ) projection of Einstein’s equations, (i.e., the Raychaudhuri equation) yields an evolution law for the entropy  $s = \hat{\alpha}dA$  of a local surface element which is very analogous to what one would expect. Indeed, it yields

$$\frac{ds}{dt} - \tau \frac{d^2s}{dt^2} = \frac{dA}{T} \left[ 2\eta\sigma_{AB}\sigma^{AB} + \zeta\theta^2 + \rho \left( \vec{\mathcal{K}} - \sigma_H \vec{v} \right)^2 \right], \quad (2.71)$$

where  $T = \frac{g}{8\pi\hat{\alpha}}$ , where  $2\eta\sigma_{AB}\sigma^{AB} + \zeta\theta^2$  are exactly the expected viscous contributions, and where  $\rho \left( \vec{\mathcal{K}} - \sigma_H \vec{v} \right)^2$  is Joule’s law.

The only unexpected term in this result is the second term on the l.h.s.; this term goes beyond usual near-equilibrium thermodynamics (which involves only the first order time derivative of the entropy), and is proportional to the second time derivative of the entropy density and to a time scale  $\tau = \frac{1}{g}$ . It is interesting to note that, for the value  $\hat{\alpha} = 1/4$ , corresponding to the Bekenstein-Hawking entropy density,  $\tau$  is equal to  $\frac{1}{2\pi T}$ , i.e., the inverse of the lowest ‘‘Matsubara frequency’’ associated to the temperature  $T$  (one also notes that  $\tau = D = 2\mathcal{D}$ , where  $D$ ,  $\mathcal{D}$  are the diffusion constants of [14]). The minus sign in front of this new term is also a particularity of BH physics. In the approximation of a constant  $\tau$ , and in solving for the non-equilibrium second law of thermodynamics, one finds that the rate of increase of entropy is given by

$$\frac{ds}{dt} = \int_t^\infty \frac{dt'}{\tau} e^{-\frac{(t'-t)}{\tau}} \left( \frac{\dot{q}}{T} \right) (t'), \quad (2.72)$$

i.e., it is defined not as the value of the heat dissipated instantaneously, nor as an integral over the past heat dissipation, but as an integral over the *future*. This highlights the acausal nature of BHs, i.e., a BH is defined as a null hypersurface which *will become stationary in the far future*. As such, it has to anticipate any external perturbation. Failing this, the null hypersurface would generically tend either to collapse, or blow up toward  $\infty$ .

We also note that the ratio of the shear viscosity  $\eta = 1/(16\pi)$  to the entropy



density  $\hat{s} = s/dA = \hat{\alpha}$  is given by

$$\frac{\eta}{\hat{s}} = \frac{1}{\hat{\alpha}16\pi} = \frac{1}{4\pi} \quad (2.73)$$

where, in the second equality, we have used the Bekenstein-Hawking value for  $\hat{s} = s/dA = \hat{\alpha} = \frac{1}{4}$ . It is interesting to note that the result  $\frac{\eta}{\hat{s}} = \frac{1}{4\pi}$  is indeed the ratio found by Kovtun, Son and Starinets in the gravity duals of strongly coupled gauge theories [13, 14].

Finally, let us note another remarkable agreement between BH dissipative dynamics and a rather general property of ordinary (near-equilibrium) irreversible thermodynamics. This agreement concerns what Prigogine has called the “minimum entropy production principle”. Let us consider the total “dissipation function”

$$D = \oint_S \dot{q} \quad (2.74)$$

as a functional of the velocity field  $v^A(x^2, x^3)$  and of the electric potential  $\phi(x^2, x^3)$  in the presence of given external influences such as an external magnetic field or tidal forces acting on the rotating BH. Then,  $D[\phi]$  or  $D[v^A]$  (imposing  $v^A_{|A} = 0$  as a constraint), reach a *minimum* when (and only when) the lowest order (Einstein-Maxwell) dynamical equations for  $\phi$  or  $v^A$  are satisfied.

### 2.5. Hawking Radiation

In this section we discuss the phenomenon of Hawking radiation, first obtained in Ref. [17] (we shall follow here the derivation of Ref. [18]). For simplicity, we will consider a 3+1 dimensional spherically symmetric BH. We remind the reader that the coefficient  $A(r)$ , associated to the time coordinate (here denoted as  $T$ ), goes to zero on the horizon, so that the horizon is an *infinite redshift surface*. It is also a *Killing* horizon, i.e., the (suitably normalized) normal vector  $\vec{\ell} = \partial/\partial t + \Omega\partial/\partial\phi$  is a Killing vector. These points will be crucial in the following. Since the coefficient of the radial coordinate is defined by  $B(r) = \frac{1}{A(r)}$  (see Section 2.1), it is singular on the horizon. To get a good coordinate system on the horizon, we first factorize  $A(r)$ ,

$$\begin{aligned} ds^2 &= -A(r) dT^2 + \frac{dr^2}{A(r)} + r^2 d\Omega^2 \\ &= -A(r) \left( dT^2 - \left( \frac{dr}{A(r)} \right)^2 \right) + r^2 d\Omega^2, \end{aligned} \quad (2.75)$$

and then introduce a new radial coordinate, the so-called *tortoise* coordinate, defined by

$$r_* = \int \frac{dr}{A(r)}. \quad (2.76)$$

Note that as  $r \rightarrow r_+$ ,  $A(r) \simeq \left(\frac{\partial A}{\partial r}\right)_{r_+} (r - r_+)$ , where  $\left(\frac{\partial A}{\partial r}\right)_{r_+}$  is (as mentioned above) equal to twice the surface gravity  $g$ . This implies

$$\begin{aligned} r_* &\simeq \int \frac{dr}{(r - r_+) \left(\frac{\partial A}{\partial r}\right)_{r_+}} \\ &\simeq \frac{\ln(r - r_+)}{2g} \end{aligned} \quad (2.77)$$

such that as  $r \rightarrow +\infty$ ,  $r_* \simeq r + 2M \ln r$  and as  $r \rightarrow r_+$ ,  $r_* \simeq \frac{\ln(r - r_+)}{2g}$ . The line element can thus be re-written as

$$ds^2 = -A(dT - dr_*)(dT + dr_*) + r^2 d\Omega^2. \quad (2.78)$$

We now switch to the so-called *Eddington-Finkelstein* coordinates,  $(t, r, \theta, \varphi)$ , where the combination  $t = T + r_*$  of  $T$  and  $r_*$  remains regular across the (future) horizon<sup>6</sup> and define  $t = T + r_*$ . The time translation Killing vector  $\partial/\partial t$  coincides with the usual one  $\partial/\partial T$ . In terms of these new coordinates the metric reads

$$ds^2 = -A(r)dt^2 + 2dt dr + r^2 d\Omega^2. \quad (2.79)$$

This metric is now regular (with a non-vanishing determinant) as the radial coordinate  $r$  penetrates within the horizon, *i.e.*, becomes smaller than  $r_+$ .

Having defined a regular coordinate system, we now consider a massless scalar field, the dynamics of which is given by the massless Klein Gordon equation

$$0 = \square_g \varphi = \frac{1}{\sqrt{g}} \partial_\mu (\sqrt{g} g^{\mu\nu} \partial_\nu \varphi) \quad (2.80)$$

The solutions to this equation in a spherically symmetric and time-independent background are given by mode functions which are themselves given simply by products of a Fourier decomposition into frequencies, spherical harmonics and a radial dependence and thus read

$$\varphi_{\omega\ell m}(T, r, \theta, \varphi) = \frac{e^{-i\omega T}}{\sqrt{2\pi|\omega|}} \frac{u_{\omega\ell m}(r)}{r} Y_{\ell m}(\theta, \varphi). \quad (2.81)$$

<sup>6</sup>Given that the horizon is an infinite redshift surface, it takes an infinite time  $T$  to fall into it, while  $r_* \simeq \ln(r - r_+)/2g$  goes to  $-\infty$  at the horizon. The sum of the two remains, however, finite.

The problem is then reduced to solving a radial equation with the radial coordinate  $r_*$ ,

$$\frac{\partial^2 u}{\partial r_*^2} + [\omega^2 - V_\ell(r(r_*))] u = 0. \quad (2.82)$$

In the case of the Schwarzschild metric (*i.e.*, when  $A(r) = 1 - 2M/r$ ) the effective radial potential  $V_\ell(r)$  is given by

$$V_\ell(r) = \left(1 - \frac{2M}{r}\right) \left(\frac{\ell(\ell+1)}{r^2}\right). \quad (2.83)$$

An essential point to note is that the effective potential vanishes both at  $\infty$  (like a massless centrifugal potential  $\ell(\ell+1)/r^2$ ), and at the horizon (where it is proportional to  $A(r)$ ). Therefore, in these two regimes (which correspond to  $r_* \rightarrow \pm\infty$ ), the solution of the wave equation behaves essentially as in flat space (see FIG. 3). The effect of the coupling to curvature is non-negligible only in an intermediate region, where the combined effect of curvature and centrifugal effects yield a *positive* potential barrier. In turn, this potential barrier yields a *grey body factor* which diminishes the amplitude of the quantum modes considered below, *i.e.*, those generated near the horizon and which must penetrate through the potential barrier on their way towards  $\infty$ . Far from the potential barrier, the general solution for  $\varphi$  is

$$\varphi_{\omega\ell m} \sim \frac{e^{-i\omega(T \pm r_*)}}{\sqrt{2\pi|\omega|}} \frac{1}{r} Y_{\ell m}(\theta, \varphi). \quad (2.84)$$

The quantification of the scalar field  $\varphi$  is rather standard (and similar to what one does when studying the amplification of quantum fluctuations during cosmological inflation). The quantum operator for the scalar field is decomposed into mode functions, *i.e.*, the eigenfunctions of the Klein Gordon equation, with coefficients given by creation and annihilation operators. The subtlety lies, however, in the definition of positive and negative frequencies.

Let us start by formally considering the simpler case of a quantum scalar field  $\hat{\varphi}(x)$  in a background spacetime which becomes stationary *both* in the infinite past, and in the infinite future. In that case, one can define positive and negative frequencies in the usual way, in the two asymptotic regions  $t \rightarrow \pm\infty$ . The coefficient of the positive frequency modes, say  $p(x)$ , then defines an annihilation operator  $\hat{a}$ . However, there are two sorts of positive-frequency ( $p(x)$ ), and negative-frequency ( $n(x)$ ) modes. The *in* ones  $p_i^{in}, n_i^{in}$  (defined in the asymptotic region  $t \rightarrow -\infty$ , and then extended everywhere by solving the Klein-Gordon equation), and the *out* ones  $p_i^{out}, n_i^{out}$  (defined in the asymptotic region  $t \rightarrow +\infty$ ). The operator-valued coefficients of these modes define some corresponding *in*

and *out* annihilation or creation operators, so that we can write the field operator  $\hat{\varphi}(x)$  as (here  $i$  is a label that runs over a basis of modes)

$$\begin{aligned}\hat{\varphi}(x) &= \sum_i \hat{a}_i^{in} p_i^{in}(x) + (\hat{a}_i^{in})^\dagger n_i^{in}(x), \\ &= \sum_i \hat{a}_i^{out} p_i^{out}(x) + (\hat{a}_i^{out})^\dagger n_i^{out}(x).\end{aligned}\tag{2.85}$$

Here, the modes are normalized as  $(p_i, p_j) = \delta_{ij}$  and  $(n_i, n_j) = -\delta_{ij}$ , where  $(\cdot, \cdot)$  is the Klein-Gordon scalar product, i.e.,  $\sim i \int d\sigma^\mu (\varphi_1^* \partial_\mu \varphi_2 - \partial_\mu \varphi_1^* \varphi_2)$ . The operators  $a_i$  and  $a_j^\dagger$  are correspondingly normalized in the usual way as  $[a_i, a_j^\dagger] = \delta_{ij}$ . One defines both an *in vacuum*  $|in\rangle$  and an *out vacuum*  $|out\rangle$  as the states that are respectively annihilated by  $a_i^{in}$  or  $a_i^{out}$ . Then, the phenomenon of particle creation corresponds to the fact that the *out* vacuum differs from the *in* one. More quantitatively, the expectation value of the number of *out* particles, in the mode labelled by  $i$ , which will be observed when the quantum field is in the *in* vacuum state is given by

$$\begin{aligned}\langle N_i \rangle &= \langle in | (a_i^{out})^\dagger a_i^{out} | in \rangle \\ &= \sum_j |T_{ij}|^2\end{aligned}\tag{2.86}$$

where we have introduced the transition amplitude  $T_{ij} = (p_i^{out}, n_j^{in})$  from an initial negative frequency mode  $n_j^{in}$  into a final positive frequency one  $p_i^{out}$ . These transition amplitudes (also called Bogoliubov coefficients) enter the calculation because, as is easily deduced from the double expansion of the field  $\hat{\varphi}(x)$  above, they give the part of  $a_i^{out}$  which is proportional to  $(a_j^{in})^\dagger$ . The application of the previous general formalism to the BH case is delicate since a BH background is not asymptotically stationary in the infinite future (because of the BH interior where the Killing vector  $\partial/\partial t$  is spacelike), and is asymptotically stationary in the infinite past only if we do consider explicitly the collapse leading to the formation of a BH from an initially stationary star. However, Hawking showed how to essentially bypass these difficulties by focussing on two types of modes:

- The high-frequency modes coming from the infinite past, which reach the horizon with practically no changes (because of their high-frequency nature) and,
- the outgoing modes, viewed in the asymptotically flat region and in the far future.

Concerning the outgoing modes, they can be unambiguously decomposed in positive- and negative-frequency parts, because, as explained above, their asymptotic behaviour is given by a sum of essentially flat-spacetime modes, (2.84). One

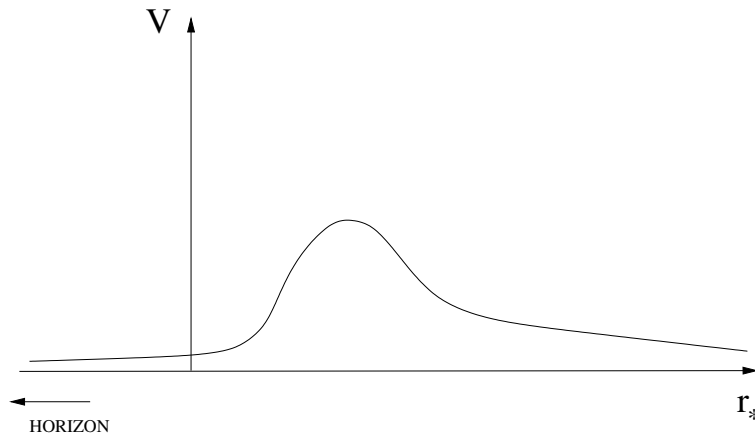


Figure 3. This figure is a schematic representation of the effective gravitational potential in the neighborhood of a BH. Note that as far as the particles are concerned, the spacetime is essentially flat both at infinity and near the horizon. The tidal-centrifugal barrier that separates the horizon from infinity gives rise to the grey body factor.

then defines the outgoing  $p_i^{out}$ 's as being proportional to  $e^{-i\omega(T-r_*)}$  with a *positive*  $\omega$ .

Let us now focus on the definition of positive- and negative-frequency modes near the horizon. We recall that, as mentioned at the beginning of this section, there is a physically infinite redshift between the surface of the horizon and asymptotically flat space at infinity. If one is interested in particle creation with a finite given frequency, as observed at infinity, the corresponding wave packets will have very high frequency near the horizon and can therefore be approximated by very localized wave packets. Given that the spacetime geometry in the vicinity of the horizon is regular, with a finite radius of curvature, it can be regarded as a piece of flat spacetime locally if one looks in a small enough region. In this approximation, the calculation can be performed in a single step.

We wish to compute the average number of final outgoing particles<sup>7</sup> seen in the *in* vacuum. Then the average number of outgoing particles of type  $p_i^{out}$  is

<sup>7</sup>Note that the “out” label, in the general discussion of particle creation above, referred to “final” particles (as defined in the final, asymptotic, stationary spacetime background). In the case of a BH background, the “final” spacetime is made of two separate asymptotic regions: (i) the outgoing wave region at spatial infinity, and (ii) the vicinity of the (spacelike?) singularity within the BH. The definition of positive- and negative-frequency modes in the latter region is ill-defined. However, luckily, the calculation of the physically relevant flux of final, outgoing modes can be performed without worrying about the physics near the BH interior singularity. In other words, it is enough to consider as “out” positive-frequency modes  $p_i^{out}$  only the ones outgoing at spatial infinity (*i.e.*, on “scri<sup>+</sup>”), though they do not constitute a complete basis of final modes.

given by  $\sum_j |T_{ij}|^2$ , where  $T_{ij} = (p_i^{out}, n_j^{in})$  is the transition amplitude from an initial negative frequency mode  $n_j^{in}$  into a final *outgoing* positive frequency one  $p_i^{out}$  (recorded at spatial infinity). To compute this transition amplitude, we need to describe what is an initial negative frequency mode  $n_j^{in}$ . As said above, Hawking suggested that only high-frequency initial modes are important, and that they essentially look the same (some kind of WKB wave) in the real *in* region (in the far past, before the formation of the BH) as in the vicinity of the horizon. Our technical problem is then reduced to characterizing what is a negative frequency mode  $n_j^{in}$  as seen in a small neighborhood of the horizon, which looks like the Minkowski vacuum.

To do this, it is convenient to have a technical criterion for characterizing positive and negative frequency modes in (a local) Minkowski spacetime. Locally, one can perform a Fourier decomposition of the wave packet and use the mathematical fact that the Fourier space properties are mapped onto analytic continuation properties in  $x$ -space. This relation can then be used to define positive and negative frequency modes. This is easy to see. Consider a general *negative frequency* wave packet in Minkowski spacetime. It has the form  $\varphi_-(x) = \int_{C^-} d^4k \tilde{\varphi}(k) e^{ik_\mu x^\mu}$  where  $k_\mu$  is *timelike-or-null* and *past-directed*, i.e.,  $k^\mu \in C^-$ . We now perform a complex shift of the spacetime coordinate,  $x_\mu \rightarrow x^\mu + iy^\mu$ , where  $y^\mu$  is *timelike-or-null* and *future-directed* (i.e.,  $y^\mu \in C^+$ ), then, the  $e^{ik_\mu x^\mu}$  term will be suppressed by a  $e^{-k_\mu y^\mu}$  term, where the scalar product  $k_\mu y^\mu$  is *positive* because it involves two timelike vectors that point in opposite directions (we use the “mostly plus” signature). This ensures that a negative-frequency wavepacket can indeed be analytically continued to complex spacetime points of the form  $x^\mu + iy^\mu$ , with  $y^\mu \in C^+$ .

The strategy for applying this criterion to characterizing negative-frequency modes  $n_j^{in}$  in the vicinity of the horizon is then the following. One starts from a wavepacket which is not purely a “negative-frequency” one near the horizon, but which has the property of evolving into an *outgoing* positive-frequency wave packet (so that it will have a non-zero transition amplitude to some  $p_i^{out}$ ). Then, one modifies the initial wavepacket so that it becomes a purely negative-frequency mode  $n_j^{in}$  near the horizon.

When looking at a wavepacket of the form of  $\varphi_\omega^{out}(t, r) \propto e^{-i\omega(T-r_*)}$  (with positive  $\omega$ ) just outside the horizon, one must first switch to well-defined coordinates to examine its physical content. We therefore replace the Schwarzschild-type time coordinate  $T$  by the Eddington-Finkelstein time coordinate,  $t = T + r_*$  which is regular on the horizon. After rearranging terms according to  $T - r_* =$

$(T + r_*) - 2r_*$  the previous (outgoing, positive-frequency) wave reads

$$\begin{aligned} [\varphi_\omega^{\text{out}}(t, r)]_{r_+} \propto e^{-i\omega(T-r_*)} &= e^{-i\omega t} e^{2i\omega r_*} \\ &= e^{-i\omega t} e^{i\frac{\omega}{g} \ln(r-r_+)} \\ &= e^{-i\omega t} (r - r_+)^{\frac{i\omega}{g}}. \end{aligned} \quad (2.87)$$

This describes the behaviour, just outside the horizon, of a wavepacket which will become (modulo some grey-body factor) an outgoing positive frequency wavepacket at  $\infty$ . However, locally on the horizon, it is neither a positive nor a negative frequency wavepacket because, at this stage, it is defined only outside the horizon, but not inside. Let us now show how one must continue this wavepacket inside the horizon, so that it becomes a genuine negative-frequency wavepacket “straddling” the horizon. Using the criterion explained above, we can “continue” the wavepacket inside the horizon by a suitable *analytic continuation*. More precisely, we need an analytic continuation of the form  $x^\mu \rightarrow x^\mu + iy^\mu$ , where  $y^\mu$  belongs to the future lightcone to ensure that we shall then be dealing with a local negative frequency wavepacket. It is easy to see, from a spacetime diagram of the lightcone on the horizon, that the vector  $\partial/\partial r$  is everywhere null and past-directed, such that  $r \rightarrow r - \varepsilon$ , where  $\varepsilon > 0$ , is everywhere null and future directed. The analytic continuation of  $\varphi_\omega^{\text{out}}(t, r)$  to  $r \rightarrow r - i\varepsilon$  will therefore define for us a good local negative-frequency mode  $n_j^{\text{in}} = n_{\omega\ell m}^{\text{in}}$ . One easily sees that this analytic continuation in  $r$  generates a new component to the wavepacket which is located inside the BH (i.e., for  $r < r_+$ ). More precisely, a one line calculation yields

$$\begin{aligned} n_{\omega\ell m}^{\text{in}}(r, t) &= N_\omega \varphi_\omega^{\text{out}}(t, r - i\varepsilon) \\ &= N_\omega \left[ \theta(r - r_+) \varphi_\omega^{\text{out}}(r - r_+) + \right. \\ &\quad \left. e^{\frac{\pi\omega}{g}} \theta(r_+ - r) \varphi_\omega^{\text{out}}(r_+ - r) \right], \end{aligned} \quad (2.88)$$

where the second term is the wavefunction inside the horizon that has acquired an additional exponential factor due to the rotation  $e^{-i\pi}$  in the complex plane from  $r > r_+$  to  $r < r_+$ . The overall factor  $N_\omega$  is a normalization factor (needed because we have extended the mode inside the BH), such that

$$\langle n_{\omega\ell m}^{\text{in}}(r, t) n_{\omega'\ell'm'}^{\text{in}}(r, t) \rangle = \delta(\omega - \omega') \delta_{\ell\ell'} \delta_{mm'}, \quad (2.89)$$

from which we obtain (when remembering that  $\varphi_\omega^{\text{out}}$  was correctly normalized)

$$|N_{\omega\ell m}|^2 = \frac{1}{e^{2\pi\omega/g} - 1}. \quad (2.90)$$

The physical meaning of equation (2.88) is the description of the splitting of the in mode  $n_j^{in} = n_{\omega\ell m}^{in}$  into a positive-frequency wave outgoing from the horizon and a wave falling from the horizon towards the singularity. One can read off from it the needed transition amplitude  $T_{ij} = (p_i^{out}, n_j^{in})$ . It is essentially given by the factor  $N_\omega$ , which must, however, be corrected by a grey-body factor  $\sqrt{\Gamma_\ell(\omega)}$  taking into account the attenuation of the outgoing wave  $e^{-i\omega(T-r_*)}$  as it crosses the curvature + centrifugal potential barrier  $V_\ell(r)$  on its way from the horizon to  $\infty$ . Then (using Fermi's golden rule), one easily finds that the general result (2.86) yields a rate of particle creation given by

$$\frac{d\langle N \rangle}{dt} = \sum_{\ell, m} \int \frac{d\omega}{2\pi} \frac{\Gamma_\ell(\omega)}{e^{\frac{2\pi\omega}{g}} - 1}. \quad (2.91)$$

One recognizes here a thermal (Planck) spectrum (corrected by a grey-body factor). From the Planck factor, one reads off the Hawking temperature,  $T = \hbar \frac{g}{2\pi}$ . This result fixes the dimensionless coefficient  $\hat{\alpha}$  in the Bekenstein entropy to the famous result  $\hat{\alpha} = \frac{1}{4}$ , *i.e.*,

$$S_{BH} = \frac{A}{4G\hbar}. \quad (2.92)$$

Let us end by two final comments. First, the generalisation of the Hawking radiation to a more general rotating and/or charged BH is given essentially by replacing in the result above the frequency  $\omega$  by  $\omega - \omega_0$  where  $\omega_0 = m\Omega + eV$  exhibits the couplings of the created particles to the angular velocity  $\Omega$  and the electric potential  $V$  of the BH. Then, in astrophysically realistic conditions, the ‘‘Hawking’’ part of the particle creation (*i.e.*, the thermal aspect) is too small to be relevant, while the combined effect of the grey body factor and of the zero-temperature limit of  $(e^{\frac{2\pi(\omega-\omega_0)}{g}} - 1)^{-1}$  yield potentially relevant particle creation phenomena in Kerr-Newman BHs, associated to the ‘‘superradiance’’ of modes with frequencies  $\mu < \omega < \omega_0$ , where  $\mu$  is the mass of the created particle (see, *e.g.*, [18] for more details and references). We conclude by noting that the situation just described is not only technically similar to the one in the inflationary scenario for cosmological perturbations, but also physically similar in that, in both cases, *transplanckian frequency modes* in the ultraviolet are redshifted to a finite, observable frequency.

### 3. Experimental tests of gravity

Before discussing various possibilities of string-inspired phenomenology (and of possible string-inspired deviations from Einstein's theory of General Relativity) we give an overview of what is known experimentally about the gravitational sector.



### 3.1. Universal coupling of matter to gravity

The standard model of gravity is Einstein's General Relativity (GR). In GR, all fields of the standard model of particle physics (SM) are universally coupled to gravity by replacing the flat spacetime metric  $\eta_{\mu\nu}$  by a curved spacetime one  $g_{\mu\nu}$ . In "standard GR" one also assumes that gravity is the only long range coupling (apart from electromagnetism). We shall see below, how the presence of other long range interactions (coupled to bulk matter) modify the usual "pure GR" phenomenology. The action for the matter sector,  $S_{SM}$ , has the structure

$$S_{SM} = \int d^4x \left[ -\frac{1}{4} \sum \sqrt{g} g^{\mu\alpha} g^{\nu\beta} F_{\mu\nu}^a F_{\alpha\beta}^a - \sum \sqrt{g} \bar{\psi} \gamma^\mu D_\mu \psi - \frac{1}{2} \sqrt{g} g^{\mu\nu} \overline{D_\mu H} D_\nu H - \sqrt{g} V(H) - \sum \lambda \sqrt{g} \bar{\psi} H \psi - \sqrt{g} \rho_{\text{vac}} \right], \quad (3.1)$$

where  $D$  denotes a (gauge and gravity) covariant derivative, while the dynamics of  $g_{\mu\nu}$  is described by the Einstein-Hilbert action,  $S_{EH}$ ,

$$S_{EH} = \int d^4x \frac{c^4}{16\pi G} \sqrt{g} g^{\mu\nu} R_{\mu\nu}(g). \quad (3.2)$$

The total action is therefore given by

$$S = S_{EH}[g_{\mu\nu}] + S_{SM}[\psi, A_\mu, H; g_{\mu\nu}], \quad (3.3)$$

and its variation w.r.t.  $g_{\mu\nu}$  yields the well-known Einstein field equations

$$R_{\mu\nu} - \frac{1}{2} R g_{\mu\nu} = \frac{8\pi G}{c^4} T_{\mu\nu} \quad (3.4)$$

where  $T^{\mu\nu} = \frac{2}{\sqrt{g}} \frac{\delta \mathcal{L}_{SM}}{\delta g_{\mu\nu}}$ . The universal coupling of any type of particle to  $g_{\mu\nu}$  is made manifest in  $S_{SM}$  while  $S_{EH}$  contains all the information on the propagation of gravity. For instance, expanding  $S_{EH}$  in powers of  $h_{\mu\nu}$  (where  $g_{\mu\nu} \equiv \eta_{\mu\nu} + h_{\mu\nu}$ ), one obtains, at quadratic order in  $h_{\mu\nu}$ , the spin-two Pauli-Fierz Lagrangian. Higher orders in  $h_{\mu\nu}$  contain an infinite series of nonlinear self-couplings of gravity:  $\partial\partial h h h h$ ,  $\partial\partial h h h h h$ , etc. As we shall see, this nonlinear structure has been verified experimentally to high accuracy (both in the weak-field regime, where the cubic vertex  $\partial\partial h h h$  has been checked, and in the strong-field regime of binary pulsars, where the fully nonlinear GR dynamics has been confirmed). In the following, we discuss, successively, (i) the experimental tests of the coupling of matter to gravity, and (ii) the tests of the dynamics of the gravitational field: kinetic terms (describing the propagation of gravity), and cubic and higher gravitational vertices.

The universal nature of matter’s coupling to gravity, *i.e.*, the coupling of matter to a universal deformation of spacetime, has many experimental consequences. These experimental consequences can be derived by using a simple theorem by Fermi and Cartan. Given any pseudo-Riemannian manifold, for instance a curved spacetime endowed with a metric  $g_{\mu\nu}$ , and given any worldline  $\mathcal{L}$  in this spacetime (not assumed to be a geodesic), there always exists a coordinate system such that, all along  $\mathcal{L}$ ,  $g_{\mu\nu}(x^\lambda) = \eta_{\mu\nu} + \mathcal{O}(\vec{x}^2)$ , where  $\vec{x}$  denotes the *spatial* deviation away from the central worldline  $\mathcal{L}$ . It is important to note that there is no linear term in  $\vec{x}$ , but only  $\vec{x}^2$  effects, *i.e.*, tidal effects. There exists a very simple and intuitive demonstration of this Fermi-Cartan theorem. Let us view the curved manifold as being some “brane” embedded within a *flat* ambient auxiliary manifold. For instance, consider an ordinary 2-surface  $\Sigma$  within a three-dimensional flat euclidean space. Given any (smooth) curve  $\mathcal{L}$  traced on  $\Sigma$ , we can take a flat sheet of paper and progressively “apply” (or “fit”) this sheet on  $\Sigma$  along the curve  $\mathcal{L}$ . The orthogonal projection of  $\Sigma$  onto this applied flat sheet defines a map from  $\Sigma$  to a coordinatized flat manifold which has the property enunciated above. Note that, in this “development” of the neighbourhood of  $\mathcal{L}$  within  $\Sigma$  onto a flat sheet, the shape (as seen on the flat sheet) of the “developped” curve  $\mathcal{L}$  is generically not a straight line. It is only when  $\mathcal{L}$  was a *geodesic* line on  $\Sigma$ , that its development will be a straight line. This proof, and its consequences, are valid in any dimension and signature.

Here, we have in mind applying this result to the “center of mass” worldline  $\mathcal{L}$  of an arbitrary body moving in a background spacetime, or more generally of any sufficiently small laboratory (containing several bodies, between which we can neglect gravitational effects). We assume that we can neglect the backreaction of the body (or bodies) on the spacetime. In the approximation where we can neglect the tidal effects (linked to the  $\mathcal{O}(\vec{x}^2)$  terms in  $g_{\mu\nu}$  in Fermi coordinates), we can consider that we have a body, or a small lab, moving in a flat spacetime. In other words, the theorem of Fermi and Cartan tells us that we can essentially “efface” (modulo small, controllable tidal effects) the background gravitational field  $g_{\mu\nu}$  all along the history of a small lab, or a body. This “effacement property” is telling us, for instance, that the physical properties we can measure in a small lab will be independent of where the lab is, and when the measurements are made. In particular, all the (dimensionless) coupling constants<sup>8</sup> that enter the interpretation of local experiments (such as various mass ratios, the fine-structure constant, etc.) must be independent of where and when they are (locally) measured (*constancy of the constants*). A second consequence of this effacement property is that local physics should be Lorentz  $SO(3,1)$  invariant, because this is a symmetry of

---

<sup>8</sup>We assume here that the cutoff length scale  $\epsilon = 1/\Lambda$  of any low-energy effective QFT description of the physics in a small lab is fixed, when measured in units of  $ds = \sqrt{g_{\mu\nu} dx^\mu dx^\nu}$ .

the (approximate) flat spacetime appearing after one has effaced the tidal effects (*local Lorentz invariance*).

Moreover, in absence of coupling to other long-range fields (such as electromagnetism for a charged body), the center of mass of an isolated body (viewed as moving in a flat spacetime) must follow a straight worldline (principle of inertia). We therefore conclude (by the theorem above) that  $\mathcal{L}$  has to be a geodesic in the original curved spacetime. This is true independently of the internal properties of the object. One may thus conclude that isolated neutral bodies fall along geodesics independently of the internal properties of the object, since at no point in the demonstration had we to rely on any internal properties of the object. This is therefore a proof of the *weak equivalence principle*, *i.e.*, all bodies in a gravitational field fall with the same acceleration. Note, once again, that the absence of other long range fields besides  $g_{\mu\nu}$  that could influence the object considered is crucial.

Finally, another universality property, that of the gravitational redshift, may be shown by a comparison of the GR formulation with the Newtonian one. In lowest order approximation, the deviation of the  $g_{00}$  component of the metric from  $\eta_{00} = -1$  is twice the Newtonian potential  $U(x)$ . Indeed, comparing the action for a geodesic,

$$S_E = -m \int dt \sqrt{-g_{\mu\nu} \dot{x}^\mu \dot{x}^\nu} \quad (3.5)$$

with

$$S_{\text{Newton}} = \int dt \left[ \frac{1}{2} m \dot{x}^2 + mU(x) \right], \quad (3.6)$$

one finds  $g_{00} = -1 + \frac{2}{c^2} U(x) + \mathcal{O}\left(\frac{1}{c^4}\right)$  where  $U = \sum_a \frac{Gm_a}{|\vec{x} - \vec{x}_a|}$ .

Experimentally, one may transfer electromagnetic signals from one clock to another identical clock located in a gravitational field. If we are in a stationary situation (*i.e.*, if there exists a coordinate system w.r.t. which the physics is independent of time  $x^0 = ct$ ), the time translation invariance of the background shows that electromagnetic signals will take a *constant coordinate time* to propagate from clock 1 to clock 2. We can then use the link  $d\tau_i = \sqrt{-g_{00}(\vec{x}_i)} dt_i$  between the proper time (at the location of clock  $i$  ( $i = 1, 2$ )) and the corresponding coordinate time, as well as the (approximate) result above for  $g_{00}$ . Finally, we conclude that two identically constructed clocks located at two different positions in a static external Newtonian potential exhibit, when intercompared by electromagnetic signals, the (apparent) difference in clock rate

$$\frac{\tau_1}{\tau_2} = \frac{\nu_2}{\nu_1} = 1 + \frac{1}{c^2} [U(\vec{x}_1) - U(\vec{x}_2)] + \mathcal{O}\left(\frac{1}{c^4}\right). \quad (3.7)$$

This gravitational redshift effect is proportional to the difference in the Newtonian potential between the two locations, independently of the constitution of the clocks (say Hydrogen maser, or Cesium clock, etc.). This is a property known as the *universality of the gravitational redshift*.

The various consequences, discussed above, of the universal character of the coupling of matter to gravity are usually summarized under the generic name of *equivalence principle*. In the next section, we discuss the experimental tests of the equivalence principle and their accuracy.

### 3.2. Experimental tests of the coupling of matter to gravity

#### 3.2.1. How constant are the constants?

The best tests of the ‘‘constancy of the constants’’ concern the fine structure constant  $\alpha = e^2/\hbar c \simeq 1/137.037$ , and the ratio of the electron mass to that of the proton  $\frac{m_e}{m_p}$  (see Ref. [21] for a review). There exist several types of tests, based, for instance, on geological data (e.g., measurements made on the nuclear decay products of old meteorites), or on measurements (of astronomical origin) of the fine structure of absorption and emission spectra of distant atoms, as, e.g., the absorption lines of atoms on the line-of-sight of quasars at high redshift. Such kinds of tests all depend on the value of  $\alpha$ . There exist, in addition, several laboratory tests such as, for example, comparisons made between several different high-stability clocks. However, the best measurement of the constancy of  $\alpha$  to date is the Oklo phenomenon<sup>9</sup>. It sets the following (conservative) limits on the variation of  $\alpha$  over a period of two billion years [22–24]

$$-0.9 \times 10^{-7} < \frac{\alpha^{\text{Oklo}} - \alpha^{\text{today}}}{\alpha^{\text{today}}} < 1.2 \times 10^{-7}. \quad (3.8)$$

Converting this result into an average time variation, one finds

$$-6.7 \times 10^{-17} \text{ yr}^{-1} < \frac{\dot{\alpha}}{\alpha} < 5 \times 10^{-17} \text{ yr}^{-1}. \quad (3.9)$$

---

<sup>9</sup> The Oklo phenomenon was discovered by scientists at the *Commissariat à l'énergie atomique* (CEA) in France. A study of the uranium ore in a Gabonese mine revealed an unusual depletion in  $U^{235}$  (used in fission reactors) w.r.t. the usual proportion. Uranium ore is a mix of two isotopes, with, in usual samples, 99.28%  $U^{238}$  and 0.72%  $U^{235}$ . By contrast, the Oklo ore had only  $\ll 0.72\%$  of  $U^{235}$ . It was realized that a natural fission process took place, prompted by the presence of ground water, in Oklo some two billion years ago, and lasted for about two million years. Scientists analysed in detail the 2 billion year-old fission decay products. One can then infer from these measurements the scattering cross-sections of slow neutrons on various isotopes. Then, modulo some further assumptions about the dependence of various nuclear quantities on  $\alpha$ , one could constrain the variation of  $\alpha$  between the time of the fission reaction (roughly two billion years ago) and now. For details about the analysis and interpretation of Oklo data see [22] and references therein.

Note that this variation is a factor of  $\sim 10^7$  smaller than the Hubble scale, which is itself  $\sim 10^{-10} \text{ yr}^{-1}$ . Comparably stringent limits were obtained using the Rhenium 187 to Osmium 187 ratio in meteorites [25] yielding an upper bound  $\frac{\Delta\alpha}{\alpha} = (8 \pm 8) \times 10^{-7}$  over  $4.6 \times 10^9$  years. Laboratory limits were also obtained from the comparison, over time, of stable atomic clocks. More precisely, given that  $\frac{v}{c} \sim \alpha$  for electrons in the first Bohr orbit, direct measurements of the variation of  $\alpha$  over time can be made by comparing the frequencies of atomic clocks that rely on different atomic transitions. The upper bound on the variation of  $\alpha$  using such methods is  $\frac{\dot{\alpha}}{\alpha} = (-0.9 \pm 2.9) \times 10^{-15} \text{ yr}^{-1}$  [26]. It should be mentioned that a few years ago claims were made concerning observational evidence of non-zero time variations of  $\alpha$  and  $\frac{m_e}{m_p}$  from analyses of some astronomical spectra (see Ref. [21]). Other recent astronomical data indicate no variability of these constants (see Ref. [21] and the chapter 18 of the Review of Particle Physics<sup>10</sup> for references).

### 3.2.2. Tests of local Lorentz invariance

We should first mention that the Michelson-Morley experiment<sup>11</sup> has been repeated (with high accuracy) and strong limits have been obtained on a possible anisotropy of the propagation of light. In its modern realizations (Brillet and Hall, 1979), it has been performed with laser technology on rotating platforms. This experiment is now viewed as a test of the isotropy of space on the moving Earth, and thereby as a test of local Lorentz invariance. There also exists another idea for testing the isotropy of space, and although its interpretation is not totally clear, it is a conceptually interesting idea. This is why we choose to outline it in these lectures.

For simplicity, consider the hydrogen atom. Assuming the isotropy of space, *i.e.*, the existence of a SO(3) symmetry, we know that there should exist a degeneracy in the energy levels, given by the magnetic quantum number  $m$ . However, it is interesting to understand how the SO(3) symmetry comes about dynamically (and therefore, how it might be dynamically violated). The Hamiltonian for the electron is given by

$$\hat{H} = -\frac{\hbar^2}{2m} \Delta - \frac{e^2}{r} \quad (3.10)$$

where the first term is the kinetic term ( $\Delta$  being the Laplacian), and the second term is the Coulomb potential. Note that in fact,  $\Delta = \delta^{ij} \partial_{ij}$  and  $r^2 = \delta_{ij} x^i x^j$ , such that both terms depend on the same spatial structure  $\delta_{ij}$ , the flat metric,

<sup>10</sup>Available on <http://pdg.lbl.gov/>

<sup>11</sup>First performed as part of a series of experiments, beginning in Potsdam in 1881 (by Michelson alone) and then in the US until 1887 (by both Michelson and Morley) to test the existence of the *aether*.

thereby ensuring the SO(3) symmetry. However, both terms also come from an underlying field theoretic formulation: (i) the non-relativistic electron kinetic energy term  $\propto \Delta = \delta^{ij} \partial_{ij}$  comes from the kinetic term in the Dirac action,  $\bar{\psi} \gamma^\mu \partial_\mu \psi - m \bar{\psi} \psi$ , with  $\{\gamma^\mu, \gamma^\nu\} = \eta_{\mu\nu}$ , while (ii) the  $e^2/r$  term is the static Green's function of the electromagnetic field, which comes from inverting the kinetic term of the photon  $\eta^{\alpha\mu} \eta^{\beta\nu} F_{\alpha\beta} F_{\mu\nu}$ , which manifestly depends, by assumption, on the same spacetime metric  $\eta_{\mu\nu}$ . Einstein assumed that, in order to take into account the coupling to gravity, it was sufficient to replace  $\eta_{\mu\nu}$  by the same  $g_{\mu\nu}$  both for the electron and the photon. By contrast, let us consider the possibility that electrons (“matter”) and photons (“electromagnetism”) have a different coupling to gravity, e.g., described by saying that they couple to two different (spatial) metrics, say

$$\begin{aligned} g_{ij}^{\text{matter}} &= \delta_{ij} \\ g_{ij}^{\text{em}} &= \delta_{ij} + h_{ij}, \end{aligned} \quad (3.11)$$

Then, computing the new propagators for the electron and the photon in their respective metrics, one finds that the SO(3) symmetry would be violated by tensor terms, appearing in the Hamiltonian, of the form  $\delta H \sim \frac{e^2}{2} h_{ij} \frac{x^i x^j}{r^3}$ . This is a violation, at a deep level, of the universality discussed in the previous section. The usual SO(3) symmetry implies that all energy levels with magnetic quantum number  $m$  are degenerate. But if tensor terms violating SO(3) were to exist, then, observable effects would include potentially measurable quadrupole-type splittings in the energy levels, which, applied to the atomic nucleus (whose energy levels are a more sensitive probe of anisotropy), are  $\propto \langle I M | \hat{Q}_{ij} | I M \rangle$ , where  $I$  and  $M$  are the nuclear spin quantum numbers, and where  $\hat{Q}_{ij}$  is a symmetric tracefree tensor operator that couples to the tracefree part of  $h_{ij}$ . Such types of measurements have been performed on the energy levels of nuclei with impressively high accuracy, the current upper bound being

$$\left| h_{ij} - \frac{h_{kk}}{3} \delta_{ij} \right| \leq 10^{-27}. \quad (3.12)$$

The universality of space is thus valid to one part in  $10^{27}$ , showing how delicate Einstein's postulate is.

### 3.2.3. Universality of free fall

The most recent limits on the deviation from the universality of free fall have been obtained by Eric's Adelberger's group [27]. In particular, they compared the acceleration of a Beryllium mass and a Copper one in the Earth's gravitational field and found

$$\left( \frac{\Delta a}{a} \right)_{\text{Be-Cu}} = (-1.9 \pm 2.5) \times 10^{-12}, \quad (3.13)$$

where  $\Delta a = a_{\text{Be}} - a_{\text{Cu}}$ . Other limits exist, such as, for instance, the fractional difference in acceleration of earth-core-like ( $\sim$  iron) and moon-mantle-like (silica) bodies,

$$\left(\frac{\Delta a}{a}\right)_{\text{Earth-core-Moon-mantle}} = (3.6 \pm 5.0) \times 10^{-13}. \quad (3.14)$$

There are also excellent limits concerning celestial bodies. In particular the possible difference in the accelerations of the Earth and the Moon towards the Sun have been measured using laser ranging (with 5 mm accuracy) with retro-reflectors (corner cubes) placed on the Moon, giving the result [28]

$$\left(\frac{\Delta a}{a}\right)_{\text{Earth-Moon}} = (-1.0 \pm 1.4) \times 10^{-13}. \quad (3.15)$$

One should, however, remember that only a fraction ( $\sim 1/3$ ) of the Earth mass is made of iron, while the rest is mostly silica (which is the main material the Moon is made of). As, independently of the equivalence principle, silica must fall like silica, one loses a factor 3, so that the resulting bound on a possible violation of the equivalence principle is only around the  $5 \times 10^{-13}$  level, which is comparable to laboratory bounds.

#### 3.2.4. Universality of the gravitational redshift

We conclude the section on the tests of the coupling of matter to gravity by just mentioning that the universality of the gravitational redshift, namely the apparent change in the frequencies of two similar clocks in a gravitational field, has been tested by comparing the frequencies of hydrogen masers at the Earth surface and in a rocket. Vessot and Levine (1979) in Ref. [29] verified that the fractional change in the measured frequencies is consistent with GR to the  $10^{-4}$  level:

$$\frac{\Delta\nu}{\nu} = (1 \pm 10^{-4}) \frac{\Delta U}{c^2}. \quad (3.16)$$

The universality of this redshift has also been verified by measurements involving other types of clocks.

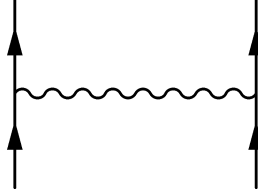
### 3.3. Tests of the dynamics of the gravitational field

#### 3.3.1. Brief review of the theoretical background

Until now we have only considered the coupling between matter and gravity, and various tests of its universality. We now discuss the tests of the *dynamics of the gravitational field*, i.e., tests probing either the propagator of the gravitational field, or the cubic or higher order gravitational vertices (for more detailed reviews

see Refs. [30, 31]). We first consider the weak field regime, regime in which we can write  $g_{\mu\nu} = \eta_{\mu\nu} + h_{\mu\nu}$ , where  $h_{\mu\nu}$  is numerically much smaller than one. For instance, in the solar system,  $h_{\mu\nu} \sim 10^{-6}$  on the surface of the Sun,  $\sim 10^{-8}$  on the Earth orbit around the Sun, or  $\sim 10^{-9}$  on the Earth surface. With values so small, it is clear that the solar system will not allow one to test many nonlinear terms in the perturbative expansion of  $g_{\mu\nu}$ .

We start by considering the gravitational interaction between two particles of masses  $m_A$  and  $m_B$ . At linear order in  $h_{\mu\nu}$ , we will have an interaction corresponding to the following (classical Feynman-like) graph



To compute explicitly what the preceding graph means, we must start from the full action describing two gravitationally interacting bodies  $A$  and  $B$ :

$$S = -m_A \int ds_A - m_B \int ds_B + \int \frac{\sqrt{g}R}{16\pi G}. \quad (3.17)$$

Expanding  $S$  in the deviations of  $g_{\mu\nu}$  away from  $\eta_{\mu\nu}$ , one obtains (denoting  $h \equiv \eta^{\mu\nu}h_{\mu\nu}$ )

$$S = -m_A \int \sqrt{-\eta_{\mu\nu}dx_A^\mu dx_A^\nu} - m_B \int \sqrt{-\eta_{\mu\nu}dx_B^\mu dx_B^\nu} + \frac{1}{2} \int h_{\mu\nu}T_A^{\mu\nu} + \frac{1}{2} \int h_{\mu\nu}T_B^{\mu\nu} + \int \frac{1}{32\pi G} h^{\mu\nu} \square \left( h_{\mu\nu} - \frac{1}{2} h \eta_{\mu\nu} \right) + \mathcal{O}(h^2 T) + \mathcal{O}(h^3), \quad (3.18)$$

where  $T_A^{\mu\nu}$  is the (flat-space limit) of the stress-energy tensor of particle  $A$  (given by a  $\delta$ -function localized on the worldline of  $A$ ), and where the kinetic term of  $h_{\mu\nu}$  is the one corresponding to the harmonic gauge (*i.e.*,  $\partial_\nu(\sqrt{g}g^{\mu\nu}) = 0$ ). Inverting this kinetic term yields for  $h_{\mu\nu}$  the following lowest-order equation (corresponding to Einstein's equations at linearized order)

$$\square h_{\mu\nu} = -\frac{16\pi G}{c^4} \left( T_{\mu\nu} - \frac{1}{D-2} T \eta_{\mu\nu} \right). \quad (3.19)$$

with  $T_{\mu\nu} = \eta_{\mu\alpha}\eta_{\nu\beta}(T_A^{\alpha\beta} + T_B^{\alpha\beta})$ . We can then “integrate out”  $h_{\mu\nu}$  by solving the latter field equation for  $h$ , and replacing the result in the original action. Modulo



self-interaction terms  $\propto T_A^{\mu\nu} \square^{-1} P_{\mu\nu\rho\sigma} T_A^{\rho\sigma}$ , the action then splits into the sum of three terms, a term  $-m_A \int \sqrt{-\eta_{\mu\nu}} dx_A^\mu dx_A^\nu$ , describing the free propagation of body  $A$ , a similar term for  $B$ , and an interaction term,

$$S^{\text{int}} = -\frac{8\pi G}{c^4} \int T_A^{\mu\nu} \square^{-1} \left( T_{\mu\nu}^B - \frac{1}{D-2} T^B \eta_{\mu\nu} \right). \quad (3.20)$$

More explicitly, if we introduce the scalar Green's function  $G(x)$ , such that  $\square G(x) = -4\pi \delta^D(x)$ , this lowest-order interaction term reads

$$S^{\text{int}} = 2G \int \int ds_A ds_B m_A u_A^\mu u_A^\nu P_{\mu\nu}^{\rho\sigma} G(x_A(s_A) - x_B(s_B)) m_B u_{B\rho} u_{B\sigma}, \quad (3.21)$$

in which one easily identifies the usual structure of a Feynman graph (namely the one depicted above), with the coupling constant  $G$  in front, and a graviton propagator (comprising the scalar Green's function, together with the spin-two projection operator  $P_{\mu\nu}^{\rho\sigma}$ , which can be read off the previous explicit result) sandwiched between two source terms.

In the stationary approximation, the scalar Green's function reduces to the usual Newtonian propagator  $1/r$ . If one further neglects the relative velocity of the two worldlines one can replace the spacetime velocities  $u_A^\mu$  and  $u_B^\mu$  by  $(1, 0, 0, 0, \dots)$ . This yields the usual Newtonian interaction term  $G \int dt m_A m_B / r$ . However, the “one-graviton exchange” diagram above contains many Einsteinian effects that go beyond the Newtonian approximation. To compute them explicitly, we first need the explicit expression of the relativistic scalar Green's function  $G(x)$ . As we are deriving here the part of the gravitational interaction which is “conservative” (*i.e.*, energy conserving), we must use the *time-symmetric* (half-advanced half-retarded) Green's function. In four dimensions, it is given by  $\delta((x_A - x_B)^2)$ . It is the sum of two terms (a retarded and an advanced one), as depicted in FIG. 4. Note in passing that this classical time-symmetric propagator corresponds to the real part of the Feynman propagator. Indeed, for a massless scalar particle in  $D = 4$  the Feynman propagator (in  $x$  space) is proportional to

$$\frac{i}{x^2 + i\varepsilon} = iPP \frac{1}{x^2} + \pi \delta(x^2), \quad (3.22)$$

where the first term on the r.h.s. is a distributional “principal part” (it is pure imaginary and “quantum”), while the second (real) term is the classical contribution (classically the interaction propagates along the light cone, see FIG. 4). Note that, contrary to the Newtonian picture where the interaction is instantaneous, we have here an interaction which depends both on the future and on the past<sup>12</sup>.

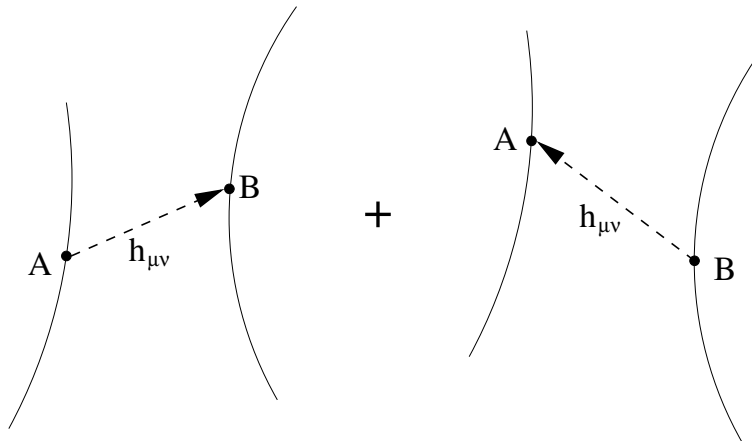


Figure 4. Time-symmetric half-advanced half-retarded contributions to the gravitational interaction between particles A and B.

When considering the case (of most importance in applications) where  $A$  and  $B$  move slowly relative to  $c$ , the time-symmetric propagator can be expanded in powers of  $1/c$ . The first term in this expansion yields the usual Newtonian instantaneous interaction, while all the higher-order terms can be expressed in terms of successive derivatives of the positions of  $A$  and  $B$ , (so that the acausality formally disappears, and is replaced by a dependence of the Lagrangian on derivatives higher than the velocities, *i.e.*, accelerations, derivatives of accelerations, and so forth. Actually, such higher-derivative terms start appearing only at the so-called “second post-Newtonian” (2PN) order, *i.e.*, the order  $\mathcal{O}(\frac{1}{c^4})$ . Such higher-order post-Newtonian (PN) contributions are important for some applications (binary pulsars, coalescing black holes), and have been computed up to the 3PN ( $\mathcal{O}(\frac{1}{c^6})$ ), as well as 3.5 PN ( $\mathcal{O}(\frac{1}{c^7})$ ) levels. Here we shall consider only the first post-Newtonian, 1PN, level, *i.e.*,  $\mathcal{O}(\frac{1}{c^2})$ . At this level, the action can be written entirely in terms of the velocities of  $A$  and  $B$  (taken at the same instant  $t$  in some Lorentz frame). By expanding the time-symmetric acausal one-graviton-exchange action written above to order  $1/c^2$  one finds the following explicit 1PN Lagrangian (now considered for an  $N$ -body system made of masses

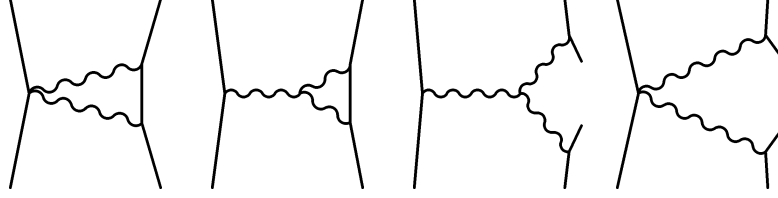
<sup>12</sup>This “acausal” behaviour is due to our considering the conservative (“Fokker”) action. If we were computing the “real” classical equations of motion of the two particles, we would use only a *retarded* Green’s function. The equations of motion so obtained would then be “causal” and would automatically contain some (physically needed), time-asymmetric “radiation reaction” terms. The trick, used here, to employ an acausal time-symmetric Green’s function is a technical shortcut allowing one to derive the action yielding the conservative part of the equations of motion.

labelled  $A, B = 1, 2, \dots, N$ .)

$$\begin{aligned} \mathcal{L}^{2\text{-body}} = & \frac{1}{2} \sum_{A \neq B} \frac{Gm_A m_B}{r_{AB}} \left[ 1 + \frac{3}{2c^2} (v_A^2 + v_B^2) - \right. \\ & \left. \frac{7}{2c^2} \vec{v}_A \cdot \vec{v}_B - \frac{1}{2c^2} (\vec{n}_{AB} \cdot \vec{v}_A) (\vec{n}_{AB} \cdot \vec{v}_B) + \mathcal{O}\left(\frac{1}{c^4}\right) \right], \end{aligned} \quad (3.23)$$

Note that the coefficients  $3/2, 7/2, 1/2$ , etc., arise from the spin 2 nature of the graviton, *i.e.*, they are uniquely fixed by Einstein's propagator.

When considering a gravitationally bound  $N$ -body system, we must remember that there is a link  $v^2 \sim \frac{GM}{r}$ , due to the "virial theorem". This link says that the  $\frac{v^2}{c^2}$  contributions in the one-graviton-exchange graph considered above must be completed by computing non-linear interaction graphs containing more gravitons, namely the ones of order  $G^2/c^2$  involving two powers of the coupling constant  $G$ . These contributions correspond to the terms  $\mathcal{O}(h^2 T)$  or  $\mathcal{O}(h^3)$  in the  $h$ -expansion of the exact Einstein action. In terms of Feynman-like diagrams, this means the following graphs:



Note, in particular, that these terms involve the graviton cubic vertex (whose structure will therefore be probed by solar-system experiments). Note also that some of these terms involve only two bodies (being proportional, say, to  $m_A m_B^2$ ), while others can involve three distinct bodies ( $\propto m_A m_B m_C$ ). The full  $G^2/c^2$  result (containing both two-body and three-body terms) is found to be equal to

$$\mathcal{L}^{3\text{-body}} = -\frac{1}{2} \sum_{B \neq A \neq C} \frac{G^2 m_A m_B m_C}{r_{AB} r_{AC} c^2}, \quad (3.24)$$

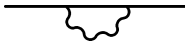
where the factor of  $1/2$  is a prediction from Einstein's theory. Note that the summation is restricted by  $B \neq A \neq C$  which allows for the two-body terms where  $B = C$ .

When looking at the nonlinear diagrams above one sees some "loops" made by graviton propagator lines closing up on a matter worldline. This may seem paradoxical because we are considering here classical gravitational effects, and classical theory is usually thought of as involving only tree diagrams. Indeed, if

we replace all our “source worldlines” (drawn above as continuous worldlines) by separate external sources (*i.e.*, by replacing the line describing  $T_A^{\mu\nu}(x)$  by separate “blobs” on which graviton propagators start or end), we see that all the diagrams above open up and become tree diagrams. However, the presence of loops in the diagrams used here do correspond to essentially some of the same physical effects that “quantum loops” describe. This is particularly clear for the diagrams below (which are included in the classical calculations)



It is clear that these diagrams describe the self-gravity effects of a mass  $m_A$  on itself. As such, they do describe the classical limit of quantum loops such as the simplest one-loop diagram



which describes the back action of the emission and reabsorption of a graviton on a quantum particle. Another similarity between “classical loops” and quantum ones, is that, in practice, multi-loops are associated to the presence of multiple integrals which are increasingly difficult to compute.<sup>13</sup> In addition, the loop diagrams depicted in the penultimate graph lead (like quantum loops) to formally divergent integrals. The origin of these divergences is that we have been describing the gravitationally interacting bodies as “pointlike”, *i.e.*, mathematically described by a  $\delta$ -function (on a worldline). There are several ways of dealing with this technical problem. One can complete the formal perturbative calculations done with point-like bodies by another approximation scheme in which each body is locally viewed (in its own rest frame) as a weakly perturbed isolated body. The development of such a dual perturbation method [32, 33] shows that the non-point-like, internal structure of non-rotating *compact* bodies (neutron stars or black holes) will enter their translational dynamics only at the 5PN

<sup>13</sup>Note that classical diagrams must all be computed in  $x$ -space. An increasing number of loops signals the presence of intermediate vertices in  $x$ -space on which one must integrate.

level ( $\sim G^6/c^{10}$ ), corresponding to 5 loops ! Knowing this, one expects that the use of a gauge-invariant regularization method for treating gravitationally-interacting point masses should give a physically unique answer up to 5 loops (excluded). Using *dimensional regularization*, one finds that all self-gravity effects are unambiguous and finite at 1PN and 2PN [33]. Recent work has pushed the calculation to the 3PN (*i.e.*, 3 loop) level. Again, one finds, either (when using a convenient gauge) a finite answer [34], or, when using the harmonic gauge, an equivalent answer after renormalizing the position of the worldline used in the  $\delta$ -function source [35].

### 3.3.2. Experimental tests in the solar system

The 1PN-level results described above are accurate enough for describing the gravitational dynamics in the solar system. Testing the validity of GR's description of the gravitational field's dynamics is then achieved by verifying the agreement of the coefficients introduced above with experimental measurements. In this section, we will see that these GR-predicted coefficients agree with their experimentally measured value to better than the  $10^{-5}$  level for the coefficients entering the one-graviton-exchange term, and to about the  $10^{-3}$  level for the additional 1PN multi-graviton term. There are many observables that can be used to test relativistic gravity in the solar system. One may use the advance of the perihelion of planets, the deflection, by the local curvature, of light reaching the Earth from distant stars, the additional time delays suffered by electromagnetic signals compared to their flat spacetime counterparts, or also, general relativistic corrections to the Moon's motion using the laser ranging technique already mentioned in previous sections.

When testing Einstein's predictions it is convenient to embed GR within a class of alternative gravity theories. For instance, one could consider not only the interaction of matter with the usual Einstein (pure spin-2) graviton but also an interaction with a long-range scalar field  $\varphi$ , *i.e.*, a spin-zero massless field, coupled to the trace of  $T^{\mu\nu}$  with strength  $\sqrt{G}\alpha(\varphi)$ . This leads to an additional attractive force, so that the effective gravitational constant measured in a Cavendish experiment is  $G_{\text{eff}} = G(1 + \alpha^2)$ . This also modifies the  $v^2/c^2$  terms in the two-body action introduced above by terms proportional to  $\alpha^2$ . These modifications are often summarized by writing the 1PN-level metric generated by an  $N$ -body system in the form

$$ds^2 = - \left( 1 - \frac{2U}{c^2} + 2(1 + \bar{\beta}) \frac{U^2}{c^4} \right) c^2 dt^2 + \left( 1 + 2(1 + \bar{\gamma}) \frac{U}{c^2} \right) \delta_{ij} dx^i dx^j,$$

where  $U = G_{\text{eff}} \sum_A m_A/r_A$  is the (effective) Newtonian potential and where

the two dimensionless coefficients  $\bar{\beta}$  and  $\bar{\gamma}$  encode the two possible (Lorentz-invariant) deviations from GR which enter the 1PN level. For an additional coupling to a scalar with  $\varphi$ -dependent coupling strength  $\alpha(\varphi)$ , one finds that the “post-Einstein” parameter  $\bar{\gamma}$  is given by  $\bar{\gamma} = -2\alpha^2/(1 + \alpha^2)$ . As for the other “post-Einstein” parameter  $\bar{\beta}$  it measures a possible modification of the (cubic-vertex related) three-body action  $\mathcal{L}^{3\text{-body}}$  written above, and it is given by  $\bar{\beta} = +\frac{1}{2}\beta\alpha^2/(1 + \alpha^2)^2$  where  $\beta$  denotes the derivative of the scalar coupling  $\alpha$  w.r.t. the field  $\varphi$ .

The most accurate test of GR in the solar system is the one made using the Cassini spacecraft by the authors of Ref. [36]. This test is (essentially) only sensitive to the post-Einstein parameter  $\bar{\gamma}$  (*i.e.*, it depends only on the graviton propagator and the coupling to matter but not on nonlinear terms). This experiment used electromagnetic signals sent from the Earth to the Cassini spacecraft and transponded back to Earth, and monitored the ratio between the electromagnetic frequency  $\nu + \Delta\nu$  recorded back on Earth to the initial frequency  $\nu$ . This ratio was used to probe the change in the geometry of spacetime in the vicinity of the Sun as the line of sight moved, especially when it was nearly grazing the Sun. The theoretical prediction for the experimental quantity measured in this experiment is

$$\left(\frac{\Delta\nu}{\nu}\right)^{2\text{-way}} = -4(2 + \bar{\gamma}) \frac{GM_{\text{sun}}}{c^3 b} \frac{db}{dt} \quad (3.25)$$

where  $b$  is the impact parameter, *i.e.*, the distance of closest approach of the signal’s trajectory to the center of the Sun. The experimental data gave the following result for the parameter  $\bar{\gamma}$

$$\bar{\gamma} = (2.1 \pm 2.3) \times 10^{-5}. \quad (3.26)$$

This confirms GR (namely  $\bar{\gamma}^{GR} = 0$ ) to the  $\mathcal{O}(1) \times 10^{-5}$  level.

The three-graviton vertex can be probed by considering a body, having a non-negligible gravitational self-binding energy, in an external gravitational field. Indeed, as emphasized by Nordtvedt [37, 38], the free fall acceleration of a self-gravitating body is, in most gravity theories (except GR) sensitive to its gravitational binding energy. For instance, the Earth and the Moon will have, in a general theory, a slightly different acceleration of free fall towards the Sun. The effect is proportional to the combination of post-Einstein parameters  $4\bar{\beta} - \bar{\gamma}$ . Lunar laser ranging data have allowed one to put a stringent upper limit on such a possibility [28], namely

$$4\bar{\beta} - \bar{\gamma} = (4.4 \pm 4.5) \times 10^{-4}. \quad (3.27)$$

Thus, to date, predictions of Einstein’s theory in the linear (one-graviton-exchange)

approximation have been verified to the  $10^{-5}$  level, while some of the cubically nonlinear aspects have been verified to the  $10^{-3}$  level.

The tests discussed up to now concern the quasi-stationary, weak-field regime, as it can be probed in the solar system. We shall now discuss the tests obtained in binary pulsar data, which have gone beyond the solar-system tests in probing part of the strongly nonlinear regime of gravity.

### 3.3.3. Objects with strong self-gravity: binary pulsars

Binary pulsars were discovered by Hulse and Taylor in 1974. Such systems are made of two objects going around each other in very elliptical orbits. Both objects are neutron stars<sup>14</sup>, of which one is a pulsar, *i.e.*, a rotating, magnetized object that emits a beam of electromagnetic noise (which includes radio waves, as well as other parts of the electromagnetic spectrum). When one looks at the geometry generated by a neutron star, and computes deviations from flat space of the metric components, one finds (on the surface of the star)

$$g_{00} = -1 + \frac{2GM}{c^2 R} \simeq -1 + 0.4 \quad (3.28)$$

for a star of (typical) mass  $1.4M_{\odot}$ , and radius  $R = 10$  km. This is a 40% deviation from flat space. By contrast, we recall that, in the solar system, the largest metric deviation from flat space occurs on the Sun's surface and is of order  $GM/(c^2 R) \sim 10^{-6}$ . We should therefore a priori expect that such objects might provide tests that go beyond the solar system ones in probing some of the strong-field aspects of relativistic gravity. In addition, in the solar system, the time-irreversible radiative aspects of gravity (*i.e.*, radiation reaction) are negligible (this is why we focussed above on time-symmetric interactions). Here, not only are strongly nonlinear effects relevant, but one must also take into account the time-dissymmetric effects linked to using a *retarded* propagator  $\propto \delta\left(t - \frac{|x_A - x_B|}{c}\right) / |x_A - x_B|$ . The corresponding time delay  $\frac{|x_A - x_B|}{c}$  is typically  $\simeq 1$  sec (since typical separations between the two objects are of order 300,000 km) and plays an essential role in the equations of motion of a binary pulsar. As a consequence, binary pulsars have given us firm experimental evidence for the reality of gravitational radiation, and for the fact that on-shell gravitational radiation is described by two transverse tensorial degrees of freedom travelling at the velocity of light.

In practice, only a subset of the known binary pulsars can be used for testing the strong nonlinear regime of GR, and/or its radiative regime. Among these, the

<sup>14</sup>Except in a few cases where the companion is another compact (though less compact) star remnant, a white dwarf.

very best ones are PSR1913+16 (where the numbers 19h13m and +16 deg measure angles on the sky), PSR1534+12, PSRJ1141-6545, and PSRJ0737-3039, the first *double* binary pulsar (made of two radio pulsars, simultaneously emitting toward the Earth).

>From the theoretical point of view, methods have been developed to deal with strongly self-gravitating objects, both in Einstein's theory and in alternative theories (see [39] for a recent review, and references). To adequately discuss the observations of binary pulsars, one has had to push the post-Newtonian perturbative calculation to the 2.5 PN level, *i.e.*, to order  $(v/c)^5$ . This odd power of the ratio  $v/c$  is linked to the time-dissymmetric, retarded nature of the propagator (together with some nonlinear effects). It is the first PN level where radiation reaction effects arise. Any experimental test of the presence of such  $(v/c)^5$  terms in the equations of motion is a probe of the reality of gravitational radiation. In addition, as mentioned above, one must carefully treat, and disentangle, the various strong-field effects that are linked to the self-gravity of each neutron star in the system.

The existing experimental tests are based on the *timing* of binary pulsars. Each time the beam of radio waves sweeps across the Earth, one observes a pulse of electromagnetic radiation. The data consists in recording the successive arrival times, say  $t_N$  (with  $N = 1, 2, 3, \dots$ ), of these pulses. Were the pulsar fixed in space, these arrival times would be equally spaced in time, *i.e.*,  $t_N = t_0 + NP$ , where  $P$  would be the (fixed) period of the pulsar. However, in a binary pulsar, the sequence of arrival times is a more complicated function of the integer  $N$  than such a simple linear dependence. Indeed, one must take into account many effects: the fact that the pulsar moves on an approximately elliptical orbit, the deviation of this orbit from a usual Keplerian ellipse, the deviation of the orbital velocity from the usual Kepler areal velocity law, the existence of various additional relativistic effects: gravitational redshift, second-order (relativistic) Doppler effect, time-delay when the electromagnetic pulse passes near the companion, radiation reaction effects in the orbital motion, etc. To compute all these effects, one needs to solve Einstein's equations of motion with high ( $\sim (v/c)^5$ ) accuracy.

The final result of these theoretical calculations is to derive the so-called *DD timing formula*, which gives the  $N^{\text{th}}$  pulse arrival time  $t_N$  as an explicit function of various "Keplerian" ( $p^K$ ), and "post-Keplerian" ( $p^{\text{PK}}$ ) parameters, say

$$t_N - t_0 = F [N; p^K; p^{\text{PK}}]. \quad (3.29)$$

Here, the Keplerian parameters ( $p^K$ ) comprise parameters that would exist in a purely Keplerian description of the timing: the orbital period  $P_b$ , the eccentricity of the orbit  $e$ , the time of passage at some initial periastron  $T_0$ , and some



corresponding angular position of the periastron  $\omega_0$ , and, finally, the projected semi-major axis  $x = \frac{a_1 \sin i}{c}$ , where  $a_1$  is the semi-major axis of the orbit of the observable pulsar<sup>15</sup> and  $i$  is the inclination angle w.r.t. the plane of the sky. The post-Keplerian parameters ( $p^{\text{PK}}$ ) then correspond to many relativistic effects that go beyond a Keplerian description, namely: a dimensionless parameter  $k$  measuring the progressive advance of the periastron  $k = \langle \dot{\omega} \rangle P_b / 2\pi$ , a parameter  $\gamma_t$  measuring the combined second-order Doppler and gravitational redshift effects, possible secular variations in Keplerian parameters  $\dot{e}$ ,  $\dot{x}$ ,  $\dot{P}_b$ , two parameters  $r$ ,  $s$  measuring the “range” and the “shape” of the additional time delay that appears when the radio waves pass near the companion, and finally a parameter  $\delta_\theta$  measuring the distortion of the orbit w.r.t an ellipse. By least-squares fitting the observed arrival times  $t_N^{\text{obs}}$  to the above general theoretical timing formula one can accurately determine the numerical values of all the Keplerian parameters, as well as some of the post-Keplerian ones. At this stage, the determination of these phenomenological parameters is (in great part) independent of the choice of a theory of gravity. On the other hand, in any specific theory of gravity, each post-Keplerian parameter is predicted to be some well-defined function of the Keplerian parameters and of the two masses,  $m_1$  and  $m_2$ , of the pulsar and its companion. For instance, *within GR* the advance of the periastron is given by

$$k^{\text{GR}}(p^{\text{K}}, m_1, m_2) = \frac{3}{c^2} \frac{(GMn)^{2/3}}{1 - e^2}, \quad (3.30)$$

where  $n = 2\pi/P_b$  and  $M = m_1 + m_2$ , while the secular variation of the orbital period (caused by radiation reaction effects) is given by

$$\dot{P}_b^{\text{GR}}(p^{\text{K}}, m_1, m_2) = -\frac{192\pi}{5c^5} \frac{1 + \frac{73}{24}e^2 + \frac{37}{96}e^4}{(1 - e^2)^{7/2}} (GMn)^{5/3} \frac{m_1 m_2}{M^2}. \quad (3.31)$$

Note that while  $k$  is proportional to  $1/c^2$  (1PN level), the secular variation of the orbital period is proportional to  $1/c^5$  (and is indeed numerically of order  $(v/c)^5$ ). The GR-predicted value for  $P_b$  is a direct reflection of the presence of  $\mathcal{O}((v/c)^5)$  time-asymmetric radiation damping terms in the equations of motion. Numerically,  $\dot{P}_b$  (which is dimensionless) is predicted to be of typical order of magnitude  $\dot{P}_b \sim 10^{-12}$ , which seems very small, but happens to be large enough to be measured with good accuracy in several binary pulsars.

The crucial point to notice is that the GR predictions (of which two are given here as examples) for the link between the post-Keplerian parameters and the masses are specific to the structure of GR, and will be replaced, in other theories of gravity, by different functions  $k^{\text{theory}}(p^{\text{K}}, m_1, m_2)$ ,  $\dot{P}_b^{\text{theory}}(p^{\text{K}}, m_1, m_2)$ ,

<sup>15</sup>In general, only one of the two objects, here labelled as 1, is a pulsar.

etc. In particular, it has been explicitly shown in various cases (and notably in the case of generic tensor-scalar theories where gravity is mediated both by a spin-2 field and a spin-0 one) that the large self-gravity of neutron stars would generically enter these functions, and drastically modify the usual prediction of GR, see [40].

To see which theory of gravity is in agreement with pulsar timing data, one can proceed as follows. Within each theory of gravity, the measurement of each post-Keplerian parameter defines a corresponding curve in the  $m_1, m_2$  plane. Therefore, in general, the measurement of two post-Keplerian parameters is sufficient to determine the (a priori unknown) numerical values of the two masses  $m_1$  and  $m_2$  (as the location where the two curves intersect). Then, the measurement of any additional post-Keplerian parameter yields a clear test of the validity of the theory considered: the corresponding third curve should pass precisely through the intersection point of the first two curves. If it does not, the theory is invalidated by the binary pulsar data considered. By the same reasoning, the measurement of  $n$  different post-Keplerian parameters yields  $n - 2$  tests of the underlying theory of gravity. Many such stringent tests have been obtained in binary pulsar observations (more precisely, nine different tests in all have been obtained when considering the data from four binary pulsars). Remarkably, *GR has been found to be consistent with all these tests*. Many alternative gravity theories have fallen by the wayside, or their parameters have been constrained so as to make the theory extremely close to GR in all circumstances (including strong-field ones).

Let us just give two impressive examples of the beautiful agreement between GR and pulsar data. In the case of the original Hulse-Taylor pulsar PSR1913+16 the ratio between the observed value of  $\dot{P}_b$  to that predicted by GR is given by

$$\left[ \frac{\dot{P}_b^{\text{obs}} - \dot{P}_b^{\text{gal}}}{\dot{P}_b^{\text{GR}} [k^{\text{obs}}, \gamma^{\text{obs}}]} \right] = 1.0026 \pm 0.0022, \quad (3.32)$$

where  $\dot{P}_b^{\text{gal}}$  is a Galactic correction. The fact that this ratio is close to one corresponds to a confirmation of the relativistic force law acting on the pulsar, of the symbolic form  $F = \frac{GM}{r^2} \left( 1 + \dots + \left( \frac{v}{c} \right)^5 \right)$ , where the crucial last term  $\sim (v/c)^5$  (i.e., an effect of order  $10^{-12}$ ) has been verified with a fractional accuracy of order  $10^{-3}$ . Note that this corresponds to an absolute accuracy of order  $10^{-15}$  compared to the leading Newtonian term  $\sim GM/r^2$  !

The timing data from the recently discovered double binary pulsar PSRJ0737-3039 led to the following ratio between the observed, and GR-predicted, values

of the post-Keplerian parameter  $s$

$$\left[ \frac{s^{\text{obs}}}{s^{\text{GR}} [k^{\text{obs}}, R^{\text{obs}}]} \right] = 0.99987 \pm 0.00050. \quad (3.33)$$

The agreement for this parameter is at the  $5 \times 10^{-4}$  level.

Summarizing: binary pulsar timing data have led to accurate confirmations of the strong-field and radiative structure of GR. Roughly speaking, these confirmations exclude any alternative theory containing long-range fields<sup>16</sup> coupled to bulk (hadronic) matter.

### 3.3.4. Tests of gravity on very large scales

So far, we have mainly focussed on tests of GR on spatial scales of several astronomical units (the size of the solar system), and on scales of 300,000 km (the typical separation between two neutron stars). We conclude this section on experimental tests of gravity by mentioning the existence of tests made on very large spatial and temporal scales. *Gravitational lensing effects* by galaxy clusters allow one to probe some aspects of relativistic gravity on scales  $\sim 100$  kpc. Here, one is talking of the effect of the curved spacetime metric generated by the cluster on light emitted by very distant quasars and passing near a galaxy cluster containing (in addition to visible galaxies) a lot of dark matter, as well as some X-ray gas. Data on the temperature distribution of the X-ray gas allows one to directly probe the Newtonian gravitational potential  $U(x)$  of the cluster (without having to assume much about the (dark) matter distribution). In turn, the potential  $U(x)$  determines the relativistic lensing of light, via the spacetime metric predicted by Einstein's theory, *i.e.*,  $-g_{00} = 1 - \frac{2U}{c^2}$ ,  $g_{ij} = \left(1 + \frac{2U}{c^2}\right) \delta_{ij}$ . According to Ref. [41], the agreement is of the order of 30%. This confirms the validity of GR on scales  $\sim 100$  kpc.

Primordial nucleosynthesis of light elements (*e.g.*, Helium, Lithium, Deuterium) in the early universe depends on both the expansion rate and on the weak-interaction reaction rate for the conversion between neutrons and protons. Given that the Hubble parameter  $H^2 \propto G\rho \propto GT^4$ , the creation of light elements at early times (and high temperatures  $T$ ) depends on Newton's constant. The comparison between theoretical predictions and observations of the abundance of light elements typically constrains the value of  $G$  at the time of Big Bang nucleosynthesis, say  $G^{\text{BB}}$  to differ by less than  $\mathcal{O}(10\%)$  from its current value  $G^{\text{now}}$  (see *e.g.*, Chapter 18 of the Review of Particle Physics, <http://pdg.lbl.gov/>).

<sup>16</sup>By which, one really means here fields with range larger than the distance between the two pulsars, *i.e.*,  $\sim 300\,000$  km.

#### 4. String-inspired phenomenology of the gravitational sector

##### 4.1. Overview

>From the previous sections, one can conclude that GR is a very well confirmed theory so that one might be tempted to require of any future theory (and especially string theory) that it lead to essentially no observable deviations from usual 4-dimensional GR. For instance, one might require that all the a priori massless scalar fields that abound in (tree level, compactified) string theory acquire large masses. However, as there is yet no clear understanding of how to fit our world within string theory, it is phenomenologically interesting to keep an open mind and explore whether there exist possibilities for deviations of GR that have naturally escaped detection so far.

String theory predicts the existence of an extended mass spectrum ( $g_{\mu\nu}(x)$ ,  $\Phi(x)$ ,  $B_{\mu\nu}$ , moduli fields, etc.) from which there could result some long range or short range modification of gravity. The existence of branes and large extra dimensions could also be sources of modified gravity (e.g., KK gravity). There could exist short distance effects at scales of order the string scale  $\ell_s$  which are observable in cosmology or in high energy astrophysics. We shall also consider possible gravitational wave signals from string-cosmology models. Finally, we refer the reader to the lectures by Juan Maldacena for a discussion of non-gaussianities in CMB data.

A phenomenologically interesting idea (though it is not supported by precise theoretical arguments) is a possible breakdown of Lorentz invariance, on large scale physics, linked to string-scale cutoff-related effects. An example of this is a modified dispersion relation of the type

$$E^2 = m^2 + \vec{p}^2 + \beta_1 \frac{E^3}{m_P} + \beta_2 \frac{E^4}{m_P^2} + \dots \quad (4.1)$$

where  $m_P$  denotes the Planck mass. One could think that because of the large value of the Planck mass, any such corrections to the usual dispersion relation are unobservable. However, there exist astrophysical phenomena, such as high energy cosmic rays, for instance high energy  $\gamma$ -rays, for which such a small change in this relation could be observed. For example, by comparing the times-of-arrival of  $\gamma$ -rays of different energies, one has been able to place strong limits on the parameter  $\beta_1$ . Such modifications of the dispersion relation have also been used in the analysis of the CMB, since, in the standard inflationary model, initial quantum fluctuations (the seeds of today's large scale structures) arise in the deep ultraviolet *i.e.*, at transplanckian scales. Note that there exist theoretical difficulties<sup>17</sup> with the inclusion of the  $\beta_1 \frac{E^3}{m_P}$  term (the one which is severely constrained

<sup>17</sup>Linked to its proportionality to  $1/m_P$ , while most theoretical models suggest a proportionality

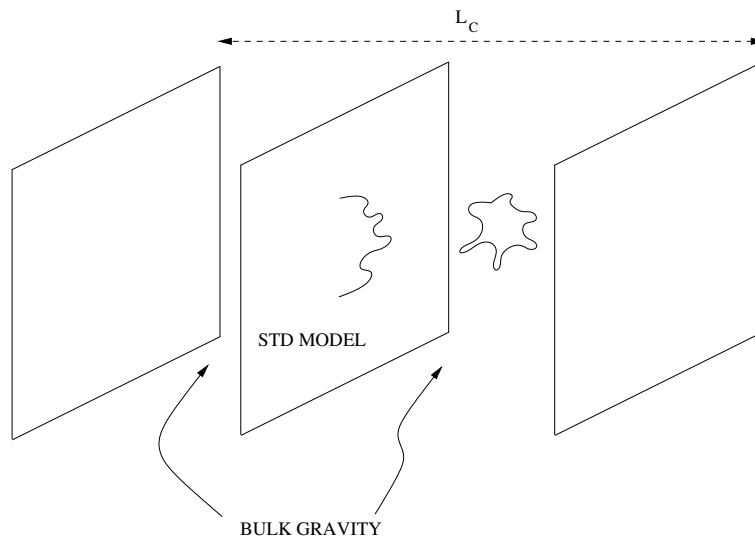


Figure 5. The ends of open strings are attached to a brane, giving rise to SM particles, while closed strings are free to propagate in the bulk.

experimentally), while the more conventional fourth order term would be too small to be observed. Note that in the case of the photon, a modification on short scales could imply a birefringence of the vacuum as  $\omega_{\pm} = |k| \left(1 \pm \beta \frac{|k|}{m_P}\right)$ . For references on these issues see [42, 43]. Speaking of string-inspired astrophysical effects, let us mention the suggestion of Ref. [44] that string theory might imply a violation of the usual Kerr bound on the spin of rotating black holes:  $J \leq GM^2$ .

Other possible predictions of string theory arise from the picture in which one considers the existence of branes on which (open string) SM particles are confined, while (closed string) gravitons are free to propagate in the bulk (FIG. 5). The extra dimensions of the bulk can then be compactified, on a Calabi-Yau or simply on a torus (thereby “localizing” gravity around the SM brane). Constraints on the size of the compactified dimensions then come either from the gravitational phenomenology, or from effects on SM particles. This is the “large” extra dimensions idea [45] which could be tested at the LHC, and so is of interest today. Other realizations include models with “very large” extra dimensions [46], but it is less clear how they are realized in string theory. In the Randall-Sundrum model [46], a brane can be like a defect in a bulk with a

---

to  $1/m_P^2$ .

negative cosmological constant, in which case the zero mode of bulk gravitational waves behaves as a surface wave localized on the brane due to the discontinuity located at the interface of the brane with the bulk. In the DGP model [47], the approximate localization of bulk gravity on the SM brane is achieved through the interplay of two dynamics for the gravitational sector: a 5D Einstein action, plus a 4D “induced” Einstein action, with a different value of Newton’s constant, on the brane. Combining the two inverse propagators, the global propagator drastically modifies gravity on large length scales  $r$ :

$$r \geq L = \frac{G_5}{G_4}. \quad (4.2)$$

In addition, even on length scales  $r \leq L$  there exist modifications of usual gravity. Indeed, the claim is that Newton’s potential is modified as [48]

$$U \simeq \frac{GM}{r} \left[ 1 - \frac{1}{L} \sqrt{\frac{r^3 c^2}{GM}} \right]. \quad (4.3)$$

At the phenomenological level, it is interesting that (*Newtonian*) gravity be modified in this way. Estimates indicate that effects are small enough to have escaped detection so far, but could be seen in refined solar system experiments (e.g., Lunar Laser Ranging). Some authors have argued that such models may have acausal behaviours, with, for instance, the appearance of closed timelike curves [49].

Another conceptually interesting idea involves the possible existence of several (parallel) Randall-Sundrum branes. The confining mechanism of gravity in the Randall-Sundrum model is such that the wavefunction of surface gravitons is exponentially decaying away from the brane. If two branes are nearby, such quasi-confined gravitational effects can tunnel from one brane to the other via exponentially small effects. As a consequence, the effective Lagrangian would contain two metric tensors with two gravitons, one massless, the other massive [50]. There are, however, theoretical difficulties with any massive gravity theory, in relation with the van Dam-Veltman-Zakharov discontinuity (see, e.g., [51] and references therein).

#### 4.2. Long range modifications of gravity

It is well known that, at tree level in string theory, there exist many massless scalar fields with gravitational strength coupling, the so-called moduli fields. Phenomenologically, one would expect that having massless scalar fields at low energies is undesirable (Would a theory containing such massless fields not immediately fail the GR tests discussed in the section above?). General arguments suggest that such scalar fields should not be expected to remain massless after

supersymmetry breaking [52]. Recently, a large “industry” has been devoted to try to construct explicit compactification models where all moduli are fixed, and actually acquire very heavy masses, which is needed if inflation is to happen in the usual way. Here however, in the spirit of keeping an open mind, we will instead assume that a scalar field remains massless in the low-energy effective theory, and discuss ways in which it might not disagree with existing tests of general relativity. In other words, we suppose there exists a flat or almost flat direction in the total scalar potential  $V(\varphi)$ , such that there remains a massless field after supersymmetry breaking. Let us mention in this respect the idea suggested, in particular, by Eliezer Rabinovici [53] that the ultimate explanation for the smallness of the cosmological constant might be a mechanism of spontaneous breaking of an underlying scale invariance. In that case, we would expect to have an associated massless Goldstone boson (the “dilaton”, in the original sense of the word).

#### 4.2.1. The cosmological attractor mechanism

Let us discuss here the idea of the *least coupling principle*, realized via a cosmological attractor mechanism (see e.g., Refs [54, 55]), which can reconcile the existence of a massless scalar field in the low energy world with existing tests of GR (and with cosmological inflation). Note that, to date, it is not known whether this mechanism can be realized in string theory. We assume the existence of a massless scalar field  $\Phi$  (i.e., of a flat direction in the potential), with gravitational-strength coupling to matter. *A priori*, this looks phenomenologically forbidden but we are going to see that the cosmological attractor mechanism (CAM) tends to drive  $\Phi$  towards a value where its coupling to matter becomes naturally  $\ll 1$ . In the string frame, we start with an effective action of the generic form

$$S_{\text{eff}} = \int d^4x \sqrt{\hat{g}} \left[ B_g(\Phi) \frac{\hat{R}}{\alpha'} + \frac{B_\Phi(\Phi)}{\alpha'} \left( 4\Box\Phi - 4(\nabla\Phi)^2 \right) - B_F(\Phi) \frac{k}{4} F_{\mu\nu}^2 - B_\Psi(\Phi) \Psi D \bar{\Psi} - \frac{1}{2} B_\chi(\Phi) \left( \hat{\nabla}\hat{\chi} \right)^2 - \frac{1}{2} m_\chi^2(\Phi) \chi^2 \right],$$

where  $\Phi$  is the massless dilaton field,  $\chi$  is the inflaton, to which has been associated a simple chaotic-inflation-type potential term, with the exception that here  $m_\chi$  is a function of  $\Phi$ . In heterotic string theory for instance,  $B_g$ ,  $B_\Phi$ ,  $B_F$ ,  $B_\Psi$  and  $B_\chi$  are given by expansions in powers of the string coupling  $g_s = e^\Phi$ , as

$$B_i = e^{-2\Phi} + c_0^{(i)} + c_1^{(i)} e^{2\Phi} + \dots \quad (4.4)$$

where the first term is the tree level term, followed by an infinite series of correction terms involving positive powers of  $g_s$  (or non-perturbative functions of

$g_s$ ). Switching to the Einstein frame, and redefining  $\hat{g}_{\mu\nu}$  and the nonstandard  $\Phi$  kinetic terms according to

$$\begin{aligned} \hat{g}_{\mu\nu} &\rightarrow g_{\mu\nu} = C B_g(\Phi) \hat{g}_{\mu\nu}, \\ \varphi &= \int d\Phi \left[ \frac{3}{4} \left( \frac{B'_g}{B_g} \right)^2 + 2 \frac{B'_\Phi}{B_g} + 2 \frac{B_\Phi}{B_g} \right]^{1/2}, \end{aligned} \quad (4.5)$$

(where a prime denotes  $d/d\Phi$ ), the effective action turns into

$$S_{\text{eff}} = \int d^4x \sqrt{g} \left[ \frac{\tilde{m}_p^2}{4} R - \frac{\tilde{m}_p^2}{2} (\nabla\varphi)^2 - \frac{\tilde{m}_p^2}{2} F(\varphi) (\nabla\chi)^2 - \frac{1}{2} m_\varphi^2(\chi) \chi^2 \right] + \dots, \quad (4.6)$$

with  $\tilde{m}_p^2 \equiv \frac{1}{4\pi G}$ , and in which the  $\chi$  terms are important during inflation while additional terms that include the gauge fields and ordinary matter such as

$$\begin{aligned} -\frac{1}{4} B_F(\varphi) F_{\mu\nu}^2 - \sum_A \int m_A [B_F(\varphi(x_A))] \times \\ \sqrt{-g_{\mu\nu}(x_A) dx_A^\mu dx_A^\nu} - V_{\text{vac}}(\varphi) \end{aligned} \quad (4.7)$$

are relevant in the matter dominated era.

As we shall see, the CAM leads to some generic predictions even without knowing the specific structure of the various coupling functions, such as e.g.,  $m_\chi(\varphi), m_A(B_F(\varphi)), \dots$ . The basic assumption one has to make is that the string-loop corrections are such that there exists a *minimum* in (some of) the functions  $m(\varphi)$  at some (finite or infinite) value,  $\varphi_m$ . During inflation, the dynamics is governed by a set of coupled differential equations for the scale factor,  $\chi$  and  $\varphi$ . In particular, the equation of motion for  $\varphi$  contains a term  $\propto -\frac{\partial}{\partial\varphi} m_\chi^2(\varphi) \chi^2$ . During inflation (i.e., when  $\chi$  has a large vacuum expectation value, this coupling drives  $\varphi$  towards the special point  $\varphi_m$  where  $m_\chi(\varphi)$  reaches a minimum. Once  $\varphi$  has been so attracted near  $\varphi_m$ ,  $\varphi$  essentially (classically) decouples from  $\chi$  (so that inflation proceeds as if  $\varphi$  was not there). A similar attractor mechanism exists during the other phases of cosmological evolution, and tends to decouple  $\varphi$  from the dominant cosmological matter. For this mechanism to efficiently decouple  $\varphi$  from all types of matter, one needs the special point  $\varphi_m$  to approximately minimize all the important coupling functions. This can be naturally realized by assuming that  $\varphi_m$  is a special point in field space: for instance it could be the fixed point of some  $Z_2$  symmetry of the  $T$ - or  $S$ -duality type (so that one could say that ‘‘symmetry is attractive’’). An alternative way of having such a special



point in field space is to assume that  $\varphi_m = +\infty$ <sup>18</sup> is a limiting point where all coupling functions have finite limits. This leads to the so-called *runaway dilaton* scenario [55]. In that case the mere assumption that  $B_i(\Phi) \simeq c_1^i + \mathcal{O}(e^{-2\Phi})$  as  $\Phi \rightarrow +\infty$  implies that  $\varphi_m = +\infty$  is an attractor where all couplings vanish.

#### 4.2.2. Observable consequences of the Cosmological Attractor Mechanism

Before discussing the observational predictions of the CAM, let us remind the reader of a few facts that are relevant for studying the possible effects of a string-inspired modification of gravity. The main source of modification of gravity comes from the fact that the “moduli” field  $\varphi$  will influence the values of the masses of the (low-energy) particles and nuclei. This means that the classical action of, say an atom  $A$ , will be

$$- \int m_A(\varphi) ds_A = - \int m_A(\varphi) \sqrt{-g_{\mu\nu} dx_A^\mu dx_A^\nu} \quad (4.8)$$

where  $g_{\mu\nu}$  is the Einstein-frame metric. Then, one finds that the scalar field  $\varphi$  will be coupled to the atom  $A$  with the strength  $\alpha_A \sqrt{G}$ , where the dimensionless coupling strength  $\alpha_A$  (with the same normalization as the one discussed above for usual tensor-scalar theories<sup>19</sup>) is simply given by

$$\alpha_A = \frac{\partial}{\partial \varphi} \ln m_A(\varphi). \quad (4.9)$$

To see better the various ways in which  $\varphi$  might enter into  $m_A$ , let us consider for instance the various parts constituting the mass of an atom:

$$m_A(\varphi) = Zm_p + Nm_n + Zm_e + E_{\text{SU3}}^{\text{nucleus}} + E_{\text{U1}}^{\text{nucleus}}, \quad (4.10)$$

where  $Z$  is the atomic number,  $m_p$  the mass of the proton,  $N$  the neutron number,  $m_n$  the mass of the neutron,  $m_e$  the mass of the electron,  $E_{\text{SU3}}^{\text{nucleus}}$  and  $E_{\text{U1}}^{\text{nucleus}}$  the nuclear and Coulomb interaction energies of the nucleus, respectively. In addition, one must note that the mass of the proton is given by

$$m_p(\varphi) = a\Lambda_{\text{QCD}}(g_3^2(\varphi)) + b_u m_u(\varphi) + b_d m_d(\varphi) + c_p \Lambda_{\text{QCD}} \alpha_{\text{em}}(\varphi). \quad (4.11)$$

The main scale that determines the mass of the proton is  $\Lambda_{\text{QCD}}$ . It depends on all the moduli including the massless field  $\varphi$  and is roughly of the form

$$\Lambda_{\text{QCD}}(\varphi) = C_g^{1/2}(\varphi) B_g^{-1/2}(\varphi) \exp\left[-\frac{8\pi B_F(\varphi)}{b_3}\right] \tilde{M}_{\text{string}}. \quad (4.12)$$

<sup>18</sup>This is viewed as a strong-(bare)-coupling limit, by contrast to the usual weak-coupling limit  $\varphi \rightarrow -\infty$  and  $\Phi \rightarrow -\infty$ .

<sup>19</sup>In particular, the effective Newton constant for a Cavendish experiment between a body made of atoms  $A$  and another one made of atoms  $B$  is  $G_{AB}^{\text{eff}} = G(1 + \alpha_A \alpha_B)$ .

Here,  $C_g$  is the conformal factor from the string to the Einstein frame. The most important contribution to the  $\varphi$  dependence of  $\Lambda_{\text{QCD}}$  is that given by the  $\varphi$  dependence of the exponential term. This dependence comes from the well-known running (via the  $\beta$ -function of  $\text{SU}(3)$ ) of some (unified) gauge coupling constant between its value  $1/g_3^2 \propto B_F(\varphi)$  considered at a GUT-scale cut-off (here approximately related to  $\tilde{M}_{\text{string}}$ ), to a value of order unity at the confining scale  $\Lambda_{\text{QCD}}$ . The other contributions to the mass of the proton are the quark masses, which are determined by the vev of the Higgs boson and by the Yukawa coupling constants, which, again, are expected to be functions of  $\varphi$  at high energy. There also exists a contribution from the electromagnetic sector since part of the mass of the proton is a function of the fine structure constant  $\alpha_{\text{em}}(\varphi)$ . Finally the nuclear binding energy of a nucleus is quite important and must also be expressed as a function of basic scales. In an approximate form it reads

$$E_{\text{SU3}}^{\text{nucleus}} \simeq (N + Z) a_3 + (N + Z)^{2/3} b_3 \quad (4.13)$$

where

$$a_3 \simeq a_3^{\text{chiral limit}} + \frac{\partial a_3}{\partial m_\pi^2} m_\pi^2(\varphi). \quad (4.14)$$

In the chiral limit (*i.e.*, taking the quark masses to zero) one gets a non-zero limit  $a_3^{\text{chiral limit}}$  to which must be added a term approximately proportional to the squared pion mass. In turn,  $m_\pi^2$  is proportional to the product of  $\Lambda_{\text{QCD}}$  and  $m_u + m_d$ , both of which are expected to be functions of  $\varphi$ . Incidentally, let us note that there exists a delicate balance between attractive and repulsive nuclear interactions [56], which implies a strong sensitivity of the binding energy of nuclei to the value of the quark masses [57]. A recent result shows that if the quark masses were to increase by 50% (at one  $1\sigma$ , or 64% at  $2\sigma$ ), all heavy nuclei would fall apart because there would be no nuclear binding [58].

At leading order, the mass of any nucleus is a pure number times  $\Lambda_{\text{QCD}}$ . In this approximation,  $m_A$  would depend universally on  $\varphi$  (via  $\Lambda_{\text{QCD}}(\varphi)$ ), and the scalar coupling strength  $\alpha_A$  would be independent of the atomic species  $A$  considered. As a consequence, there would be no violation of the universality of free fall. This shows that the violations of the universality of free fall will depend on the small fractional corrections in  $m_A$  proportional to the ratios

$$\frac{m_u}{\Lambda_{\text{QCD}}}, \quad \frac{m_d}{\Lambda_{\text{QCD}}}, \quad \text{and} \quad \alpha_{\text{em}}. \quad (4.15)$$

When differentiating the mass of an atom w.r.t.  $\varphi$ , say

$$m_A(\varphi) = \mathcal{N} \Lambda_{\text{QCD}} \left( 1 + \varepsilon_A^\sigma \frac{m_u + m_d}{\Lambda_{\text{QCD}}} + \varepsilon_A^\delta \frac{m_d - m_u}{\Lambda_{\text{QCD}}} + \varepsilon_A^{\text{em}} \alpha_{\text{em}} \right), \quad (4.16)$$

where  $\mathcal{N}$  is a pure number (which depends on  $N$  and  $Z$ ), one obtains for the scalar coupling strength  $\alpha_A(\varphi) = \frac{\partial}{\partial\varphi} \ln m_A(\varphi)$  an (approximate) expression of the form

$$\alpha_A(\varphi) \simeq \alpha_{\text{had}}(\varphi) + \varepsilon_A^\sigma \frac{\partial}{\partial\varphi} \left( \frac{m_u + m_d}{\Lambda_{\text{QCD}}} \right) + \varepsilon_A^\delta \frac{\partial}{\partial\varphi} \left( \frac{m_d - m_u}{\Lambda_{\text{QCD}}} \right) + \varepsilon_A^{\text{em}} \frac{\partial}{\partial\varphi} \alpha_{\text{em}}, \quad (4.17)$$

where  $\alpha_{\text{had}} \equiv \frac{\partial}{\partial\varphi} \ln \Lambda_{\text{QCD}}(\varphi)$ . When the CAM has attracted  $\varphi$  near a value  $\varphi_m$  which minimizes all the separate coupling functions entering the various ingredients of  $m_A(\varphi)$ , each term in the above expression for  $\alpha_A(\varphi)$  will be (approximately) proportional to the small difference  $\varphi - \varphi_m$ . As a consequence all the contributions to  $\alpha_A(\varphi)$  will be small, so that all the observable deviations from GR will be naturally small.

Let us describe more precisely the possible observable consequences of the CAM. In this mechanism, the couplings of the massless scalar field to the various physical sectors are not assumed to be initially small (they are given by the various coupling functions  $B_i(\varphi)$  entering the Lagrangian, and these functions are “of order unity”). However, via its coupling to cosmological evolution, the scalar field is driven towards a point where the couplings to matter become small, but not exactly zero. Indeed, one can analytically estimate the “efficiency” of the cosmological evolution in driving  $\varphi$  towards  $\varphi_m$ , and one finds some expression for the difference<sup>20</sup>  $\delta\varphi \equiv \varphi - \varphi_m$  [54, 55]. The deviations from GR are all proportional to the small quantity  $\delta\varphi^2$  because the scalar coupling strengths  $\alpha_A, \alpha_B$  are proportional to  $\delta\varphi$ , and all “post-Einstein” observables contain two scalar couplings, say  $\alpha_A\alpha_B$  when talking about the scalar exchange between  $A$  and  $B$  (for instance the modified gravitational constant for a Cavendish experiment involving two bodies made of atoms  $A$  and  $B$  is  $G_{AB} = G(1 + \alpha_A\alpha_B)$ ). In addition to predicting small values for the (approximately composition-independent) “post-Einstein” parameters  $\bar{\gamma}$  and  $\bar{\beta}$  this mechanism also predicts various (small) violations of the equivalence principle.

For instance, the above expressions for the ingredients entering  $m_A$  and  $\alpha_A$  lead to generic predictions about the type of violation of the universality of free fall that one might expect in string theory. Indeed, one finds that the fractional difference in the free fall acceleration of two bodies (made of atoms  $A$  and  $B$ )

<sup>20</sup>When  $\varphi_m$  is infinite,  $\delta\varphi \equiv \varphi - \varphi_m$  is replaced, e.g., by  $e^{-c\varphi}$ .

takes the form

$$\frac{a_A - a_B}{\langle a \rangle} \simeq 2 \times 10^{-5} \alpha_{\text{had}}^2 \left[ \Delta \left( \frac{E}{M} \right) + c_B \Delta \left( \frac{N+Z}{M} \right)_{AB} + c_D \Delta \left( \frac{N-Z}{M} \right)_{AB} \right], \quad (4.18)$$

with

$$\frac{E}{M} = \frac{Z(Z-1)}{(N+Z)^{1/3}}. \quad (4.19)$$

where  $(\Delta Q)_{AB} \equiv Q_A - Q_B$ , and where the first, second and third terms in the brackets are contributions from the Coulomb energy of the nucleus ( $\propto \alpha_{\text{em}}$ ), and from the  $\varphi$ -dependence of the sum and difference of the quarks masses, i.e.,  $m_u + m_d$  and  $m_u - m_d$ .

This mechanism also predicts (approximately composition-independent) values for the post-Einstein parameters  $\bar{\gamma}$  and  $\bar{\beta}$  parametrizing 1PN-level deviations from GR. They are of the form

$$\bar{\gamma} = -2 \frac{\alpha_{\text{had}}^2}{1 + \alpha_{\text{had}}^2} \simeq -2\alpha_{\text{had}}^2, \quad (4.20)$$

and

$$\bar{\beta} = \frac{1}{2} \frac{\alpha_{\text{had}}^2 \frac{\partial \alpha_{\text{had}}}{\partial \varphi}}{(1 + \alpha_{\text{had}}^2)^2} \simeq \frac{1}{2} \alpha_{\text{had}}^2 \frac{\partial \alpha_{\text{had}}}{\partial \varphi}. \quad (4.21)$$

In this model, one in fact violates all tests of GR. However, all these violations are correlated. For instance, using the numerical value  $\Delta \left( \frac{E}{M} \right) \simeq 2.6$  (which applies both to the pair Cu–Be and to the pair Pt–Ti), one finds the following link between equivalence-principle violations and solar-system deviations

$$\left( \frac{\Delta a}{a} \right) \simeq -2.6 \times 10^{-5} \bar{\gamma}. \quad (4.22)$$

Given that present tests of the equivalence principle place a limit on the ratio  $\Delta a/a$  of the order of  $10^{-12}$ , one finds  $|\bar{\gamma}| \leq 4 \times 10^{-8}$ . Note that the upper limit given on  $\bar{\gamma}$  by the Cassini experiment was  $10^{-5}$ , so that in this case the necessary sensitivity has not yet been reached to test the CAM.

As another example, one can compute the evolution of the fine structure constant w.r.t. time. Given that it is a function of  $\varphi$ , and that  $\varphi$  evolves as a function of cosmological evolution due to its coupling to matter,  $\alpha_{\text{em}}$  is indeed a function of time, and its time derivative can be written as

$$\frac{d}{dt} \ln \alpha_{\text{em}} \sim \pm 10^{-16} \sqrt{1 + q_0 - \frac{3\Omega_m}{2}} \sqrt{10^{12} \frac{\Delta a}{a}} \text{ yr}^{-1}. \quad (4.23)$$

The first square root on the r.h.s. of this equation can also be written as

$$\frac{\Omega_m \alpha_m + 4\Omega_v \alpha_v}{\Omega_m + 2\Omega_v}. \quad (4.24)$$

where  $\Omega_m$  denotes the fraction of the cosmological closure density due to dark matter, and  $\alpha_m$  the scalar coupling to dark matter, while  $\Omega_v$  and  $\alpha_v$  denote the corresponding quantities for “dark energy” (or “vacuum energy”). For instance, if we assume  $\alpha_v \sim 1$  (so that  $\varphi$  is a kind of “quintessence”) while  $\alpha_m \ll 1$ , we see from the result above that the current experimental limit  $\frac{\Delta a}{a} < 10^{-12}$ , implies the following upper bound on a possible time variation of the fine-structure constant:  $\frac{d}{dt}(\ln \alpha_{\text{em}}) \leq 10^{-16} \text{ yr}^{-1}$ . This upper bound is below the current laboratory limits on  $\dot{\alpha}/\alpha$ , but comparable to the Oklo limit mentioned above. When working out the generic predictions of the *runaway dilaton* version of the cosmological attractor mechanism, one finds that it naturally predicts (when assuming an inflationary potential  $\propto \chi^2$ ) a level of deviation from GR of order  $-\bar{\gamma} \sim 4C \times 10^{-8}$ , corresponding, for instance, to a violation of the equivalence principle at the level  $\Delta a/a \sim C \times 10^{-12}$ . Here,  $C$  is a combination of model-dependent dimensionless parameters, which are generically expected to be “of order unity”. This suggests (if  $C$  is smaller, but not much smaller than 1) that the current sensitivity of equivalence principle experiments may be close to what is needed to test the deviations from GR predicted by such a runaway dilaton. Let us note in this respect that ongoing improved lunar laser ranging experiments will probe  $\Delta a/a$  to better than the  $\sim 10^{-13}$  level, and that the CNES satellite mission MICROSCOPE (to be launched in the coming years) will reach  $\Delta a/a \sim 10^{-15}$ . Another more ambitious satellite mission (which is not yet approved), STEP (Satellite Test of the Equivalence Principle), plans to probe violations of the equivalence principle down to the  $10^{-18}$  level<sup>21</sup>. In addition, post-Newtonian solar system experiments at the  $10^{-7}$  level would be of interest. The approved micro-arcsecond global astrometry experiment GAIA will probe  $\bar{\gamma} \sim 10^{-7}$ , while the planned laser experiment LATOR might reach  $\bar{\gamma} \sim 10^{-9}$ . In addition, the comparison of cold-atom clocks might soon reach the interesting level  $\frac{d}{dt}(\ln \alpha_{\text{em}}) \sim 10^{-16} \text{ yr}^{-1}$ .

Finally, let us mention that one can combine the basic mechanism of the CAM (which consists in using the coupling of  $\varphi$  to matter, *i.e.*, the presence of a term of the form  $a(\varphi)\rho_{\text{matter}}$  in the action) with the presence of a “quintessence”-like potential  $V(\varphi) \propto 1/\varphi^p$ . This yields the “chameleon” mechanism [60] in which both the value  $\varphi_m$  towards which  $\varphi$  is attracted, and the effective mass (or inverse range) of  $\varphi$ , depend on the local matter density  $\rho_{\text{matter}}$ . Whatever be

<sup>21</sup>Let us also mention the suggestion [59] that atom interferometry might be used for testing the equivalence principle down to the  $\Delta a/a \sim 10^{-17}$  level.

one's opinion concerning the a priori plausibility of having some nearly massless moduli field surviving in the low-energy physics of string theory, it is clear that such experiments are important and could teach us something new about reality.<sup>22</sup>

## 5. String-related signals in cosmology

### 5.1. Alternatives to slow-roll inflation

In the usual inflationary scenario, the period of exponential expansion is based on the slow roll mechanism, *i.e.*, one has to assume a sufficiently flat potential so that the scalar field, the inflaton, slowly rolls down to its minimum in such a way that the approximate equality  $p_\varphi \simeq -\rho_\varphi$  lasts sufficiently long, say for a minimum of 60–70 e-folds. The simplest inflationary Lagrangian reads

$$\mathcal{L} = -\frac{1}{2} (\partial\varphi)^2 - V(\varphi) \quad (5.1)$$

with a usual kinetic term and a potential  $V(\varphi)$ . This simple inflationary framework leads to specific predictions such as a relation between the ratio of tensor to scalar primordial perturbations and the “distance” in field space over which  $\varphi$  runs during inflation (the so-called Lyth bound, see the lectures by Juan Maldacena in these proceedings). Let us, however, emphasize that these predictions (which lead to constraints on the model) do depend on the assumption that inflation is realized by the simple action (5.1) with a slow-roll potential. There are, however, other ways of realizing inflation, in which these constraints might be relaxed. Let us note in this respect that inflation can be realized even if the potential  $V(\varphi)$  in (5.1) is *not* of the slow-roll type [61]. Moreover, one may have inflation without a potential at all if the Lagrangian is a complicated enough function of  $X \equiv -(\partial\varphi)^2$ . Indeed, if one has an action of the type  $\mathcal{L} = p(X)$ , one finds that there can exist attractors toward a de Sitter expansion phase, corresponding to a line where the effective equation of state deduced from  $\mathcal{L} = p(X)$  is  $p = -\rho$  (e.g., k-inflation [62]; ghost inflation [63]). To have a “graceful exit” from this de Sitter phase one needs, for instance, to introduce some additional  $\varphi$  dependence in  $\mathcal{L}$ . It has been suggested in [64] that such a mechanism might be realized in string theory, via a Dirac-Born-Infeld-type action, say

$$p(X, \varphi) = -\frac{\varphi^4}{\lambda^2} \left( \sqrt{1 - \frac{\lambda\dot{\varphi}^2}{\varphi^4}} - 1 \right) - V(\varphi). \quad (5.2)$$

<sup>22</sup>For instance, if one considers it very unlikely that such a field can exist, these experiments are important because they can *falsify* string theory. By contrast, if one finds a violation of the equivalence principle which is nicely consistent with the prediction (4.18) for the composition dependence of a moduli field, this might be viewed as a *confirmation* of string theory.

In such a “DBI inflation”, the use of non-standard kinetic terms greatly relaxes the restrictions imposed on the flatness of the potential  $V(\varphi)$  which must be imposed in the usual case of (5.1). It also tends to produce larger non-gaussianities in the CMB [65]. Let us also point out that the use of a non-linear kinetic term might significantly affect the Lyth bound. For instance, if one considers the action

$$\mathcal{L} = p(X, \varphi) = K(X) - V(\varphi), \quad (5.3)$$

where  $K(X)$  is a non-linear function of the kinetic term  $X \equiv -(\partial\varphi)^2$ , one finds the following modified form of the relation between the ratio  $r$  of tensor to scalar primordial perturbations and the derivative of  $\varphi$  w.r.t. the number of e-folds  $N$ :

$$\frac{r}{8} = \left( \frac{d\varphi}{dN} \right)^2 a \quad (5.4)$$

Here  $a$  is an additional amplification factor, which is given by the following expression in terms of the kinetic function  $K(X)$

$$a = \frac{2K'}{\sqrt{1 + 2X \frac{K''}{K'}}} = \begin{cases} 1 \text{ for } K = \frac{X}{2}, \\ 1 \text{ for DBI type: } -\sqrt{1-X}, \\ \gg 1 \text{ for, e.g., } -\frac{1}{2\alpha}(1-X)^\alpha, \text{ with } \alpha < \frac{1}{2}. \end{cases}$$

A large amplification factor  $a \ll 1$  would (formally) correspond to a relaxed Lyth bound on the excursion of  $\varphi$ , given a minimum number  $N$  of e-folds. It is interesting to note that  $a = 1$  (unchanged Lyth bound) in the DBI-type square root model. However, we note that a more general power  $\alpha$ , with  $\alpha < 1/2$ , would formally relax the Lyth bound. [A more detailed study is, however, necessary for seeing whether the bound is *physically* relaxed.]

The present section presented only a very partial and sketchy picture. It was only intended as an illustration that folklore results and constraints on inflationary models do depend on using the standard slow-roll action (5.1), and that there exist other mechanisms in which those results and constraints might be different and possibly relaxed.

## 5.2. Cosmic superstrings

### 5.2.1. Phenomenological origin

The existence and detection of *cosmic superstrings* is an exciting possibility that was first suggested in Ref. [66], then kept alive for a number of years, and recently revived dramatically notably in Ref. [67] and in other papers [68–70]. They arise in brane antibrane scenarios where the inflaton is the brane-antibrane

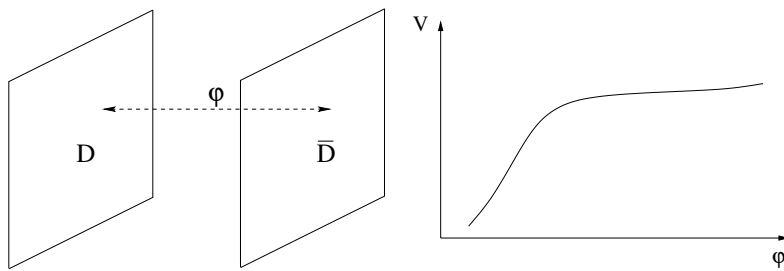


Figure 6. Left: The brane-antibrane distance as a scalar field  $\varphi$ . Right:  $V(\varphi)$  behaves as  $c_1 - c_2\varphi^{-4}$  for large brane-antibrane separations

separation (see e.g., [71]). In such scenarios, for large enough brane-antibrane separations, the potential behaves like  $c_1 - c_2/\varphi^4$  such that it satisfies the slow roll conditions (FIG. 6). When the branes are near, some of the modes connecting the two branes become tachyonic, *i.e.*, a complex field (with kinetic term  $-\partial T \partial \bar{T}$ ) having a potential  $V(|T|^2)$  with wrong-sign curvature near  $T = 0$ . This instability can generate topological defects since the phase of the vev of  $T$  need not be uniformly the same all over space. Contrary to the situation in which strings are created at the beginning of inflation and then diluted away, this scenario naturally produces strings at the end of inflation so that they are not diluted by the expansion. For causality reasons, the value of the field's vev in a given Hubble patch should be uncorrelated to that in other Hubble patches. This is what creates a network of strings and one can then compute the initial density and correlation length of the string network. The string tension  $\mu$  in Planck units, *i.e.*, the dimensionless parameter  $G\mu$ , where  $G$  is Newton's constant, was initially thought to be high, of the order of  $10^{-3}$  at best, because of the string theoretic origin of these objects and of the then expected relation between  $\alpha'$  and the Planck length. However, in models with warping factors and large fluxes, the string tension can be lowered to much smaller values. In practice, the string tension is tuned to fit current CMB data. Tye and collaborators [68] find a window of the type  $10^{-12} < G\mu < 10^{-6}$ , while in the more detailed KKLM model [67] one finds  $G\mu \sim 10^{-10}$ .

In trying to gain insight into the observational predictions that can be made from cosmic superstring models, one must consider not only the stretching by the cosmological expansion of an initial network of cosmic strings with a correlation length of the order of the Hubble scale, but also string interactions. A string can for instance self-intersect or two strings can intersect and reconnect. The Hubble expansion tends to locally straighten out the strings while interconnections tend to produce loops and small-scale structure. Given an initial correlation length and



reconnection probability  $p$ , working out the time evolution of a string network is essentially a classical problem. Two types of strings develop, long strings with correlation length of the order of the time scale  $t$ , and small loops that lose energy by gravitational radiation [72–74].

In order to define the typical size of string loops (at the time they are formed) we introduce a dimensionless parameter  $\alpha$  such that  $\ell_{\text{loop}}(t) = \alpha ct$ . It was initially thought that  $\alpha = 50 G\mu$ , an estimate linked to the idea that gravitational damping is the essential mechanism which determines the lifetime of loops. More recently, it has been suggested that  $\alpha$  might be significantly different from  $50 G\mu$ . There is, however, no consensus on the “correct” value of  $\alpha$ . Estimates vary between  $\alpha \sim (50 G\mu)^\beta$ , with  $\beta > 1$  (leading to “small loops”) and  $\alpha \sim 0.1$  (leading to large loops). [For an introduction to this problem, and references, see e.g., the talk of Joe Polchinski at the 2007 String meeting in Madrid.] Happily, some of the predictions we shall discuss below (notably those concerning the observability of gravitational waves from a cosmic string network) are rather insensitive to the value of  $\alpha$ .

Several numerical simulations confirm the tendency of string networks to display a scale-invariant behavior [75, 76]. There have been recent attempts at refining the theoretical description of string networks [77, 78]. However, there is, to date, no consensus among experts as to the typical size distribution of loops (i.e., the dominant gravitational wave-emitting string type). In several simulations, the distribution of the size of loops is bimodal, with one peak at  $\alpha \sim 0.1$  and another peak at the UV cutoff. It has been argued by Vilenkin and collaborators that only the “large loop” part, i.e.,  $\alpha \sim 0.1$ , will survive.

In the following, assuming KKLMMT-type brane inflation and the stability of strings over cosmologically interesting time scales, we discuss the phenomenological predictions made by treating  $p$  and  $\alpha$  as free parameters and their possible observable signals.

### 5.2.2. Observational signatures

Partly for historical reasons, the phenomenology of cosmic strings has been studied mostly in the context of CMB observations. Slow-roll inflation generates a random  $\frac{\delta T}{T}$  angular distribution on the sky that fits well the observations. Adding a random network of cosmic strings generates additional (non-Gaussian) fluctuations in the CMB which have less angular structure (the string has a lensing effect proportional to its velocity  $v$  over the sky,  $\delta T/T \sim 8\pi G\mu v\gamma$ ). CMB observations can then be used to place an upper bound on  $G\mu$ , of order  $5 \times 10^{-7}$ . Much smaller values of the string tension will not lead to any observable signature in the CMB. Let us also mention that cosmic (super)strings might be detected via their gravitational lensing of galaxies, or microlensing of stars.

By contrast to the CMB (or lensing) observations, which are only sensitive to

string tensions  $G\mu > 10^{-7}$ , existing or planned gravitational wave interferometers could detect cosmic (super)strings with tensions in the much wider range  $10^{-15} < G\mu < 10^{-6}$ . Let us recall that a gravitational wave (GW) detector is actually measuring tidal forces, and more precisely a component of the Riemann tensor projected “along” a detector having a quadrupolar structure<sup>23</sup>. In other words, a GW antenna measures the second time derivative  $\ddot{h}(t)$  of a projection of the metric fluctuation  $h_{\mu\nu}$ . Current detectors are sensitive down to the level  $h \sim 10^{-22}$ , for frequencies  $f \sim 100$  Hz.

The GW signal from a string network is an incoherent background of GWs made of the superposition of all GWs ever emitted by string loops (from zero to very large redshifts). This signal is distributed over a very large spectrum of frequencies (including wavelengths of the size of the universe, as well as very short ones). In order to determine the frequency distribution, the number of loops and how they evolve, one needs to know the evolution of the universe during the inflationary, radiation and matter dominated eras.

Besides detecting the GWs from a string network in a man-made interferometer, another observational possibility lies in the timing of isolated millisecond pulsars. In a stationary spacetime, the pulses emitted by an isolated pulsar would be observed on Earth (after correcting for the Earth motion) at very regular intervals. By contrast, in presence of a fluctuating background of GWs, the times of arrival of successive pulses would fluctuate, and exhibit some red noise. Pulsar timing over some time interval  $T$  (which is typically several years) is most sensitive to the part of the GW frequency spectrum with frequencies  $f \sim 1/T$ . Therefore, pulsar timing is most likely to detect long wavelength GWs (several light years long).

Along with LIGO-type ground based interferometers, a space-based one, the Laser Interferometer Space Antenna (LISA) has been conceived, with arm lengths of the order of  $10^6$  km instead of the 3 or 4 km ones constructed on the ground. LISA can therefore explore much smaller frequencies. The best achievable sensitivity for LIGO-type instruments is reached for frequencies  $f \sim 100$  Hz, *i.e.*, rather fast events lasting  $\sim 10^{-2}$  seconds, while space experiments may probe events with periods  $\sim 1000$  secs, which are quite slow events (see FIG. 7). In Ref. [74], the possible existence of sharp gravitational wave bursts above the background caused by string cusps was pointed out. For a typical oscillating loop, there occurs a cusp once or twice per oscillation with the extremity of the cusp going at the velocity of light and emitting a strong gravitational wave signal in the direction in which the cusp is moving. Statistically, these events are random. A GW burst will be detected if it happens to be emitted towards the

---

<sup>23</sup>This is the spin-2 analog of saying that electromagnetic antennas are sensitive to the projection of the electric field along the direction of a dipolar antenna.

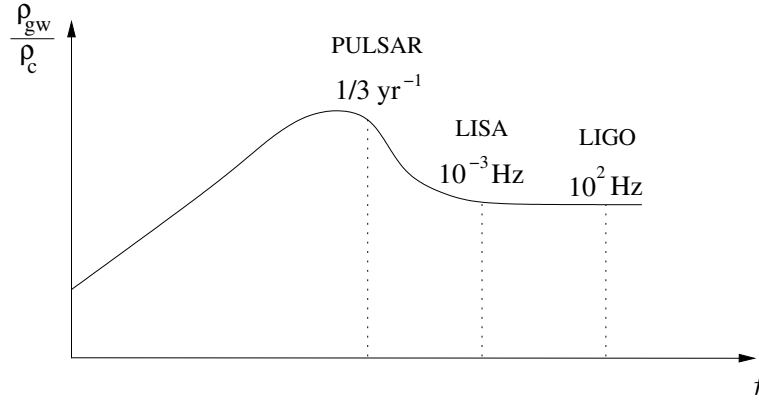


Figure 7. Expected frequency distribution of the ratio  $\Omega_{GW} = \frac{\rho_{GW}}{\rho_c}$  for the stochastic gravitational wave background of cosmic strings.

detector. Under some conditions, these cusps can create signals which stand much above the quasi-Gaussian random mean square background “GW noise”. This raises the exciting possibility that LIGO/VIRGO/GEO or LISA might detect GW signals emitted by giant superstrings at cosmological distances.

Let us now give an introduction to the physics behind the occurrence of those cusps, and the associated emission of GW bursts.

### 5.2.3. String dynamics

We consider the string position  $X^\mu$  as a function of the worldsheet coordinates  $\tau$  and  $\sigma$ . We treat the string dynamics in a locally flat spacetime. Introducing the lightcone coordinates in conformal gauge,

$$\sigma_{\pm} = \tau \pm \sigma, \quad (5.5)$$

$X^\mu(\tau, \sigma)$  satisfies

$$\frac{\partial}{\partial \sigma_+} \frac{\partial}{\partial \sigma_-} X^\mu(\tau, \sigma) = 0 \quad (5.6)$$

such that the generic string solution is the sum of left and right movers

$$X^\mu(\tau, \sigma) = \frac{1}{2} [X_+^\mu(\sigma_+) + X_-^\mu(\sigma_-)] \quad (5.7)$$

in which the factor 1/2 is introduced for convenience. The Virasoro constraints read

$$\begin{aligned} (\partial_+ X_+^\mu)^2 &= 0 \\ (\partial_- X_-^\mu)^2 &= 0 \end{aligned} \quad (5.8)$$

In the time gauge, the worldsheet is sliced by constant coordinate time hyperplanes  $X^0 = x^0 = \tau$ , so that

$$X^0(\tau, \sigma) = \tau = \frac{1}{2}(\sigma_+ + \sigma_-). \quad (5.9)$$

We thus have  $X_+^0 = \sigma_+$  and  $X_-^0 = \sigma_-$ . Then  $\partial_\pm X^0 = 1$  contributes a  $-1$  in the Virasoro constraints, so that

$$(\partial_+ X_+^\mu)^2 = -1 + (\partial_+ X^i)^2, \quad (5.10)$$

and similarly for the  $-$  equation. This means that the derivatives (w.r.t. their argument) of the spatial components  $X_\pm^i(\sigma_\pm)$  of the left and right modes are constrained to be *unit euclidean vectors*:

$$\left(\dot{X}_\pm^i\right)^2 = 1. \quad (5.11)$$

The  $X_\pm^i$  are periodic and the time derivative of the spatial component of  $X$  are unit vectors. We may now use a representation first introduced in Ref. [79]. The derivatives  $\dot{X}_\pm^i$  can be seen as drawing two curves on the unit sphere (the Turok-Kibble sphere). In addition, as  $X_\pm^i$  is periodic in three-dimensional space (there is no winding), we have  $\int d\sigma_\pm \dot{X}_\pm^i = 0$ . As a result, the ‘‘center of mass’’ of both left and right moving curves must be at the center of the sphere. This implies that the two curves generically<sup>24</sup> intersect twice [80]. Now, the main point is that an intersection between the two curves represents a *cusp*. More technically, such an intersection corresponds to particular points on the string worldsheet at which the two null (see (5.8)) tangent vectors  $\dot{X}_+^\mu$  and  $\dot{X}_-^\mu$  are parallel in spacetime. In general, the string worldsheet intersects locally the light cone along the two distinct directions  $\dot{X}_+^\mu$  and  $\dot{X}_-^\mu$ . The cusps are special points where the worldsheet is *tangent to the lightcone* (see FIG. 8). This is a singularity of the classical worldsheet at which a strong gravitational wave signal is emitted along the common null vector. Let us now indicate how one computes the emission of gravitational wave bursts from cuspy strings. We consider Einstein’s theory in the linearized approximation,

$$g_{\mu\nu}(x) = \eta_{\mu\nu} + h_{\mu\nu}(x). \quad (5.12)$$

We use the harmonic gauge,  $\partial^\nu \bar{h}_{\mu\nu} = 0$ , so that Einstein’s equations simplify to

$$\square \bar{h}_{\mu\nu} = -16\pi G T_{\mu\nu}(x), \quad (5.13)$$

<sup>24</sup>There exist, however, specially contrived curves that can avoid intersecting.

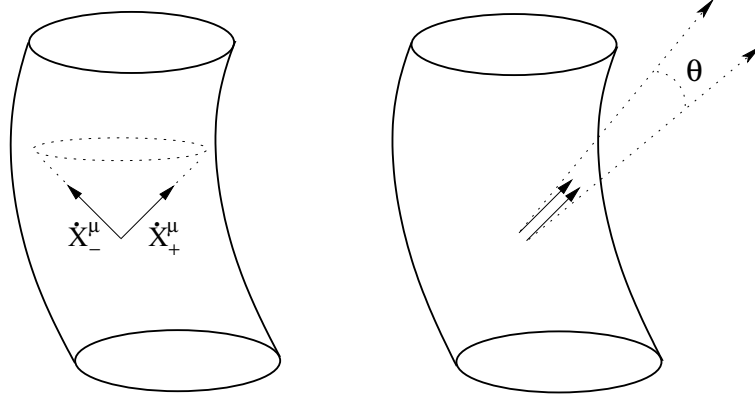


Figure 8. Left: The lightcone generically intersects the worldsheet into two separate null directions corresponding to the velocity of the left and right movers. Right: When a cusp occurs, the two null vectors are parallel and the worldsheet is tangent to the lightcone. There results a large burst of outgoing gravitational radiation.

where

$$\bar{h}_{\mu\nu} = h_{\mu\nu} - \frac{1}{2}h\eta_{\mu\nu}. \quad (5.14)$$

The stress-energy tensor is obtained by differentiating the Nambu action w.r.t.  $g_{\mu\nu}$ . Taking its Fourier transform, one finds

$$T^{\mu\nu}(k^\lambda) = \frac{\mu}{T_\ell} \int_{\Sigma_\ell} d\tau d\sigma \dot{X}_+^{(\mu} \dot{X}_-^{\nu)} e^{-\frac{i}{2}k \cdot (X_+ + X_-)} \quad (5.15)$$

where  $(\mu\nu)$  indicates symmetrization over the indices  $\mu, \nu$ , and where, in the exponential, we have replaced  $X^\mu$  by the half-sum of the left and right movers. The fundamental period of a loop of length  $\ell$  is  $T_\ell = \frac{\ell}{2}$ . Note that  $\ell$  is the invariant total length  $\frac{E_0}{\mu}$ , where  $\mu$  is the string tension. In string theory, one usually uses a worldsheet gauge where  $\ell$  is either 1 or  $2\pi$  but here one finds it more convenient to use a gauge where  $\sigma$  and  $\tau$  are connected to an external definition of time (namely  $X^0 = x^0 = \tau$ ).

We wish to compute the integral giving  $T^{\mu\nu}(k^\lambda)$  over a periodic domain  $\Sigma_\ell$  in the  $\tau, \sigma$  plane. We can rewrite the integral as an integral over  $d\sigma_+ d\sigma_-$ . This yields the famous left-right factorization of closed string amplitudes<sup>25</sup> and the Fourier transform of the string stress-energy tensor reads

$$T^{\mu\nu}(k) = \frac{\mu}{\ell} I_+^{(\mu} I_-^{\nu)}, \quad (5.16)$$

<sup>25</sup>Though we are doing here a classical calculation, one recognizes that the result is given by the graviton vertex operator.

where

$$I_{\pm}^{\mu} = \int_0^{\ell} d\sigma_{\pm} \dot{X}_{\pm}^{\mu}(\sigma_{\pm}) e^{-\frac{i}{2}k \cdot X_{\pm}}. \quad (5.17)$$

By solving Einstein's equation (5.13), one finds that the spacetime-Fourier transform of the source on the r.h.s. actually gives the time-Fourier transform of the asymptotic GW amplitude (emitted in the direction  $n^i = k^i/k^0$ ), i.e., the time-Fourier transform of the quantity  $\kappa_{\mu\nu}(t-r, \vec{n})$  appearing in the asymptotic expansion

$$\bar{h}_{\mu\nu}(t, \vec{x}) = \frac{\kappa_{\mu\nu}(t-r, \vec{n})}{r} + \mathcal{O}\left(\frac{1}{r^2}\right). \quad (5.18)$$

Here the  $1/r$  decrease in amplitude as a function of distance away from the string is caused by the retarded Green's function in 3+1 dimensions.  $\kappa_{\mu\nu}$  is a function of both the time variable and the angle of emission. As we just said, the time-Fourier transform of  $\kappa^{\mu\nu}$  is proportional to the spacetime-Fourier transform  $T^{\mu\nu}(k)$  of the source, and is explicitly given by

$$\begin{aligned} \kappa_{\mu\nu}(f, \vec{n}) &= |f| \int dt e^{2\pi i f(t-r)} \kappa^{\mu\nu}(t-r, \vec{n}) \\ &= 2G\mu |f| I_{+}^{(\mu}(\omega, \omega\vec{n}) I_{-}^{\nu)}(\omega, \omega\vec{n}). \end{aligned} \quad (5.19)$$

This formula shows that we can compute what is observed in a GW detector as a function of string tension, frequency, and the product of two integrals involving left and right moving modes.

We can then estimate the generic features of the GW burst emitted by a cusp by noticing that, in the Fourier domain, each integral  $I_{\pm}^{\mu}$  is dominated (when considering large frequencies:  $f \gg T_{\ell}^{-1}$ ) by the singular behaviour of the two integrands  $\dot{X}_{\pm}^{\mu}(\sigma_{\pm}) e^{-\frac{i}{2}k \cdot X_{\pm}}$  near a cusp. The calculation proceeds by (Taylor) expanding the vectors  $X_{\pm}^{\mu}$  and  $\dot{X}_{\pm}^{\mu}$  in powers of  $\sigma_{\pm}$ . One finds that the first few leading terms in this expansion can be gauged away, so that the signal amplitude is much smaller than what could have (and had) been initially thought. After Fourier transforming back to the time domain, it is finally found that [74]

$$\begin{aligned} \kappa(t) &\propto |t-t_c|^{1/3}, \\ \ddot{\kappa}(t) &\propto |t-t_c|^{-5/3}. \end{aligned} \quad (5.20)$$

As this result seems to crucially depend on the presence of a mathematically singular behaviour of the *classical* string worldsheet at a cusp, one might worry that quantum effects could blur away the sharp cusp, and make the above classical burst signal disappear. It was checked that this is not the case [81] (the basic reason being that, finally, the strong GW burst signal is emitted by a large segment of the string around the cusp).

#### 5.2.4. Gravitational waves from a cosmological string network

In order to understand the observational signature of a cosmic string network and not just a single string, one must combine the analysis of the previous section with the cosmological expansion of a Friedman-Lemaître universe and with an integration over redshift. A crucial point is then to estimate the number density of string loops. This density can be analytically estimated as a function of the string parameters, such as the reconnection probability  $p$ , and the string tension  $G\mu$ . Note that the reconnection probability is expected to be quite different for cosmic superstrings compared to the traditionally considered field-theory strings. Field theory strings are expected to reconnect, when they cross, with essentially unit probability ( $p \simeq 1$ ), while fundamental or  $D$ -strings are expected to reconnect with a smallish probability,  $10^{-3} < p < 1$  [82] (because of the presence of the string coupling, and other factors).

The loop number density can be approximately estimated as [83]

$$n_\ell \sim \frac{1}{p 50 G\mu t^3} + \dots \quad (5.21)$$

where the first term on the r.h.s. comes from loops that were created at redshifts  $\leq 1$ , while the ‘...’ denotes a possible additional contribution from high-redshift strings. When the loop-size parameter  $\alpha$  is smaller or equal to the “traditionally expected” value  $50G\mu$ , the contribution from high-redshift strings is negligible (because strings decay in less than a Hubble time). By contrast, when  $\alpha \gg 50G\mu$ , the strings survive over many Hubble times, and the contribution of high-redshift strings starts to dominate the loop density. Note the somewhat unexpected feature displayed by the first term in  $n_\ell$ , namely that it increases both as  $G\mu$  and/or  $p$  are decreased. This feature is one of the features which allow GW signals from strings to be detected down to very small values of the string tension (contrary to CMB effects). Indeed, as  $G\mu$  is decreased, though each individual string signal will decrease proportionally to  $G\mu$ , there will be more emitting loops. After integrating over redshifts, one finds that the observable signal is a complicated, *non monotonic* function of  $G\mu$ . The numerical estimates of Ref. [83] considered the case in which the loop size parameter  $\alpha < 50G\mu$ , in which case the first term in (5.21) is dominant. If, on the other hand, one assumes  $\alpha \sim 0.1$  (as is suggested by some numerical simulations [75]), strings survive longer so that higher redshift contributions are non-negligible. It has been found that in such cases these contributions increase the number of loops (which increases the GW signal) but tend to drown the cusp signal within the quasi-Gaussian random-mean-square GW background [84].

Based on current detector capabilities and on the sensitivity estimates for future detectors, one finds that if  $\alpha \leq 50G\mu$ , LIGO could detect  $G\mu \geq 10^{-12}$  while LISA could detect  $G\mu \geq 10^{-14}$ . On the other hand, if  $\alpha \gg 50G\mu$  LISA

could reach  $G\mu \geq 10^{-16}$ . One has looked in the current LIGO data for the possible presence of a background of GW's, but without success so far [85]. The best current bound on  $G\mu$  comes from pulsar timing [86] and is roughly at the  $G\mu \leq 10^{-9}$  level (which is about three orders of magnitude more stringent than the limits than can be obtained from CMB data).

Gravitational wave detectors are thus excellent probes of cosmic (super)strings. There is therefore the possibility that they could confirm or refute KKLMMT-type scenarios in a large domain of parameter space. However, there are large uncertainties in string network dynamics which prevent one from being able to make reliable analytical estimates. If one is in a region of parameter space where the rather specific cusp-related signals are well above the r.m.s. background one might find rather direct experimental evidence for the existence of cosmic strings. There would however remain the task of discriminating between string theoretic strings and field theoretic ones. One way would be (assuming one could strongly reduce the string network uncertainties) to determine the reconnection probability  $p$  from its influence on the loop number density, and, thereby, on the recurrence rate of observed signals. Another more ambitious possibility would be to exploit the presence of two populations of strings, namely D and F strings, in D-brane anti D-brane annihilation, and attempt to measure two different values of  $G\mu$ , the ratio of which satisfies  $\mu_D = \mu_F/g_s$ .

## 6. Conclusion

We hope that these lectures have shown that gravity phenomenology is a potentially interesting arena for eventually confronting string theory to reality.

## Acknowledgement

TD wishes to thank the organizers of this Les Houches session for putting together a timely and interesting programme. He is especially grateful to Nima Arkani-Hamed, Michael Douglas, Igor Klebanov and Eliezer Rabinovici for informative discussions. ML wishes to thank the organizers of the school and the lecturers for a very stimulating time in les Houches.

## Bibliography

- [1] R. Penrose, Riv. Nuov. Cimento. **1** (1969) 252.
- [2] D. Christodoulou, Phys. Rev. Lett. **25** (1970) 1596.



- [3] D. Christodoulou, R. Ruffini Phys. Rev. D **4** (1971) 3552.
- [4] S.W. Hawking, Phys. Rev. Lett. **26** (1971) 1344.
- [5] J. Bardeen, B. Carter and S.W. Hawking, Comm. Math. Phys. **31** (1973) 161.
- [6] S.W. Hawking, and J.B. Hartle, Comm. Math. Phys. **27** (1972) 283.
- [7] R.S. Hanni, and R. Ruffini, Phys. Rev. D **8** (1973) 3259.
- [8] T. Damour, Phys. Rev. D **18** (1978) 3598.
- [9] T. Damour, in: “Quelques propriétés mécaniques, électromagnétiques, thermodynamiques et quantiques des trous noirs”; Thèse de Doctorat d’Etat, Université Pierre et Marie Curie, Paris VI, 1979. available (see files these1.pdf to these6.pdf) on <http://www.ihes.fr/~damour/Articles/>
- [10] T. Damour, in: “Surface Effects in Black Hole Physics”; Proceedings of the Second Marcel Grossmann Meeting on General Relativity, (edited by R. Ruffini, North Holland, 1982) pp 587-608; available (see file surfaceeffects.pdf) on <http://www.ihes.fr/~damour/Articles/>
- [11] R.L. Znajek, MNRAS **185** (1978) 833.
- [12] K. S. . Thorne, R. H. . Price and D. A. . Macdonald, “Black Holes: The Membrane Paradigm,” *New Haven, USA: Yale Univ. Press (1986) 367p.*
- [13] P.K. Kovtun, D.T. Son and A.O. Starinets, Phys. Rev. Lett. **94** (2005) 111601.
- [14] D. T. Son and A. O. Starinets, Ann. Rev. Nucl. Part. Sci. **57** (2007) 95 [arXiv:0704.0240 [hep-th]].
- [15] B. Carter, in: *Black Holes*, Proceedings of 1972 Les Houches Summer School, (edited by C. DeWitt and B. S. DeWitt, Gordon and Breach, NY, 1973).
- [16] J. Bekenstein, Phys. Rev. D **7** (1973) 2333.
- [17] S.W. Hawking, Comm. Math. Phys. **43** (1975) 199.
- [18] T. Damour, and R. Ruffini, Phys. Rev. D **14** (1976), 332.
- [19] E.ourgoulhon, Phys. Rev. D **72**, 104007 (2005) [arXiv:gr-qc/0508003].
- [20] E.ourgoulhon and J. L. Jaramillo, Phys. Rept. **423**, 159 (2006) [arXiv:gr-qc/0503113].
- [21] J.P. Uzan, Rev. Mod. Phys. **75** (2003) 403.
- [22] T. Damour, and F. Dyson, Nucl. Phys. B **480** (1996) 37.
- [23] A.I. Shlyakhter, in: ATOMKI Report A/1 (Debrecen, Hungary) 1983.
- [24] Y. Fujii, Nucl. Phys. B **573** (2000) 337.
- [25] K.A. Olive, M. Pospelov, Y.-Z. Qian, G. Manhes, E. Vangioni-Flam, A. Coc, and M. Casse, Phys. Rev. D **69** (2004) 027701.
- [26] S. Bize *et al.*, Phys. Rev. Lett. **90**, 150802 (2003) H. Marion *et al.*, Phys. Rev. Lett. **90**, 150801 (2003); M. Fischer *et al.*, Phys. Rev. Lett. **92**, 230802 (2004).
- [27] C.D. Hoyle, U. Schmidt, B.R. Heckel, E.G. Adelberger, J.H. Gundlach, D.J. Kapner, and H.E. Swanson Phys. Rev. Lett. **86** (2001) 1418; E.G. Adelberger, B.R. Heckel, and A.E. Nelson, Ann. Rev. Nucl. Part. Sci. **53** (2003) 77; C.D. Hoyle, D.J. Kapner, E.G. Adelberger, J.H. Gundlach, U. Schmidt, and H.E. Swanson, Phys. Rev. D **70** (2004) 042004; D.J. Kapner, T.S. Cook, E.G. Adelberger, J.H. Gundlach, B.R. Heckel, C.D. Hoyle, and H.E. Swanson, Phys. Rev. Lett. **98** (2007) 021101.
- [28] J. G. Williams, S. G. Turyshev and D. H. Boggs, Phys. Rev. Lett. **93**, 261101 (2004) [arXiv:gr-qc/0411113].
- [29] R.F.C. Vessot, M.W.A. Levine, General Relativity and Gravitation **10** (1979) 181.
- [30] C. Will, Living Rev. Relativity **4** (2001).
- [31] See chapter 18 (“Experimental tests of gravitational theory”, by T. Damour) in W.-M. Yao *et al.* (Particle Data Group), J. Phys. G **33**, 1 (2006); a 2007 partial update for the 2008 edition is available on the PDG WWW pages (URL: <http://pdg.lbl.gov/>).

- [32] P. D. D'Eath, Phys. Rev. D **12**, 2183 (1975).
- [33] T. Damour, Gravitational radiation and the motion of compact bodies. in *Gravitational Radiation*, edited by N. Deruelle and T. Piran, North-Holland, Amsterdam, 1983, pp 59-144.
- [34] T. Damour, P. Jaranowski and G. Schafer, Phys. Lett. B **513**, 147 (2001) [arXiv:gr-qc/0105038].
- [35] L. Blanchet, T. Damour and G. Esposito-Farese, Phys. Rev. D **69**, 124007 (2004) [arXiv:gr-qc/0311052].
- [36] B. Bertotti, L. Iess, and P. Tortora, Nature **425** (2003) 374.
- [37] K. Nordtvedt, Phys. Rev. **169** (1968) 1014.
- [38] K. Nordtvedt, Phys. Rev. **169** (1968) 1017.
- [39] T. Damour, arXiv:0705.3109 [gr-qc].
- [40] T. Damour, and G. Esposito-Farese, Phys. Rev. D **54** (1996) 54.
- [41] A. Dar, Nucl. Phys. (Proc. Supp.) **B28**,321(1992).
- [42] T. Jacobson, S. Liberati and D. Mattingly, Annals Phys. **321**, 150 (2006).
- [43] G. Amelino-Camelia, Lect. Notes Phys. **669**, 59 (2005) [arXiv:gr-qc/0412136].
- [44] E. G. Gimon and P. Horava, arXiv:0706.2873 [hep-th].
- [45] I. Antoniadis, N. Arkani-Hamed, S. Dimopoulos, and G. Dvali, Phys. Lett. B **436** (1998) 257.
- [46] L. Randall, and R. Sundrum, Phys. Rev. Lett. **83** (1999) 3370.
- [47] G. Dvali, G. Gabadadze, and M. Porrati, Mod. Phys. Lett. **83** (2000) 1717.
- [48] G. Dvali, A. Gruzinov, and M. Zaldarriaga, Mod. Phys. D **68** (2003) 024012.
- [49] A. Adams, N. Arkani-Hamed, S. Dubovsky, A. Nicolis and R. Rattazzi, JHEP **0610**, 014 (2006) [arXiv:hep-th/0602178].
- [50] I.I. Kogan, S. Mouslopoulos, A. Papazoglou, G.G. Ross, J. Santiago, Nucl. Phys. B **584** (2000) 313; R. Gregory, V.A. Rubakov, and S.M. Sibiryakov, Phys. Rev. Lett **84** (2000) 5928; T. Damour and I. I. Kogan, Phys. Rev. D **66**, 104024 (2002) [arXiv:hep-th/0206042].
- [51] T. Damour, I. I. Kogan and A. Papazoglou, Phys. Rev. D **67**, 064009 (2003) [arXiv:hep-th/0212155].
- [52] M. R. Douglas and S. Kachru, Rev. Mod. Phys. **79**, 733 (2007) [arXiv:hep-th/0610102].
- [53] E. Rabinovici, arXiv:0708.1952 [hep-th].
- [54] T. Damour, and A.M. Polyakov, Nucl. Phys. B **423** (1994) 532.
- [55] T. Damour, F. Piazza, and G. Veneziano, Phys. Rev. D **66** (2002) 046007; T. Damour, F. Piazza, and G. Veneziano, Phys. Rev. Lett. **89** (2002) 081601.
- [56] B.D. Serot, and J.D. Walecka, Int. J. Mod. Phys. E **6** (1997) 515.
- [57] J.F. Donoghue, Phys. Rev. C **74** (2006) 515.
- [58] T. Damour and J. F. Donoghue, arXiv:0712.2968 [hep-ph].
- [59] S. Dimopoulos, P. W. Graham, J. M. Hogan and M. A. Kasevich, Phys. Rev. Lett. **98**, 111102 (2007) [arXiv:gr-qc/0610047].
- [60] J. Khoury and A. Weltman, Phys. Rev. Lett. **93**, 171104 (2004) [arXiv:astro-ph/0309300].
- [61] T. Damour, and V.F. Mukhanov, Phys. Rev. Lett. **80** (1998) 3440.
- [62] C. Armendariz-Picon, T. Damour, and V.F. Mukhanov, Phys. Lett. B **458** (1999) 209.
- [63] N. Arkani-Hamed, P. Creminelli, S. Mukohyama, and M. Zaldarriaga, JCAP **0404** (2004) 001.
- [64] E. Silverstein, and D. Tong, Phys. Rev. D **70** (2004) 103505.
- [65] M. Alishahiha, E. Silverstein, and D. Tong, Phys. Rev. D **70** (2004) 123505.
- [66] E. Witten, Nucl. Phys. B **249** (1985) 557.

- [67] S. Kachru, R. Kallosh, and A. Linde, J. Maldacena, L. McAllister, and S.P. Trivedi, JCAP **0310** (2003) 013.
- [68] S. Sarangi, and S.-H. Tye Phys. Lett. B **536** (2002) 185.
- [69] G. Dvali, and A. Vilenkin JCAP **0403** (2004) 010.
- [70] E.J. Copeland, R.C. Myers, and J. Polchinski, JHEP **0406** (2004) 013.
- [71] G. Dvali, and S.-H Tye, Phys. Lett. B **450** (1999) 72.
- [72] A. Vilenkin, Phys. Rev. D **23** (1981) 852.
- [73] A. Vilenkin and E. P. S. Shellard, *Cosmic Strings and Other Topological Defects* Cambridge University Press, Cambridge, 2000.
- [74] T. Damour, and A. Vilenkin, Phys. Rev. Lett. **85** (2000) 3761; T. Damour, and A. Vilenkin, Phys. Rev. D **64** (2001) 064008.
- [75] V. Vanchurin, K. Olum, and A. Vilenkin, Phys. Rev. D **72** (2005) 063514; V. Vanchurin, K. Olum, and A. Vilenkin, Phys. Rev. D **74** (2006) 063527.
- [76] C. Martins, and E. Shellard, Phys. Rev. D **73** (2006) 043515.
- [77] J. Polchinski, and J.V. Rocha, Phys. Rev. D **75** (2007) 123503.
- [78] F. Dubath, and J.V. Rocha, Phys. Rev. D **76** (2007) 024001.
- [79] T.W.B. Kibble, and N. Turok, Phys. Lett. B **116** (1982) 141.
- [80] N. Turok, Nucl. Phys. B **242** (1984) 520.
- [81] D. Chialva, and T. Damour, JCAP **0608** (2006) 003.
- [82] M. G. Jackson, N. T. Jones and J. Polchinski, JHEP **0510**, 013 (2005) [arXiv:hep-th/0405229].
- [83] T. Damour, and A. Vilenkin, Phys. Rev. D **71** (2005) 063510.
- [84] C.J. Hogan, Phys. Rev. D **74** (2006) 043526.
- [85] B. Abbott *et al.* [LIGO Collaboration], Astrophys. J. **659**, 918 (2007) [arXiv:astro-ph/0608606].
- [86] F. A. Jenet *et al.*, Astrophys. J. **653**, 1571 (2006) [arXiv:astro-ph/0609013].